ELECTRON MICROSCOPIC STUDIES ON THE REPRODUCTION AND DEVELOPMENT OF TWO BRITTLE-STARS, AMPHIPHOLIS KOCHII AND OPHIURA SARSII (ECHINODERMATA: OPHIUROIDEA)

(With 7 Tables, 10 Text-Figures and 43 Plates)

A DISSERTATION

submitted to the Graduate School, Hokkaido University,

in partial fulfillment of the requirements for the degree

DOCTOR OF SCIENCE

By

MASAKANE YAMASHITA, OSAKA

CONTENTS

I. INTRODUCTION

Brittle-stars constitute the class Ophiuroidea, one of the five classes of the phylum Echinodermata, which includes about 2,000 existing species. This class, therefore, surpasses in number of species the other classes of echinoderms, except for asteroids. It is no exaggeration to say that the ophiuroids are mostly prosperous in comparison with the other members of echinoderms, in the meanings that they are most active by means of well movable arms and that they are found on all types of bottom of the seas at any latitudes and at the depth from intertidal zone to abyssal region, down to 7,000 m. In spite of their prosperity, however, our knowledges of the ophiuroids, especially of their reproduction and development, are very poor as compared with those of the other echinoderms. For example, there has been no published study concerning the fine structure of the ophiuroid gonads except some light microscopic investigations briefly treated (Smith, 1940; Patent, 1976). As for the fine structure of the gonads in echinoderms, detailed observations of the spermatogenesis have been extensively made with special attentions to the acrosome formation (Longo and Anderson, 1969a; Dan and Shirakami, 1971; Atwood, 1974; Pladellorens and Subirana, 1975; Bickell et al., 1980). All the foregoing observations on the acrosome structure agree in that the acrosome of the echinoderms is circular in shape. On the other hand, as to the beginning of the acrosome formation with an appearance of the proacrosomal vesicle, variation is found among five classes of the echinoderms; in the holothuroid the proacrosomal vesicle is initially recognized

in the spermatogonium (Atwood, 1974; Pladellorens and Subirana, 1975), in the crinoids it is in the spermatocyte (Bickell, et al., 1980), and in the echinoid and asteroid in the spermatid (Longo and Anderson, 1969a; Dan and Shirakami, 1971). However, in the ophiuroid the time of beginning of the acrosome formation is unknown up to date, because there has been no detailed examination about the ophiuroid spermatogenesis.

Concerning the reproductive cycle of the echinoderms, many analytical studies have been made, especially for the echinoids, but the close relationship between the reproductive cycle and environmental changes is still unclear. Based upon a superficial correlation between them, several authors have suggested that the reproductive periodicities might be controlled by environmental factors such as water temperature (Boolootian, 1966; Pearse and Phillips, 1968; Chatlynne, 1969; Pearse, 1969a, b, 1970; Lessios, 1981), salinity (Lessios, 1981), lunar periodicity (Pearse, 1975), tidal change (Pearse, 1972), food supply (Fuji, 1960b; Pearse and Giese, 1966; Pearse, 1969a, b: Gonor, 1973a), and photoperiod (Holland, 1967; Pearse, 1969a). To date, however, experimental studies to clarify the relationship between the reproductive cycle and these environmental factors have been confined to only a few investigations (Cochran and Engelmann, 1975; Pearse, 1981; Pearse and Eernisse, 1982). Concerning the reproductive cycle of ophiuroids, the same situation as that for the echinoids is also present: several examinations have been published until now, but the effect of the external factors on gametogenesis has never been experimentally confirmed (Patent,

1969; Fenaux, 1970, 1972; Lönning, 1976; Tyler, 1977; Hendler, 1979; Tyler and Gage, 1980, 1982; Gage and Tyler, 1982).

As for the development of the ophiuroids, it has been reported that they have various developmental pattern, among which planktotrophic development, which includes free-living ophiopluteus, is well known as a typical ophiuroid developmental pattern (Hyman, 1955; Hendler, 1975). Recently, several reports on ophiuroid development have been published, but these have been concerned with the different developmental pattern known as abbreviated development (Fenaux. 1963, 1969; Patent, 1970; Stancyk, 1973; Hendler, 1977, 1978; Mladenov, 1979; Oguro et al., 1982). Moreover, many of these studies have been chiefly concerned with ecological aspects rather than embryological one. Observations made through ophiopluteus development are scarce, in spite of the fact that many ophioplutei have been found by means of plankton-hauls (Mortensen, 1913, 1920, 1921, 1931, 1937, 1938, Thorson, 1934). To date, detailed studies on the development of the ophiopluteus have been confined to only the three species Ophiothrix fragilis (MacBride, 1907), Ophiocoma nigra (Narasimhamurti, 1933) and Ophiopholis aculeata (Olsen, 1942). In addition, there is no report on the fertilization process of the ophiuroids. The small number of papers about ophiuroid development, including fertilization, are mainly due to the difficulty of artificially inducing their spawning in the laboratory. Indeed, no chemical substances inducing their spawning have been reported, whereas KCl and 1-methyladenine are known to induce spawning in other groups.

Since the pioneering works of the Colwins (1961a, b; 1963a, b), there have been many reports of electron microscopic observations on the early fertilization process in animals (cf., Colwin and Colwin, 1967; Austin, 1968). However, observations on the latter fertilization process, including male and female pronuclear formation and their association, are confined to only a few species (cf., Longo, 1973). Moreover, many of the observations concerning early fertilization process were carried out in polyspermic conditions in order to increase the opportunity for cutting ultrathin sections containing the region of sperm-egg interaction. The problem, therefore, is whether these observations accurately reflect the normal, monospermic fertilization process. Indeed, it has been reported that in some mammals excess spermatozoa which are incorporated into the egg are unable to develop into male pronuclei (Hunter, 1967; Hirao and Yanagimachi, 1979). The small number of reports concerned with the latter phase of fertilization may be partly due to this troublesome phenomenon.

In echinoderms, published electron microscopic observations of fertilization process have appeared for the echinoids (Longo and Anderson, 1968), but not for the ophiuroids. Echinoid eggs are fertilized after meiosis has been completed, whereas ophiuroid eggs are fertilized during meiosis, at the first meiotic metaphase (see RESULTS, C-1). This difference in the state of egg maturation at insemination seems to be important to the subsequent fertilization process (cf., Wilson, 1925; Longo, 1973).

The present study, therefore, describes the morphology of the gonads of two brittle-stars Amphipholis kochii and Ophiura sarsii at first (A), second, the reproductive cycle of A. kochii is examined (B), third, the normal developmental process of A. kochii is reported after establishment of the spawning induction method for the ophiuroid (C), and finally, the monospermic fertilization process of A. kochii is studied (D). The morphology of the gonads is examined with electron microscopy, with special reference to the gonadal wall and spermatogenesis. The examinations of the reproductive cycle of the ophiuroids in the present studies reveal not only a gross feature of the cycle but also the growth pattern of oocytes and control mechanism of the sperm production. The developmental process of eggs in A. kochii is described up to the metamorphosis in laboratory culture. The normal, monospermic fertilization process, including acrosome reaction, sperm penetration, egg cortical reaction together with fertilization membrane and hyaline layer formation, male and female pronuclear formation and their association, is examined with electron microscopic techniques. The surface replica method and electron microscopic histochemistry are also used to describe the fetilization membrane and hyaline layer formation. The present study also attempts to analyse the mechanisms for male and female pronuclear formation and the relationship between them or to meiosis, by means of the experimental study using the meiosis inhibitors (colchicine, colcemid or cytochalasin B).

II. MATERIALS AND METHODS

1. Animals

The brittle-stars, Amphipholis kochii, were collected between the tidemarks at Abuta on the Pacific coast of south-western Hokkaido, Japan. Samplings of the animals were made at monthly intervals from June 1979 through August 1980, and in June and July from 1981 to 1983. The brittle-stars, Ophiura sarsii, were collected in Uchiura Bay, south-western Hokkaido, Japan, at the depth of about 300 m. Samplings were made from April through September, 1979.

2. Histology

a. Light microscopy (LM): The gonads, embryos and larvae were fixed in Bouin's solution for 3 hours or more, dehydrated with ethanol and embedded in paraffin. The serial sections of 3-5 μm were stained with Delafield's hematoxylin and eosin.

b. Transmission electron microscopy (TEM): The testes were prefixed with 5% glutaraldehyde (GA) in 75% sea water, washed in 150% sea water, and postfixed with 1% OsO_4 in 75% sea water. The eggs were prefixed with 5% GA in 50% sea water, washed in 100% sea water and postfixed with OsO_4 in 50% sea water. The fixed materials were dehydrated with acetone and embedded in Epon (Luft, 1961). Ultrathin sections were cut with glass knives on a Porter-Blum MT-1 ultramicrotome, stained with uranyl acetate and lead citrate (Reynolds, 1963), and observed in a JEOL JEM-100S electron microscope. To ease the examination of the fertilization process in monospermic eggs by TEM, ultrathin sections were

obtained by a further sectioning of Epon thick sections: Thick sections (1-2 μm thick) were affixed on a slide and stained with 0.1% aqueous solution of toluidine blue containing 1% sodium borate. The sections suitable for further sectioning were selected by obervation under a light microscope. To a selected section, an Epon block was attached with adhesive (Aron Alpha; Konishi Co., Ltd., Osaka, Japan). The section that adhered to the Epon block was removed from the slide using liquid nitrogen and was cut into ultrathin sections with the ultramicrotome. The ultrathin sections were mounted on collodion-coated grids and observed with TEM after ordinary double stain.

c. Scanning electron microscopy (SEM): the GA-fixed eggs or spermatozoa were affixed on a cover slip with poly-L-lysine (Mazia et al., 1975), and postfixed with OsO_4. After dehydration in ethanol, they were critical point dried in CO_2, coated with a gold, and examined in a JEOL JSM-T20 scanning electron microscope.

d. Ultrastructural histochemistry: To expose the vitelline coat, some eggs were stained with Ruthenium Red (RR) known to stain extracellular mucopolysaccharides: The GA-fixed eggs were washed in 0.2 M cacodylate buffer (pH=7.4), and postfixed in a 1:1 mixture of 2% OsO_4 in 0.2 M cacodylate buffer and RR stock solution (Luft, 1971a and b) for 3 hours in the dark. These eggs were embedded in Epon, cut into ultrathin sections and stained additionally with uranyl acetate and lead citrate in order to amplify the contrast in the tissue. Periodic acid-chromic acid-silver methenamine (PA-CrA-silver) stain was employed for

detection of polysaccharides in ultrathin sections (Rambourg et al., 1969): The prefixed eggs with GA were embedded in Epon without postfixation in OsO_4. Ultrathin sections were oxidized successively with periodic acid and chromic acid, and then stained with a silver methenamine reagent for 20 min in the dark at 60°C. Control sections were treated with the silver methenamine reagent without previous oxidation.

e. Surface replica method: Details of the egg surface were observed by means of the surface replica method: The GA-fixed eggs were washed at least three times in distilled water in order to prevent artifacts originated from salts in the fixative (Miller et al., 1983). After removal of excess water, the eggs were quickly frozen in liquid Freon without postfixation in OsO_4, and then preserved in liquid nitrogen. To expose the egg surface covered by ice, the eggs were etched at -75°C, 10^{-6} torr for 10 min in the vacuum evaporator JEOL JEE-4X. For surface replication, they were shadowed with a platinum-palladium and coated with carbon. The surface replicas were cleaned successively in sodium hypochlorite and sulfuric acid, and viewed in TEM. The surface structure of the developing fertilization membrane was also observed by the replica method: The developing fertilization membranes, which were removed mechanically from the GA-fixed eggs, were affixed on a cover slip with poly-L-lysine and dehydrated in ethanol. After critical point drying in CO_2, they were treated for the surface replication as described above. All figures of the surface replicas were photographically reversed, and platinum deposits appear white.

3. Analysis of the growth pattern of oocytes

a. Frequency polygon method: The frequency polygon method of Pearse (1965) was adopted for the examination of the growth pattern of the oocytes as follows: All those oocytes with a nucleolus found in three longitudinal sections were chosen to measure the diameter with an ocular micrometer. The diameter of each oocyte was represented by a mean of the lengths along long and short axes, because the most oocytes were somewhat elliptical in outline. The obtained diameters were separated into 10 μm size classes for examining the size-frequency distribution of the samples.

b. Instantaneous relative growth rate: The growth rate of the largest oocytes was examined by calculating the instantaneous relative growth rate according to the following formula by Brody (1945):

$$k = (\ln V_2 - \ln V_1)/(t_2 - t_1),$$

where k represents the instantaneous relative growth rate, V_1 is the largest oocyte volume at time t_1, and V_2 is the largest oocyte volume at time t_2. From the mean diameter of oocyte, i.e., the mean length of long and short axes of oocyte, the volume of oocyte was calculated on assumption that the oocyte was adequately represented as a sphere. The largest oocyte volume in each female was gained by building the intermediate volume of largest five oocytes in each female. The largest oocyte volume in each month was then obtained by averaging the largest oocyte volume of each female in a month. The resulting volume was plotted on a graph with semi-logarithmic scale against time starting on July 26th, 1979, after the spawning had occurred.

4. Analysis of the annual testicular cycle

a. Calculation for the number of cells in testis: The number of cells in the testis was calculated by the following procedure, based on the method of Holland et al. (1975): 1) Assuming that the testis is a solid cylinder with a constant diameter, the testicular volume was calculated according to its length and diameter. 2) Under the light microscope, the histological cross section of a given testis was divided into four regions, each of which is occupied mainly by spermatogonia, spermatocytes, spermatozoa together with spermatids, and others, respectively. The boundary of each region was clearly observable by histological examination (cf., Figs. 1C and D). In order to assess the percentage of each cell population in a cross section, the histological cross section of the testis was projected onto an aluminium foil by means of camera lucida. The aluminium foil was cut along the boundary of each cell region and weighed by a chemical balance. The weight of each aluminium foil was divided by the total weight. 3) To estimate the volume of one spermatogonium, spermatocyte or spermatozoon (or spermatid), an arbitrary number of cells in each cell population was projected onto an aluminium foil at a magnification of 920x. The projected foil was then weighed, and its weight was divided by the weight of the standard aluminium foil of 920 mm x 920 mm for conversion of weight to area. The resulting area was divided by the number of the cells projected to yield the area occupied by one cell. From this area, the volume of one cell was calculated on the assumption that the cell was adequately represented as a sphere. The average volume of each cell type after several measurements was

as follows: Spermatogonium; 1.0 x 10^{-6} mm^3: Spermatocyte; 3.6 x 10^{-7} mm^3: Spermatozoon (Spermatid); 2.4 x 10^{-8} mm^3. 4) In order to calculate the cell number of each cell population from a given testis, the testicular volume was multiplied by the percentage of each cell population and then divided by the volume of the one cell. Three arbitrary testes were measured for an individual, and the average number of cells was used for the data.

To assess the number of the amoeboid cells (the somatic cells in the testis), the foregoing method could not be empolyed because the locality of these cells in the testis was not cylindrical but very irregular (cf., Fig. 1E). Thus, the area of the amoeboid cell clusters in a cross section was used for estimating the number of the amoeboid cells. It was accomplished as follows: The outline of the clusters of the amoeboid cells in a cross section was projected onto an aluminium foil at a magnification of 194x, and the weight of the foil obtained was divided by the weight of the foil of 194 mm square. The average area after three measurements was used for the data.

b. Experiment on temperature influence: To examine the influence of sea water temperature on spermatogenesis, some brittle-stars collected in February, April and May were separated into two groups, each containing about five animals; one group, as a control, was kept in the aquarium at the same temperature as that of the sea water at the collection site, while the other group was kept at a higher or lower temperature than that. In these experiments, the day length at the collection site was roughly maintained. Eighteen days later, the animals were fixed,

and the number of the spermatogenic cells was claculated by the aforementioned procedure.

c. Autoradiography: The brittle-stars collected during the season from November through June were injected intracoelomically with 5 μCi of ^{3}H-thymidine (specific activity, 42 Ci/m mol). The ^{3}H-thymidine was diluted for use with one part of sea water. The injected animals were kept in the aquaria at various water temperatures including the same temperature at which the samples were collected. At intervals after the injection of 1h, 1 day, and days 3, 5, 7, 10, 14, 18, 22, 26 and 30, several animals were fixed in Bouin's solution, embedded in paraffin and sectioned in pieces 2-3 um thick. After being deparaffinized, the slides were extracted with cold 2% perchloric acid and dipped in half-diluted nuclear emulsion at 45°C; they were then exposed for 10 days at 4°C. The slides were stained with Delafield's hematoxylin and eosin after photographical development following the application of emulsion.

5. Induction of spawning and artificial insemination

The eggs of the brittle-star Amphipholis kochii were shed by temperature shock: The female brittle-stars were kept in a finger bowl (ca. 250 ml) filled with sea water at 20-25°C and then placed in a refrigerator at 4°C for 3 hours or more. When the sea water temperature in the bowl fell to 4°C, the cold sea water was replaced by warm sea water at 20-25°C. After a time lag of 30-40 min, the female brittle-stars spawned. The spawned eggs were then inseminated in sea water with low concentrations of spermatozoa (10^{2}-10^{3} cells/ml). Only when all or the vast

majority of eggs cleaved normally (an indication of monospermic fertilization) after 1.5 hours of culture at 23°C, were the eggs used for this study.

6. Culture of embryos and larvae

Embryos and larvae were reared in the sea water filtered through a 0.45 μm Millipore filter and treated with antibiotics, penicillin G (100 units/ml) and streptomycin sulfate (1 mg/ml). The culture medium was gently stirred as in the case of the culture of echioplutei (Hinegardner, 1969), and was changed daily during the early development and every other day during the latter stage. The temperature of the medium was kept constantly at 23°C or 15°C. As a food for the larvae, laboratory cultured diatom Phaeodactylum tricornutum was served.

7. DNA synthesis in fertilized eggs

In order to examine the DNA synthesis in the fertilized eggs, the eggs were incubated in sea water containing ^{3}H-thymidine (1 μCi/ml), fixed with GA and OsO_4 at various times after insemination and embedded in Epon. Epon thick sections of the eggs were fixed on glass slides and treated for autoradiography. The autoradiograms were stained with toluidine blue.

8. Inhibition of meiosis

Colchicine and its derivative colcemid were used to arrest the nuclear division in meiosis. Colchicine (500 μg/ml) or colcemid (5 μg/ml) was added to the egg suspension at 30 min

preinsemination or 5, 15, 30 or 45 min postinsemination. The fertilized eggs were allowed to incubate for 60 min at 23°C, and aliquots were fixed for TEM at 5, 15, 30, 45 and 60 min postinsemination (cf., Text-Fig. 8).

Cytochalasin B (0.5 µg/ml) was used to inhibit the cytokinesis in meiosis, i.e., the polar body formation. Since cytochalasin B inhibits sperm penetration into egg cytoplasm (cf., Schatten and Schatten, 1981), it was added to the egg suspension at 2 min postinsemination.

III. RESULTS

A. Ultrastructure of the gonads of *Amphipholis kochii* and *Ophiura sarsii*

1. General morphology of the gonads

The general morphology of the gonads in the two brittle-stars is very similar, so that the following descriptions are applicable to both species. The gonads in the disk are little sacs attached to the coelomic wall of the bursae, arranged in a row (Figs. 1A and B). There are 80-130 gonads in an individual and their maturity are concordant with one another. The gonad originates from the genital rachis (Fig. 2B), which is entirely enclosed by the genital coelomic sinus (GCS) and the genital hemal sinus, as is the case of other ophiuroids (Smith, 1940; Patent, 1976). Details of these sinuses will be described in the next section (A-2). In immature gonads, a large lumen, where post-spawning residual bodies are present, is observable at the central portion of the gonad, but it is gradually occupied by gametogenic cells as gonad maturation proceeds (Figs. 1C and 2A; cf., Figs. 16 and 17). In the testis, zonation of spermatogonia, spermatocytes and spermatozoa together with spermatids can be recognized (Figs. 1C and D). Mature spermatozoa gather to form large clusters in the lumen of the central portion of the testis (Fig. 1C). The somatic cells in the testis known as amoeboid cells are usually found during the formation assembly in the sperm mass (Fig. 1E). In the ovary, oogonia, small oocytes and large oocytes are present at the basal part, proximal part and

distal part of the ovary, respectively (Figs. 2A and B). We are able to find amoeboid cells in the ovary, although they are sometimes not distinguishable from the follicle cells.

2. Ultrastructure of the gonadal wall

a. Gonadal wall of Amphipholis kochii

The gonadal wall can be divided into two parts, an outer sac and an inner sac, in accordance with Walker's (1974) definition for the asteroid gonadal wall.

Outer sac: The outer sac of the gonadal wall consists of three units: a visceral peritoneum, a connective tissue layer covered with basal laminae, and the outer epithelium of the GCS (Fig. 3A).

The visceral peritoneum possesses flagella which are scattered sparsely on its free outer surface (Fig. 3A). There are no collar-like projections around the flagellum (Fig. 3B). The cells of the visceral peritoneum are composed of an irregular ellipsoidal nucleus with a long axis parallel to the outer surface of the visceral peritoneum, and of a cytoplasm containing a small number of mitochondria, lipid bodies and free ribosomes. Nerve processes and longitudinal muscle fibers are observable in the visceral peritoneum (Fig. 3A).

The connective tissue layer is covered by a basal lamina measuring 50 nm in thickness (Fig. 3A) and we are able to see electron-lucent ground substances, collagen fibers and cells

scattered freely in this layer (Fig. 3A).

The morphology of the cells that form the outer epithelium of the GCS is similar to that of the visceral peritoneum, except for the absence of the flagella and muscle fibers (Fig. 3A).

The GCS is narrow and the outer and inner epithelium are colosely contiguous to each other at many places (Fig. 3A). There are no structural elements in the GCS.

Inner sac: The inner sac is also composed of three units: the inner epithelium of the GCS, the genital hemal sinus covered with basal laminae, and a germinal epithelium (Fig. 3A).

The cellular components of the inner epithelium of the GCS resemble those of the visceral peritoneum. However, the muscle fibers run circularly, unlike the longitudinal fibers in the visceral peritoneum (Figs. 3A and C). The muscle fiber consists of thick and thin myofilaments measuring 30 nm and 8 nm in diameter, respectively (Fig. 3C). Nerve processes are also found in the inner epithelium of the GCS. They contain membrane-bound granules measuring 60 nm to 130 nm in diameter (Fig. 3C). These seem to be neurosecretory granules.

In the genital hemal sinus, we are able to recognize a large number of fine fibrous and granular materials, which are probably nutrients, a few collagen fibers and occasional hemal cells. The large cytoplasm of the hemal cells possesses abundant nutritive bodies (Fig. 3A).

The germinal epithelium comprises the gametogenic cells and the somatic cells known as the amoeboid cells. The amoeboid cells are usually found among the gametogenic cells or in the

central portion of the gonad and form a large assembly there (Fig. 1E). Occasionally we are able to see them make close contact with the genital hemal sinus (Figs. 3A and D). The amoeboid cells in the testes seem to be able to ingest the spermatozoa with phagocytic action (Fig. 4).

b. Gonadal wall of Ophiura sarsii

The gonadal wall is separable into an outer and inner sac (Fig. 5A), as is the case of A. kochii (cf., Fig. 3A).

Outer sac: The outer sac consists of a visceral peritoneum, a connective tissue layer covered with basal laminae, and the outer epithelium of the GCS (Fig. 5A).

The nucleus of the visceral peritoneal cell is irregular ellipsoidal and contains a thick mass of heterochromatins (Fig. 5A). The flagella are scattered sparsely on the free surface of the visceral peritoneum (Fig. 5A), as in A. kochii. The flagellated cells, however, possess collar-like projections around the flagellum (Fig. 5B), unlike A. kochii (cf., Fig. 3B). These flagellated cells have been called flagellated-collar cells by Walker (1979). Nerve processes and longitudinal muscle fibers are also present in the visceral peritoneum (Fig. 5C).

The connective tissue layer is mainly composed of electron-lucent ground substances, collagen fibers and cells scattered sparsely (Fig. 5A).

The outer epithelium of the GCS is similar to the visceral peritoneum. However, the flagella and muscle fibers are absent

in this layer, although the nerve processes are present (Fig. 5A).

The GCS is relatively broader (Fig. 5A) than that of A. kochii (cf., Fig. 3A).

Inner sac: The inner sac consists of the inner epithelium of the GCS, a genital hemal sinus covered with basal laminae, and a germinal epithelium (Fig. 5A).

The structure of the inner epithelium of the GCS resembles that of the visceral peritoneum. Circular muscle fibers are present (Fig. 5D), in place of the longitudinal muscle fibers found in the visceral peritoneum (Fig. 5C).

Abundant nutrients and hemal cells are observable in the genital hemal sinus (Fig. 5A). The hemal cells possess a large cytoplasm that includes many nutritive bodies (Fig. 5A). The nucleus of the hemal cell is ovoid and is provided with a thick mass of heterochromatins located mainly along the nuclear envelope (Fig. 5A).

The germinal epithelium comprises the gametogenic cells and the amoeboid cells. The amoeboid cells are sometimes in close contact with the genital hemal sinus (Fig. 5E). The phagocytic ability of the amoeboid cells in O. sarsii is also suggested (Fig. 5F).

3. Ultrastructure of spermatogenesis

a. Spermatogenesis in Amphipholis kochii

In order to examine the whole process of spermatogenesis, the testes during February to April were observed, since all kinds of spermatogenic cells are observable in these testes (cf., annual reproductive cycle of A. kochii; RESULTS, B-1)

Spermatogonium

The spermatogonium, 7 μm in diamter, has a large oval nucleus of about 5.5 μm along the greater axis and 4 um along the shorter (Fig. 6A). One or two nucleoli are usually found in the nucleus (Figs. 6A and 7A). The cytoplasm contains ovoid or tubular mitochondria, Golgi apparatus and two centrioles proximal or distal in situation. The mitochondria scattered in the cytoplasm show no particular distribution (Fig. 6A). The Golgi apparatus is usually located near the centrioles (Figs. 6A and B). The proacrosomal vesicles makes its appearance in the spermatogonial stage (Figs. 6C and 7A). The proacrosomal vesicle is represented as a membrane-bound coarse accumulation of fine granules (Figs. 6D and 7B). The Golgi apparatus found near the proacrosomal vesicle seems to be a contributor for the vesicle formation (Figs. 6D and 7B). The distal and proximal centrioles are perpendicular to each other, and both of them are located in the peripheral cytoplasm (Figs. 6A and B). A striated fibrous rootlet extending inward from the distal centriole is observable (Fig. 6B). Besides these organella, well-developed endoplasmic reticula, numerous free ribosomes and occasional multivesicular

bodies are also found (Figs. 6 and 7). The spermatogonium also contains electron-dense materials present either near or in contact with the nuclear envelope (Fig. 6A). These materials seem to be similar to the amorphous materials described in the echinoid germ-line cells (Houk and Hinegardner, 1981). Desmosome-like junctions joint the spermatogonia (Fig. 7B).

Spermatocyte

The primary and secondary spermatocytes are not distinguishable in feature probably because none of the morphological chracters differ from each other. The spermatocyte measures about 5 μm in diameter. The nucleus being about 3.5 μm is more condensed than that in the spermatogonium, but the density and distribution of the mitochondria, Golgi apparatus, centrioles and rootlet are similar to those found in the spermatogonium (Fig. 8A; cf., Fig. 6A). Several proacrosomal vesicles are found near Golgi apparatus (Fig. 8B). The electron-dense materials found either near or in contact with the nuclear envelope of the spermatogonia are not detected in this stage. The formation of a flagellum extending from the distal centriole begins in the spermatocytic stage. The desmosome-like junctions found between the spermatogonia are still observable during this stage.

Spermatid

The early spermatid, about 3 μm in diameter, has a circular nucleus measuring about 2.5 μm in diameter (Fig. 9A). The chromatin granules embedded in homogeneous matrix are aggregated

heterogeneously. During spermiogenesis, condensation of the chromatin is accelerated, leaving several nuclear vacuoles, and the circular nucleus becomes ellipsoidal in shape (Figs. 9A-D). The cytoplasm is confined to the posterior region of the cell, where the mitochondria reduce in number and gather to form a single doughnut-shaped mitochondrion in the mature spermatozoon (Figs. 9D-F). The developed endoplasmic reticula found during the previous stages are much reduced in this stage.

The proximal and distal centrioles remain perpendicular to each other in the early spermatid as during the previous stages (Fig. 9A), but in the later spermatids and mature spermatozoon the axis of the proximal centriole lies at an angle of about 30° from that of the distal one (Fig. 9E). The rootlet accompanied with the distal centriole disappears completely in the spermatid, and instead, a centriolar satellite complex associates the distal centriole. In the centriolar satellite region, nine spoke-like satellites emanate from the dense matrix of the distal centriole and bifurcate into secondary spokes (Fig. 10A). In transverse section through a proximal tip of the central tubules of the flagellum, nine Y-shaped connectives are found between the flagellar membrane and the peripheral tubules of the flagellum (Fig. 10B).

The desmosome-like junctions still remain in the early spermatids, but later they disappear, and intercellular bridges take a function to join the spermatids. The intercellular bridges are short and cylindrical, being marked by an annular thickening on the cytoplasmic side of the plasma membrane (Fig. 10C).

The proacrosomal vesicles fuse to form an acrosomal vesicle

in the early spermatid (Fig. 11A). At first, the acrosomal vesicle is found at a caudal part of the cell (Fig. 9A), but during spermiogenesis it is transported to the anterior portion of the cell (Fig. 9B). During this movement, a shallow indentation of the nucleus, which becomes an acrosomal fossa in the further stage, is formed beneath the acrosomal vesicle (Fig. 9B). Between the acrosomal vesicle and nucleus fibrous materials are usualy found (Fig. 11B). These materials seem to be precursors of the periacrosomal layer. The acrosomal vesicle contains electron-dense fine granules and the vesicle membrane bulges out at the anterior apex of the vesicle, producing an electron-lucent space between the membrane and the mass of the granules (Figs. 11B and C). The acrosomal granule looks like denser at the apex of the vesicle, although condition of its density differs slightly in sections (Figs. 11B and C). The vesicle membrane surrounding the basal half of the acrosome is coated with electron-dense material (Fig. 11B and C). As spermiogenesis proceeds, the indentation at the apex of the nucleus becomes deeper to form a cup-shaped acrosomal fossa (Figs. 9B, C and 11B, C).

Spermatozoon

The spermatozoon of Amphipholis kochii belongs to a typical primitive type defined by Franzen (1970).

The acrosomal vesicle, being hat-shaped, is completely bounded by a limiting membrane and measures 0.35 μm at the height of the crown and 0.55 μm in breadth at the brim (Fig. 11D). It contains fine granular substances whose condensation is denser at

the crown than at the brim (Fig. 11D). The electron-lucent space of the acrosomal vesicle in the mature spermatozoon is much thinner than that in the spermatid (Figs. 11B-D). In the basal area of the acrosomal vesicle, electron-lucent disk is not observable in the present species, whereas it is present in the ophiuroid, Ophiopholis aculeata, and the asteroids, Asterias forbesi and Ctenodiscus crispatus (Summers et al., 1975). The limiting membrane of the acrosomal vesicle at the brim is coated with electron-dense material (Fig. 11D). The periacrosomal layer is made of fine fibrous materials. A part of it is specialized into a fibrous tuft beneath the acrosomal vesicle, where the vesicle is slightly indented upward and an electron-lucent space is formed (Fig. 11D). This specialization of the periacrosomal material at the base of the acrosomal vesicle has been reported in other echinoderms (Hagiwara et al., 1967; Mabuchi and Mabuchi, 1973; Tilney et al., 1973; Summers et al., 1975; Hylander and Summers, 1975; Colwin et al., 1975; present study, next section), and it has been generally thought to be the center for the polymerization of G-actin into F-actin in order to elongate the acrosomal process during the acrosome reaction (Mabuchi and Mabuchi, 1973; Tilney et al, 1973 and 1978; Tilney, 1976 and 1978).

The nucleus measures about 1.5 μm along the antero-posterior axis and 2.3 μm in width, being highly condensed with several nuclear vacuoles (Fig. 9F). As well as the anterior pole of the nucleus, the posterior one is slightly indented to form a centriolar fossa (Fig. 9F). The single doughnut-shaped mitochondrion, about 0.8 μm in height and 1.8 μm in width, has a central cavity which houses the centrioles (Figs. 9E and F).

The flagellum being about 90 μm in length and 0.3 μm in diameter is composed of the ordinary 9+2 structure (Fig. 9F). It extends posteriorly at an angle of about 30° from the antero-posterior axis of the acrosome and nucleus (Fig. 9D). The flagellar membrane frequently expands laterally and these lateral expansions are roughly alighned with the central tubules in transverse section (Fig. 9F). These lateral expansions have also been found in other brittle-stars Ophiocoma nigra (Hylander and Summers, 1975), Ophiura sarsii (present study, next section) and in many fishes (Afzelius, 1978).

b. Spermatogenesis in Ophiura sarsii

As noted in MATERIALS AND METHODS, O. sarsii were collected during the season from April to September. During this season, the maturity of the testes, as well as ovaries, varied extensively according to individuals and showed no distinct seasonal fluctuations, suggesting an absence of a distinct annual reproductive cycle in this species. Thus, irrespective of whether the animals were collected at different months, only those testes with all kinds of spermatogenic cells were used.

Spermatogonium

The spermatogonium is distinguishable from other kinds of spermatogenic cells by their nuclear morphology: the nucleus is large, comprising patches of condensed chromatins scattered throughout the nucleoplasm and one or two prominent nucleoli (Figs. 12A and B). The cytoplasm of the spermatogonia contains

small, randomly distributed mitochondria (Figs. 12A and B), two centrioles situated perpendicular to each other (Fig. 12C), Golgi apparatus usually found near the centrioles (Figs. 12A-C), a striated rootlet associated with the distal centriole (Fig. 12D), and abundant ribosomes. It should be noted that proacrosomal vesicles produced by the Golgi apparatus are already observable in the spermatogonia (Figs. 12A and E). The proacrosomal vesicles are membrane-bound coarse accumulations of fine granules (Fig. 12E). The membrane of the proacrosomal vesicle appears more electron-dense than that of other ordinary vacuoles. The spermatogonia also contain electron-dense materials with or without surrounding membrane (Fig. 12B). Perhaps these materials are specific to the germ-line cells as suggested in the previous section (3-a, p.21). The adjacent spermatogonia are jointed by desmosome-like junctions (Fig. 12A).

Spermatocyte

The spermatocyte has a more condensed nucleus than that of the spermatogonium (Fig. 13A). The cytoplasm of the spermatocyte contains the same organella found in the spermatogonia (Figs. 13A and C). The formation of the proacrosomal vesicles are still detectable in the spermatocyte (Figs. 13A and B). The flagellum makes its appearance in the spermatocytic stage (Fig. 13C). The desmosome-like junctions found between the spermatogonia can still be observable during this stage (Fig. 13A).

Spermatid

The nucleus of the early spermatid consists of condensed

chromatins which are aggregated heterogeneously (Fig. 14A). During spermiogenesis, the condensation of the chromatins is accelerated, leaving several decondensed region known as nuclear vacuoles (Figs. 14B and C). In concord with the condensation of the chromatins, the nucleus alters its shape, from circular to ellipsoidal (Figs. 14A-C). The cytoplasm is confined to the posterior region of the spermatids where the scattered small mitochondria gather and fuse to each other, forming a single doughnut-shaped mitochondrion (Figs. 14A and B). The proacrosomal vesicles fuse to form an acrosomal vesicle (Fig. 14D). The acrosomal vesicle of the early spermatid is found in the caudal portion of the cell (Fig. 14A); during spermiogenesis it is transported to the anterior portion of the cell (Figs. 14B and C). During this movement, the homogeneous contents of the acrosomal vesicle differentiate into an electron-dense and an electron-lucent region (Fig. 14E). Close to the acrosomal vesicle on the side of the electron-lucent region, we are able to find a dense plate-like structure (Fig. 14E). The electron-lucent region becomes the basal region of the acrosomal vesicle in the subsequent stage (Figs. 14F and G). The axis of the acrosome has therefore been determined before sitting on the nucleus. The anteriorly transported acrosomal vesicle is situated in a small indentation of the nucleus (Fig. 14B). Between the indentation and the acrosomal vesicle, fibrous materials are present (Fig. 14F), and they surround the acrosomal vesicle, becoming periacrosomal layer (Fig. 14G). During spermiogenesis the indentation of the nucleus becomes deeper, especially at its

center, as well as wider (Figs. 14B and C); this is now called an acrosomal fossa. The spermatids are jointed to each other by intercellular bridges, suggesting that cytokinesis is incomplete during meiosis (Fig. 14H).

Spermatozoon

The spermatozoon comprises an ellipsoidal head, an ellipsoidal middle piece and a long flagellated tail (Figs. 15A and B), thus conforming to a typical primitive type (Franzen, 1970).

The head consists of the acrosome and the nucleus. The acrosomal vesicle is semi-circular and provided with a limiting membrane (Fig. 15A). The basal half of the acrosomal vesicle membrane is more electron-dense than that of the upper half (Fig. 15C). The contents of the acrosomal vesicle are electron-dense fine granules, which occupy the main part of the acrosome and are denser at the upper side, and an electron-lucent irregular region situated at the relatively basal part of the acrosome (Fig. 15C). Just beneath the acrosome, the dense plate-like structure is detectable (Fig. 15C), as has already been seen during the later spermiogenesis (cf. Figs. 14E-G). The periacrosomal layer is made up of fine fibrous materials (Fig. 15C). The nucleus is highly condensed with several nuclear vacuoles (Fig. 15A). The acrosomal fossa is deeper at its center (Fig. 15A). The posterior portion of the nucleus is also indented slightly (Fig. 15B): this indentation is known as a centriolar fossa.

The middle piece consists of a doughnut-shaped mitochondrion and some residual cytoplasm, including two centrioles (Fig. 15B). In contrast with the perpendicular orientation of the two

centrioles in the previous stages, the proximal centriole now lies at an angle of about 30° from the axis of the distal centriole (Fig. 15B). This reorientation of the proximal centriole has been detected during spermiogenesis. We are now able to observe a centriolar satellite complex associated with the distal centriole (Fig. 15B), instead of the rootlet present during the previous stages. It is made of nine spoke-like satellites and nine Y-shaped connectives: the former radiates from the dense matrix of the distal centriole and bifurcates into secondary spokes (Fig. 15D); the latter is detectable in the transverse section through the proximal tip of the central microtubules in the flagellum, and connects the peripheral microtubules and the flagellar membrane (Fig. 15E).

The flagellum is composed of an ordinary 9+2 structure (Fig. 15F). The flagellar membrane expands laterally and these lateral expansions are roughly alighned with the central microtubules of the flagellum when observed in a transverse section (Fig. 15F).

B. Analysis of the annual reproductive cycle of Amphipholis kochii

1. Gross features of the annual reproductive cycle

a. Annual changes of the gonad index

The annual reproductive cycle is well defined in the population of Amphipholis kochii at Abuta as shown in Text-Fig. 1. The gonad index, a rate of the gonad weight to the body weight, is higher in May-June and lower in July-October, being decreased

suddenly between June and July. No significant changes of the gonad index is found from July to October, but from November it increases constantly. Significances are found between the index values of the female and the male from March through May, with a confidence limit of 95% (t-test).

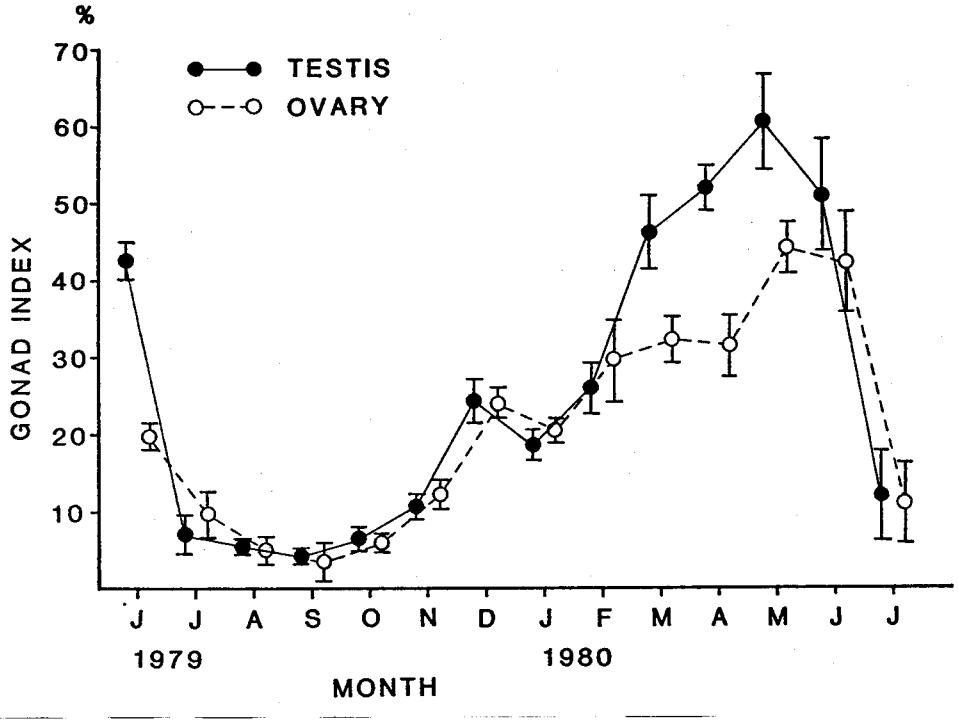

Text-Fig. 1. Monthly variations in the gonad index of Amphipholis kochii from June 1979 through July 1980. Average ± standard error.

b. Gametogenesis in annual reproductive cycle

For observing the annual cycle of the gonad, gonad condition is classified into the following six stages (Table 1):

Stage 0 (unsexuable): In this stage, the gametogenesis in both sexes rests after the shedding of the gametes, and the relict gametes degenerate into post-spawning debris in a short

phagocytic period (Fig.16A). The gonads are very small, and the sex cannot be determined even by histological observation. Along the inner side of the gonadal wall, occasionally some gonial cells without any sign of oogonia or spermatogonia can be seen (Fig. 16A).

Table 1. Characteristics of gonadal stages in Amphipholis kochii.

STAGE	OVARY			TESTIS		
	Color	Internal feature	The largest oocyte diameter	Color	Internal feature	% Of sperm
Stage 0 (Unsexuable)	Brown	Post-spawning debris	——	Brown	Post-spawning debris	——
Stage 1 (Recovering spent)	Orange	Previtellogenic oocytes	< 30 μm	Light yellow	Arrest of spermatogenesis	——
Stage 2 (Growth)	Dark orange	Vitellogenic oocytes	< 60 μm	Cream	Beginning of spermatogenesis	< 25 %
Stage 3 (Premature)	Dark orange	Cytoplasmic globules	< 80 μm	Milky white	Active spermatogenesis	25-50 %
Stage 4 (Mature)	Brown red	Cytoplasmic globules	80 μm ≦	Milky white	Large sperm mass	50 % ≦
Stage 5 (Spent)	Dark brown	Relict oocytes	——	Brown	Relict sperm	——

Stage 1 (recovering spent): The gonads are still small, but their color differs according to the sex, orange in the female and light yellow in the male. The lumen of the gonad still has a small amount of the post-spawning debris (Figs. 16B and 17A). The testis has spermatogonial layer without showing spermatogenesis in progress (Fig. 16B). Along the ovarian wall, previtellogenic oocytes being less than 30 μm in diameter can be found (Fig. 17A).

Stage 2 (growing): The cream-colored testis slowly starts spermatogenesis and the percentage of sperm in a cross section is under 25% (Fig. 16C). The ovary, dark orange in color, develops vitellogenic oocytes which attain 60 μm in diameter (Fig. 17B).

Stage 3 (premature): The testis is milky white in color and spermatogenesis is actively proceeded. Layers of spermatogonia and spermatocytes become thicker, and sperm mass is formed in the central region of the testis, with 25-50% sperm range in a cross section (Fig. 16D). The ovary is of a dark orange color, and the largest oocyte reaches 80 μm in diameter (Fig. 17C). Among the developing oocytes, cytoplasmic globules stained with both hematoxylin and eosin are found (Fig. 17D).

Stage 4 (mature): The gonads in both sexes attain their maximum volume. The testis is milky white in color, and has a large sperm mass. The percentage of sperm in a cross section reaches over 50%. On the contrary, the layers of spermatogonia and spermatocytes become thinner than those in the previous stage (Fig. 16E). The ovary now has turned brownish red, and its lumen is almost occupied by fully grown primary oocytes which are more than 80 μm in diameter (Fig. 17E). We can seldom detect the secondary oocytes or ova in the mature ovary. The cytoplasmic globules found in the premature stage are still observable. The meiotic figures of oogonia are also found in the mature ovary, as well as in the other ovaries.

Stage 5 (spent): The gonads are dark brown in the female and brown in the male, and have a small number of relics of oocytes or sperms in the lumen (Figs. 16F and 17F).

Text-Fig. 2 shows monthly changes of the relative proportion of the animals with each gonadal stage. In May-June, the number of the animals of stage 4 (mature) increases in both sexes, and in July those of stage 5 (spent) come to appear. These results indicate that the spawning period of Amphipholis kochii at Abuta is in June-July and occurs once a year. The period of stage 4 (mature) is shorter than that of other stages: this fact suggests that this species matures relatively acutely. The post-spawning resting period (stage 0) of the gonads lasts about one month around July and August.

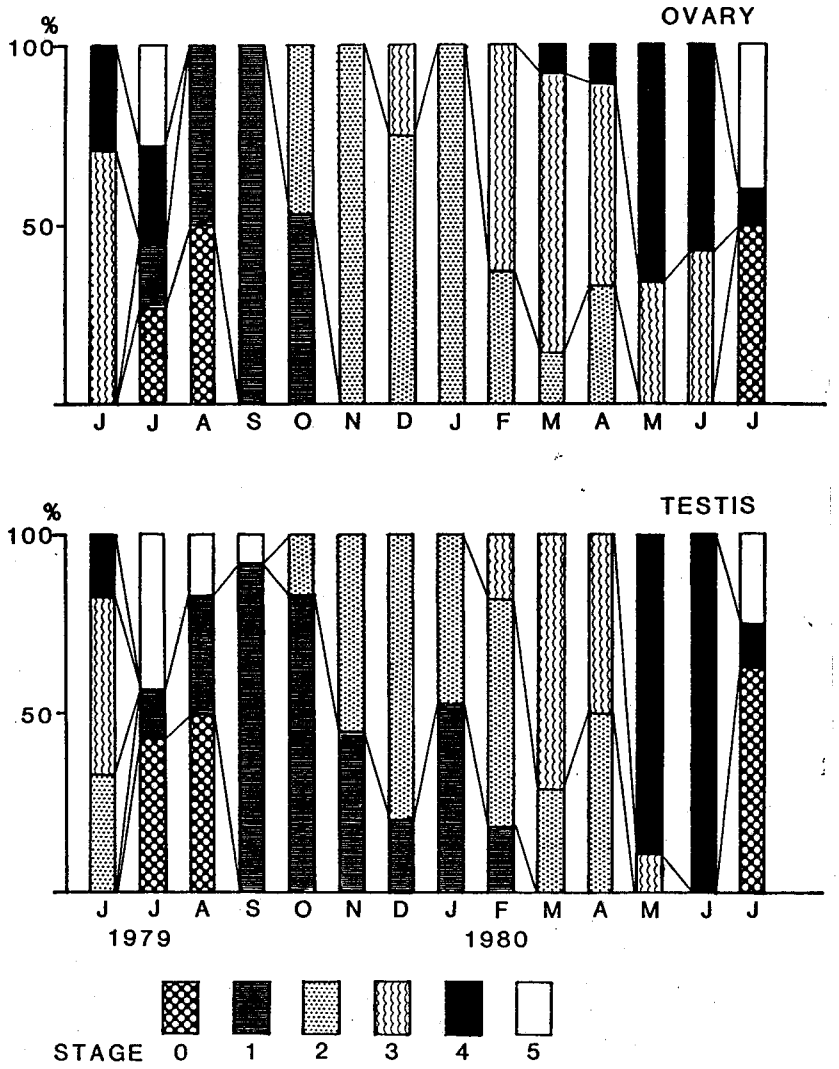

Text-Fig. 2. Monthly changes in relative proportion of the animals in each gonadal stage of Amphipholis kochii.

2. Analysis of the growth pattern of oocytes

a. Size-frequency distribution of oocytes

Monthly changes in the size-frequency distribution of the oocytes have been demonstrated by a frequency polygon method as shown in Text-Fig. 3. From these data, the following three particular features can be recognized on the oocyte growth in this species: 1) The entire population of oocytes does not grow as a single generation but grows as multiple generations. This is clearly indicated by the shape of polygon, which does not show a single peak but a diffused figure. 2) Small oocytes, under 20 μm in diameter, are present every month. 3) As maturation proceeds, the large oocyte population and the small oocyte population separate distinctly from each other; in other words, the number of medium-sized oocytes, 40-60 μm in diameter, is reduced.

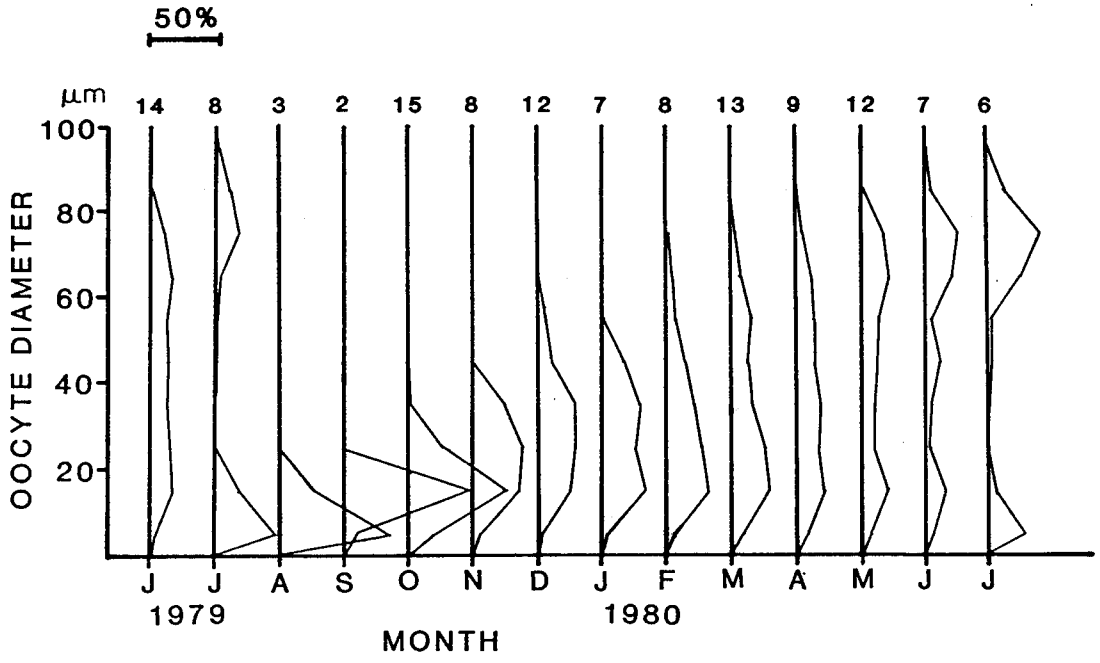

Text-Fig. 3. Monthly variations in the size-frequency distribution of oocytes in Amphipholis kochii.

b. Growth rate of the largest oocytes

Text-Fig. 4 shows the growth curve of the largest oocytes. Three stages are distinguishable on the growth pattern of the largest oocytes: a resting stage for about one month immediately after spawning, a fast growth stage from late August to December and a slow growth stage from December to June. The instantaneous relative growth rates of the oocytes in each stage are 0 in the resting stage, 0.031 in the fast growth stage, and 0.007 in the slow growth stage. These results indicate that the volumes of the oocytes increase about 3.1% per day in the fast growth stage and about 0.7% per day in the slow growth stage.

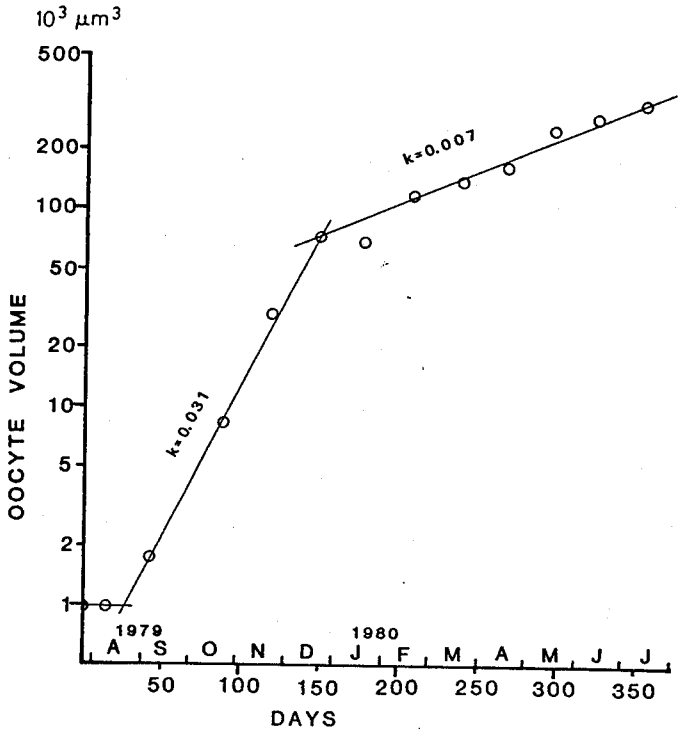

Text-Fig. 4. The growth curve for the largest oocytes in Amphipholis kochii. The instantaneous relative growth rate is shown as k.

3. Analysis of the annual testicular cycle

a. Annual cycle of spermatogenesis

Text-Fig. 5 gives monthly fluctuations in the number of the spermatogenic cells, the area of the amoeboid cell clusters and the sea water temperature at the collection site. As a whole, the following five phases are distinguishable in the annual testicular cycle.

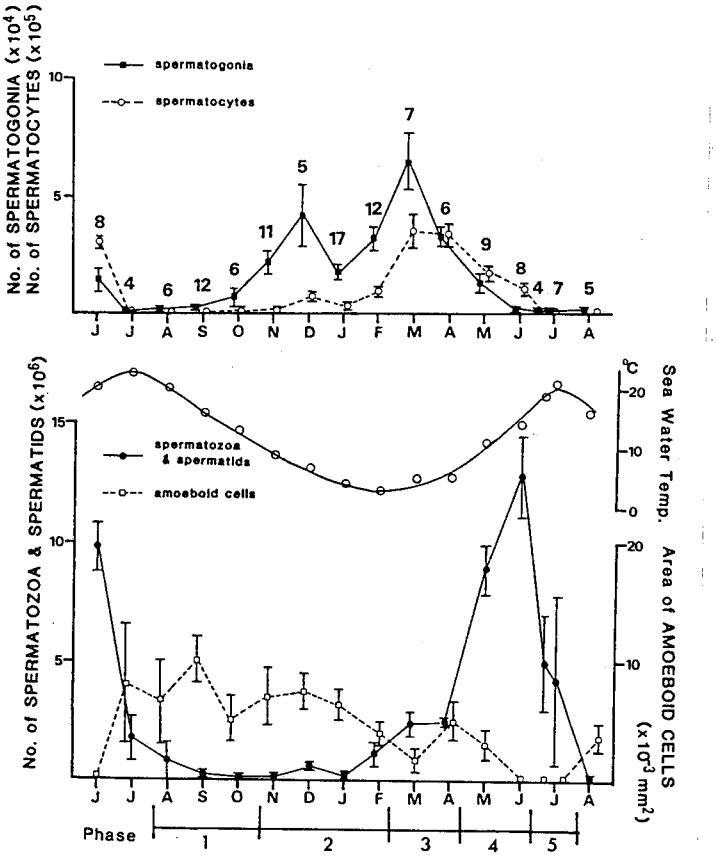

Text-Fig. 5. Monthly variations in the number of the spermatogenic cells and in the area of the amoeboid cell clusters in Amphipholis kochii. Changes of the sea water temperature at the collection site are also indicated. The numbers indicated over the upper graph show the number of the animals used each month. Average ± standard error.

Phase 1: August to October. Spermatogenesis is arrested, and the spermatocytes are absent. A small number of the relict spermatozoa are ingested by the amoeboid cells forming large clusters.

Phase 2: November to February. Spermatogenesis recommences, but the number of the spermatozoa is still very small. The clusters of the amoeboid cells are still large.

Phase 3: March to April. The spermatocytes increase abruptly in number, and the number of the spermatozoa and spermatids becomes larger than in phase 2, but much smaller than in phase 4. During this period, the sea water temperature at the collection site is still as low as during phase 2.

Phase 4: May to June. The sea water temperature rises rapidly. The number of the spermatozoa and spermatids increases abruptly, reaching maximum in June.

Phase 5: July. A sudden decrease in the number of the spermatozoa and spermatids occurs as a result of shedding (cf., B-1).

b. Influence of sea water temperature on spermatogenesis

Table 2 shows the result obtained from the experiment to examine the influence of sea water temperature on spermatogenesis. In February (phase 2), there was no significant difference in the number of the spermatogenic cells between the control and experimental groups. In April (phase 3) and May (phase 4), however, an apparent difference between the two groups was detected. In April, the number of the spermatozoa and

spermatids in the animals which had been kept at higher water temperature was significantly larger than that in the control ($P<0.05$, t-test). In May, the number of the spermatozoa and spermatids at the lower temperature was smaller than that in the control. It was also notable that in May the number of the spermatocytes at lower temperature was much larger than in the control ($P<0.1$).

These results indicate that the high water temperature accelerates the accumulation of spermatozoa and that the low water temperature inhibits it in phases 3 and 4. In phase 2, however, the water temperature has no influence on the accumulation of spermatozoa.

Table 2. Number of the spermatocytes and the spermatozoa with spermatids in *Amphipholis kochii*.

	Sea water temperature (°C)	No. of spermatocytes ($\times 10^4$)	No. of spermatozoa & spermatids ($\times 10^5$)
February	3 (control)	7.3 ± 2.0	10.1 ± 4.6
	13	4.7 ± 1.0	10.8 ± 3.1
April	5 (control)	33.6 ± 5.2	25.3 ± 1.4
	9	29.1 ± 6.7	62.6 ± 14.9
May	11 (control)	9.7 ± 3.5	93.5 ± 12.1
	4	41.4 ± 14.5	70.0 ± 31.5

c. Duration of spermatogenesis at various temperatures

Fig. 18 shows autoradiograms through the testis of the brittle-star Amphipholis kochii after the injection of ^{3}H-thymidine. Even 1 hour after the injection, the spermatogonia and spermatocytes were heavily labeled, but the spermatids and spermatozoa were not labeled at all (Fig. 18A). Several days after the injection, the spermatids or the spermatozoa became labeled (Figs. 18B and C). This feature shows the occurrence of a possible transformation of the labeled spermatogonia or spermatocytes to the spermatids or spermatozoa, in vivo. Finally, some labeled spermatozoa were found in the cytoplasm of the amoeboid cells (Fig. 18D). Under TEM, we could easily detect these spermatozoa ingested by the amoeboid cells after a phagocytic action (Fig. 4). Based upon these results, the duration necessary for the transformation from the spermatocyte to the spermatid or to the spermatozoon was determined by detecting the first appearance of the labeled spermatid or spermatozoon in the autoradiograms.

Table 3. Duration of spermatogenesis in Amphipholis kochii at various water temperatures.

	Nov		Dec	Jan	Feb		Mar		Apr		May		Jun	
Sea water temperature (°C) (collection site)	9		7	4	3		5		5		11		14	19
Sea water temperature (°C) (experiment)	9	16	7	4	3	13	5	18	5	9	11	4	14	19
Duration of spermatogenesis (days) spermatocyte - spermatid	7	5	10	18	22	5	14	3	14	7	7	22	5	3
spermatocyte - spermatozoa	14	7	14	22	30	10	18	5	18	14	10	30	7	5
spermatid - spermatozoa	7	2	4	4	8	5	4	2	4	7	3	8	2	2

Table 3 gives the duration of spermatogenesis at various temperatures as well as at the same temperature as that at the collection site. The duration of spermatogenesis faithfully correlated to the water temperature at which the animals had been kept. The same experimental temperature for cultivation yields the same duration of spermatogenesis irrespective of whether the animals had been collected at different months. In order to demonstrate the relationship between the duration of spermatogenesis and the water temperature more closely, the durations obtained in each month in Table 3 were plotted against the water temperature (Text-Fig. 6). As the water temperature became higher, the duration of spermatogenesis became shorter, and vice versa. A close relationship between the water temperature and the duration of spermatogenesis was more apparent in the early stage of spermatogenesis, from spermatocyte to spermatid, than in the later stage, from spermatid to spermatozoon or spermiogenesis.

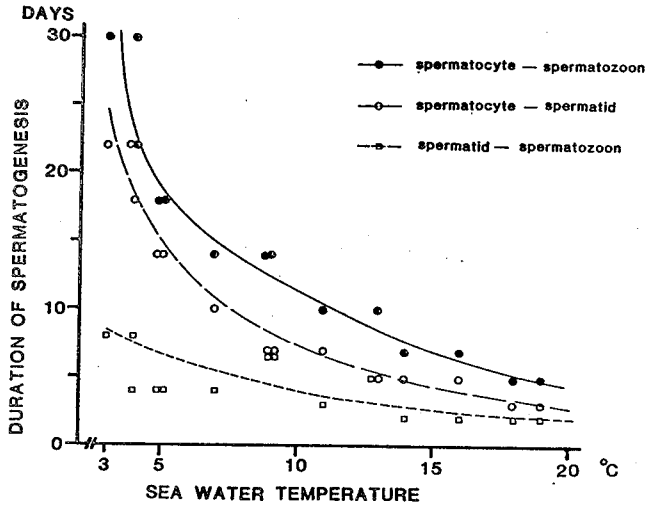

Text-Fig. 6. Correlation between the duration of spermatogenesis in Amphipholis kochii and the sea water temperature. The animals were reared at various experimental temperatures and the duration of spermatogenesis in each experiment was then measured.

d. Seasonal changes in the spermatocyte production rate (SPR)

To estimate the SPR per day throughout each month, the number of the spermatocytes (Text-Fig. 5) was divided by the duration of the spermatocytic stage (the duration from spermatocyte to spermatid, Table 3). Table 4 shows the seasonal changes in the SPR. It was apparent that the seasonal changes in the SPR had two distinct periods, one from November to February (phase 2) and the other from March to June (phases 3 and 4). The SPR in phases 3 and 4 was about six times higher than that in phase 2. The SPR was high in phase 3 though the sea water temperature was noticeably low at this season (Text-Fig. 5). In phase 2, however, the SPR was very low even at almost the same or higher water temperature than that in phase 3 (Text-Fig. 5). These results seemed to indicate clearly that the water temperature was not able to control the SPR.

Table 4. The spermatocyte production rate in Amphipholis kochii during the season from November to June.

	phase 2				Phase 3		Phase 4	
	Nov	Dec	Jan	Feb	Mar	Apr	May	Jun
No. of spermatocytes (x 10^4) (N)	1.4	7.2	3.3	9.2	34.6	33.6	17.3	9.7
Duration of spermatocytic stage (days) (D)	7	10	18	22	14	14	7	5
N / D	0.2	0.7	0.2	0.4	2.5	2.4	2.5	1.9
Spermatocyte production rate (per day)	1.0	3.5	1.0	2.0	12.5	12.0	12.5	9.5

The rate in each month is represented as a ratio to the rate obtained in November.

C. Development of Amphipholis kochii eggs in laboratory culture

1. The early embryogenesis

a. Shedding of gametes

The brittle-star Amphipholis kochii is forced to shed gametes by the temperature shock described in MATERIALS AND METHODS. The brittle-star spawns all eggs in one spawning. The number of the spawned eggs from one female is about 40,000. When both males and females are kept in a finger bowl and treated with the temperature shock, usually the males initiate to shed sperm, then the females spawn, suggesting that the shedding of sperm prior to that of eggs takes place in the field. The shedding posture is similar to those found in other ophiuroids; the disk is raised several centimeters above the bottom and contracts vigorously as shown in Fig. 19 (Mortensen, 1920; Olsen, 1942; Woodley, 1975; Hendler, 1977; Mladenov, 1979; Bowmer, 1982).

b. Fertilization

The spawned eggs are at the first meiotic metaphase and remain there until fertilized (Fig. 20A). The living unfertilized egg, about 90 μm in diameter, is opaque, brownish red and homolecithal (Fig. 20A). It is slightly heavier than sea water and tends to fall slowly to the bottom. A transparent jelly coat measuring 5 μm thick surrounds entirely the egg surface (Fig. 20A). The unfertilized eggs are fertilizable at least for 3 hours after the spawning. Naturally, fertilization occurs immediately after spawning of the eggs, because in natural conditions

the sperm is shed prior to the eggs. The early fertilization process during artificial insemination, photographed at one second intervals, is shown in Fig. 21. The fertilization cone begins to be formed within 5-10 sec postinsemination (Fig. 21A). In Fig. 21A, the acrosomal process, which must be in contact with the egg surface across the jelly coat, can hardly be detected by light microscopy in the present species. Within 15-20 sec postinsemination, the spermatozoon invades the egg cytoplasm through the fertilization cone (Figs. 21B-F). The spermatozoa which fail to contribute to fertilization remain attached to the jelly coat surface and are unable to enter the jelly coat (Fig. 22). The cortical reaction begins at the entry site of the fertilizing spermatozoon and spreads over the egg surface to the opposite pole within 10 sec of the beginning of the cortical reaction. As soon as cortical reaction occurs, the jelly coat overlying the sperm entry site begins to dissolve and completely disappears from the whole egg surface within a few minutes postinsemination (Fig. 22). When the jelly coat of the unfertilized eggs is removed by means of acid sea water (pH=5.0), these eggs are no longer fertilizable even in the normal sea water.

The fertilized egg is provided with a transparent fertilization membrane and a translucent hyaline layer (Fig. 20B). The hyaline layer around the living egg is 7-8 μm thick, much thicker than that in echinoids (about 1 μm thick: cf., McClay and Fink, 1982; Hylander and Summers, 1982). The first polar body formation occurs 15 min postinsemination at 23°C, and 15 min later, the second one is eliminated (Table 5). The first and second polar

bodies, measuring 3-4 μm in diameter, attach themselves to the outer surface of the hyaline layer or inner surface of the fertilization membrane, or sometimes they exist freely within the perivitelline space (Fig. 20C). Occasionally the first polar body subdivides into two, so that three polar bodies exist in the perivitelline space.

Details of the changes in the egg morphology before, during and after fertilization will be described in the next section (D-1).

Table 5. Timetable for the embryonic development of Amphipholis kochii egg cultured at 23°C or 15°C.

Stage	23°C	15°C
1st. polar body formation	15 (min)	——
2nd. polar body formation	30	——
2-cell	1.5 (hrs)	2 (hrs)
4-cell	2 1/6	3
8-cell	2 5/6	4
16-cell	3.5	5
Blastula	7-8	10-12
Hatch out	8.5	13-14
Gastrula	13-17	1 (days)
Spicule formation	21	1.5
Archenteron differentiation	1.1 (days)	1.8
Coelomic pouch formation	1.3	2
2-armed ophiopluteus	1.7	2
Left posterior coelomic pouch formation	1.7	3
4-armed ophiopluteus	2	4
Right posterior coelomic pouch formation	2.5	6.5
6-armed ophiopluteus	4.5	8.5
8-armed ophiopluteus	6	——
Hydrocoel formation	6.5	10.5
Hydrocoel 5-lobed	8.5	——
Metamorphosis (incipient)	12	——

c. Cleavage

Culture of the embryos and larvae was carried out at 23°C and 15°C. The following description of the embryonic development is based on the culture at 23°C. There is no significant difference between the two cultures, except for the developmental speed. The timetable of the two cultures is shown in Table 5.

Cleavage is holoblastic, equal and radial by nature. The first and second divisions cut the egg along the longitudinal axis, although the second cleavage plane is perpendicular to the first one (Figs. 20D and E). On and after the 4-cell stage, the arrangement of the blastomeres becomes irregular, because the blastomeres move so that they lie across each other (Figs. 20F and H). Occasionally some embryos, however, show the regular arrangement of 4- or 8-cell stage in the radial cleavage (Figs. 20E and G). As cleavage proceeds, the blastomeres are pushed between each other in all embryos, so as to occupy the least space as a whole, resulting in a very irregular arrangement of blastomeres. Successive divisions occur at approximately 40 min intervals, producing a spherical blastula provided with a narrower blastocoel than that in echinoid blastulae (Fig. 20I).

d. Blastula and Gastrula

The embryos hatch in the blastula stage. A swimming blastula just hatched is still surrounded by the thick hyaline layer which is thicker at the posterior pole (Fig. 20J). The primary mesenchymal cells in the vegetal polar wall immigrate into the blastocoel and occupy almost the whole space (Figs. 20J, K and 24A). Concurrently with the cellular migration, the spherical

swimming blastula becomes dorso-ventrally flattened and ellipsoidal in shape (Figs. 20J and K). It possesses many vacuoles in the animal polar wall (Figs. 20K and 24A); these vacuoles may serve as a floating device, as suggeted by Narasimhamurti (1933).

Gastrulation was achieved by an invagination of the wall cells at the vegetal pole (Figs. 20L and 24B). During the gastrulation, the embryo becomes more flattened dorso-ventrally and takes a shield shape (Fig. 20L). At this stage, the spicule formation begins in the primary mesenchyme (Fig. 23A). The spicule forms a tetraradiated shape (Fig. 23B), unlike that of other ophioplutei or echinoplutei in which the spicule is triradiated (cf. Mortensen, 1921). It consists of the rudiments of the antero-lateral, post oral, postero-lateral and body rods in the ophiopluteus (cf., Text-Fig. 7).

2. The latter embryogenesis

a. Ophiopluteus

The early 2-armed ophiopluteus has a helmet shape owing to the appearance of the first arms, the postero-lateral arms (Fig. 23C). In this larva, the archenteron differentiates into three parts; intestine, stomach and esophagus arranged from aboral to oral (Fig. 23C). The 4-armed ophiopluteus is successively formed by adding the second arms, the antero-lateral arms (Fig. 23D). In the 4-armed larva, expansion of the stomach occurs, after which the larva begins to eat diatom. At the age of 4.5 days, the larva bears its third arms, the post oral arms, resulting in a 6-armed ophiopluteus (Fig. 23E). Finally, in the larva at the

age of 6 days the fourth arms, the postero-dorsal arms, are formed (Fig. 23G). The postero-dorsal arms are supported by the postero-dorsal rods which are derived from the antero-lateral rods (Text-Fig. 7). The 8-armed ophiopluteus attains 350 μm in length along the antero-posterior axis without containing the length of the antero-lateral arms. The postero-lateral arms are most prominent in length as compared with the others and their rods are provided with a row of small spines (Text-Fig. 7). The larval skeletal system of A. kochii is very simple, without having any of the accessory rods described in other ophioplutei (Text-Fig. 7: cf., Mortensen, 1921).

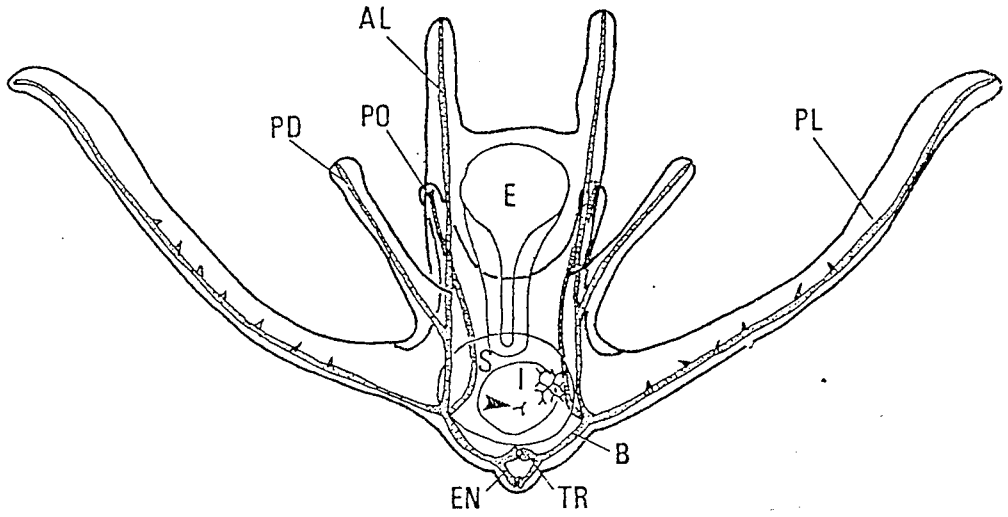

Text-Fig. 7. An 8-armed ophiopluteus of Amphipholis kochii showing a larval skeletal system. To avoid complexity, coeloms and other detailed structures are omitted. Dorsal view. Arrowheads indicate the spicules of adult skeletal system. AL, antero-lateral rod; B, body rod; E, esophagus; EN, end rod; I, intestine; PD, postero-dorsal rod; PL, postero-lateral rod; PO, post oral rod; S, stomach; TR, transverse rod.

b. Coelomic pouch differentiation

In the 2-armed ophiopluteus at the age of 1.7 days, the right and left coelomic pouches, which are derived from two outpockets of the archenteron (Fig. 24C), are found near the constricted region between the stomach and esophagus (Fig. 23C). The left coelomic pouch segregates into anterior and posterior coeloms in the 4-armed ophiopluteus (Fig. 23D), and the posterior one again segregates into a hydrocoel and a somatocoel in the 8-armed ophiopluteus (Fig. 24D). The left anterior coelom develops as an axocoel. The hydrocoel expands anteriorly along the stomach and differentiates into 5-lobes at the side of the esophagus (Figs. 23H and 24E). On the other hand, the right coelomic pouch is not well-developed, unlike the left one, although it separates into an anterior and a posterior coelom in the 4-armed ophiopluteus (Figs. 23F and 24D).

c. Metamorphosis

The following morphological changes of the ophiopluteus occur during the metamorphosis of A. kochii: The spicule of the adult skeletal system forms a triradiated shape and is bifurcated, forming a network of spicules (Text-Fig. 7). The anterior part of the larva shrinks and the larval arms degenerate except for the postero-lateral ones (Fig. 23I). The 5-lobed hydrocoel begins to surround the esophagus for forming the further pentaradial water canal system of the adult brittle-star. The anterior part of the larva becomes a young brittle-star which bears several podia (Fig. 23I). Finally, the last larval arms, the postero-lateral arms, degenerate.

D. Electron microscopic analysis of the monospermic fertilization process of *Amphipholis kochii*

1. The early fertilization process in normal eggs

a. Unfertilized eggs

On the egg surface, we are able to see two kinds of investments; one is a jelly coat and the other is a vitelline coat. The jelly coat of GA-fixed material appears to be irregular aggregations of filaments which bear many nodules (Figs. 25A and B). It is completly removed by the treatment with acid sea water (pH=5.0). The vitelline coat is a dense network of filaments measuring 50 nm in width (Fig. 26A). In contrast to the jelly coat materials, these filaments are not removed in acid sea water. This suggests that the jelly substances do not share to make these filamentous structures. Moreover, dithiothreitol (10 mM, 1 min treatment), a reagent known to remove the echinoid vitelline coat (Epel, et al., 1970), is capable of removing these filaments (Fig. 26B), justifying the identification of them as vitelline coat substances.

The vitelline coat observed by TEM is very thin, about 5 nm thick, when stained with uranyl acetate and lead citrate (Fig. 27A), but it is about 20 nm thick when stained with RR (Fig. 27B). The thickness of the vitelline coat stained with RR is not changed after removal of the jelly coat in acid sea water (pH= 5.0), indicating that materials stained with RR are derived not from jelly substances but from the original constituents of the vitelline coat. Thus RR staining seems near the thickness of the

fresh vitelline coat. The vitelline coat of A. kochii is widely separated from the ooplasmic surface in many places, like in other ophiuroids (Holland, 1979) but unlike in many echinoids (Afzelius, 1956; Endo, 1961; Anderson, 1968; Millonig, 1969). Vitelline posts, which have been observed by RR stain beneath the vitelline coat of echinoids (Kidd, 1978), could not be detected beneath the vitelline coat in A. kochii.

Electron microscopy of the egg plasma membrane shows characteristic meandering folds known as microplicae (Figs. 26A and B; Andrews, 1976), which are 0.2-0.3 μm high (Fig. 28B). In TEM of the egg cortex, the membrane-bound cortical granules, measuring 1.5-2.0 μm in diameter, are arranged in several layers (Fig. 28A), except at the animal pole where they are in a monolayer. Although individual cortical granules show varing internal structure, in general the contents are divided into two parts (Fig. 28B): a peripheral fibrous (PF) and a central fibrous (CF) part; the CF part consists of two components differing in electron density. The PF and CF parts are clearly distinguishable after PA-CrA-silver staining (Fig. 28C): Silver deposition is dense on the PF part, but slight if at all at the CF part. These observations indicate a differential distribution of polysaccharides in the cortical granule.

b. Acrosome reaction

As described in the previous part (A-2), an intact spermatozoon of A. kochii consists of an ellipsoidal head and a middle piece with a long flagellum (Figs. 29A and C). The acrosome reaction is probably induced by the contact of the spermatozoa to

the jelly coat surface. The length of the acrosomal process of an acrosome-reacted spermatozoon is about 5 μm (Figs. 29B and 30A), which corresponds to the thickness of the jelly coat surrounding the egg of this species (cf., Fig. 20A). As observed in many invertebrates (cf., Dan, 1967), the acrosome reaction involves an opening of the acrosomal vesicle by a fusion between the outer acrosomal membrane and the overlying sperm plasma membrane (Fig. 29D), followed by a projection of the basal region of the acrosomal vesicle (Fig. 29E) and the formation of the acrosomal process (Fig. 29F). The acrosomal process consists of bundle of fine filaments. In this species, the acrosomal fossa, the depression of the anterior surface of the nucleus, remains unchanged even after the acrosome reaction (Figs. 29F and 30B). This stands in contrast to the rapid disappearance of the acrosomal fossa in other non-echinoid spermatozoa, such as the asteroids (Dan and Hagiwara, 1967), the ophiuroids (Hylander and Summers, 1975), and the holothuroids (Colwin et al., 1975). We are able to observe fine fibrous structures in the acrosomal fossa after formation of the acrosomal process (Fig. 29F).

c. Sperm incorporation

Within 5-10 sec postinsemination, a spermatozoon that comes in contact with the jelly coat surface produces an acrosomal process (Fig. 30A). The process passes across the jelly coat. By a fusion of the membrane of the acrosomal process and the egg plasma membrane (Fig. 30B), the fertilizing spermatozoon invades the egg cytoplasm through the fertilization cone (Figs. 30C and

D). The fertilization cone contains free ribosomes and microfilaments (Fig. 30C). The fusion site of the fertilization cone and spermatozoon enlarges, and within 10-20 sec postinsemination, the sperm nucleus, middle piece mitochondrion and centrioles are completely incorporated into the egg cytoplasm (Figs. 30C and D). The bundle of fine filaments that supports the acrosomal process is also found within the fertilization cone (Fig. 30D).

d. Cortical reaction

An elevation of the vitelline coat from the egg surface is observable at the leading edge of the spreading cortical reaction (Fig. 31A). Opening of the cortical granules at the ooplasmic surface is resulted from a fusion of their own membrane with overlying egg plasma membrane (Fig. 31A), and the contents are discharged underneath the vitelline coat. At the site of opening of the cortical granules, we are unable to find apparent vesicular structures which would indicate multiple fusions of the cortical granule membrane with the egg plasma membrane (Anderson, 1968; Millonig, 1969; Holland, 1979). Therefore, the fusion of the membranes probably occurs only at one place in each granule. The cortical granules which are located deeply away from the egg surface are discharged by a fusion of their own membrane and the adjacent cortical granule membrane (Fig. 31C). Most of the PF material of the cortical granules disperse throughout the space between the ooplasmic surface and the vitelline coat and cause an increase in osmotic pressure of the perivitelline fluid (Figs. 31B and C). This fact is probably important for further elevation of the vitelline coat or developing fertilization membrane

because the infiltration of water into the perivitelline space is produced. Some of the PF material attaches to the elevated vitelline coat (Figs. 31B and C). The CF material, together with a small amount of surrounding PF material, remains near the egg surface and forms a hyaline layer during the subsequent stage (Fig. 31C). Not all the cortical granules release their contents; some of them remain undischarged. These undischarged cortical granules can be detected in the embryonic cells at least until the gastrula stage, as is also the case of the echinoids (Afzelius, 1956; Runnström, 1966; Anderson, 1968).

e. Fertilization membrane formation

The vitelline coat filaments are woven into a thin sheet immediately after their elevation from the egg surface (Fig. 32A). As the cortical granules are discharged, much fibrous materials are found being attached to the inner surface of the vitelline coat sheet (Fig. 32B). Judging from the TEM observation on the cortical granule exocytosis (cf., Figs. 31B and C), these fibrous materials probably correspond to the PF materials of the cortical granules. At 1 min postinsemination, the sheet takes on a trilaminated structure composed of dense outer and inner laminae with an intermediate translucent lamina (Fig. 33A), and is transformed into the fertilization membrane. Although the exact location of the vitelline coat substance within the fertilization membrane is uncertain, they are probably located at the upper region of the membrane, since the outer surface of the developing fertilization membrane does not show apparent changes

during the membrane transformation. This suggests that the materials derived from the cortical granules are added only to the inner surface of the elevated vitelline coat. At 2 min postinsemination, further PF material is added to the inner surface of the developing fertilization membrane, forming additional layers (Fig. 33B). Finally, within 3 min of insemination, the fertilization membrane is completely formed and persists till hatching. The fully-formed fertilization membrane, about 40 nm thick, consists of three layers (Fig. 33C): an outer layer, about 16 nm thick, which has already formed at 1 min postinsemination, is composed of the three laminae already described; a middle layer, about 8 nm thick, has an electron-lucent appearance; an inner layer, about 16 nm thick, consists of the same three laminae as the outer layer. The TEM image of the ophiuroid fertilization membrane resembles that of the echinoids (Afzelius, 1956; Endo, 1961; Anderson, 1968; Inoue and Hardy, 1971). A surface replica of the fully-formed fertilization membrane shows that its outer surface is very smooth, while its inner one possesses meandering grooves (Fig. 32C). We are unable to find any crystalline structures and triangular projections on the outer surface as well as the inner one of the fertilization membrane (Fig. 32C), in contrast with the echinoid fertilization membrane (Inoue et al., 1967; Inoue and Hardy, 1971; Chandler and Heuser, 1980).

f. Hyaline layer formation

After the dischage of the cortical granules, the ooplasmic surface bears many long slender microvilli (Fig. 34A), probably owing to the excess membrane produced by fusion of the cortical

granule membrane and egg plasma membrane during the discharge of the cortical granules. The released CF materials of the cortical granules fuse with one another near the egg surface and form the hyaline layer within 5 min postinsemination (Figs. 34B and C).

2. The latter fertilization process in normal eggs

a. Development of male pronucleus

The spermatozoon that penetrated the egg cortex rotates in various angles in different individuals (Figs. 35A and B). This random rotation has also been reported in other animals (Longo and Anderson, 1969b and 1970), whereas in the echinoids Arbacia punctulata, Strongylocentrotus purpuratus, and Lytechinus variegatus rotation is always 180° (Longo and Anderson, 1968; Schatten and Mazia, 1976; Schatten, 1981), although in the echinoid Clypeaster japonicus, the angle is random (Hamaguchi and Hiramoto, 1980). Dispersion of the sperm chromatin begins at a lateral portion of the spermatozoon (Figs. 35A and B), and it ends at the acrosomal fossa (Figs. 35C and D). Following chromatin dispersion, many vacuoles gather around the nucleus (Figs. 35C and D). These vacuoles elongate and surround the nucleus (Figs. 35C and D), forming the male pronuclear envelope. The ellipsoidal nucleus of the spermatozoon becomes circular as the chromatin disperses (Figs. 35A-E).

At 15 min postinsemination, at the stage of first polar body elimination, the incorporated spermatozoon develops into a male pronucleus, which is surrounded by a nuclear envelope with nuclear pores (Figs. 35E, 36A and Text-Fig. 8). At this time, the

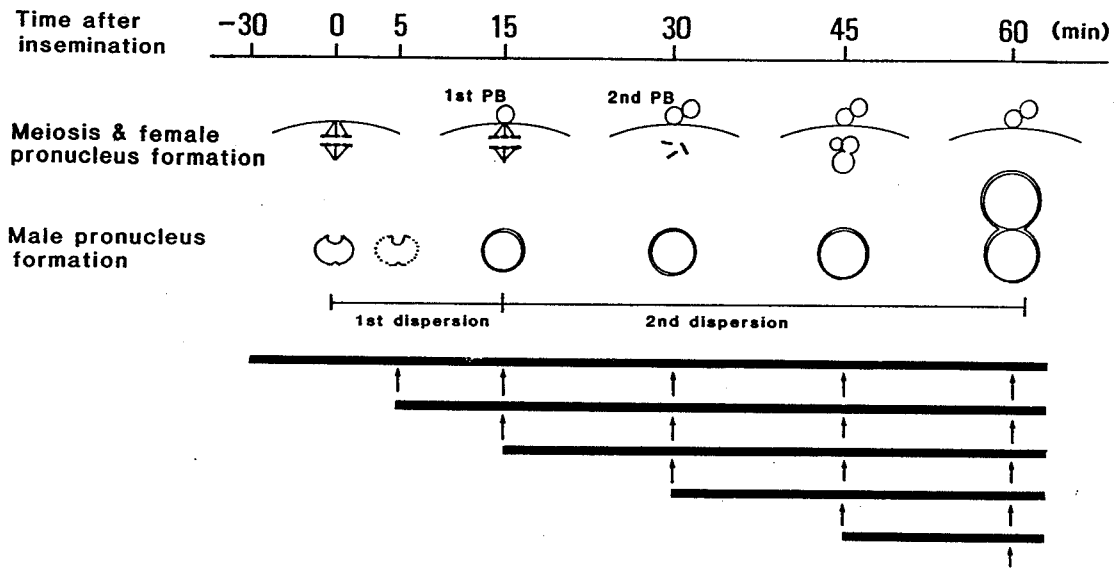

Text-Fig. 8. Schematic representation showing the schedule of meiosis and male and female pronuclear development in Amphipholis kochii. Bars indicate the treatment with colchicine or colcemid. Aliquots of the fertilized eggs were fixed at the times indicated by arrows.

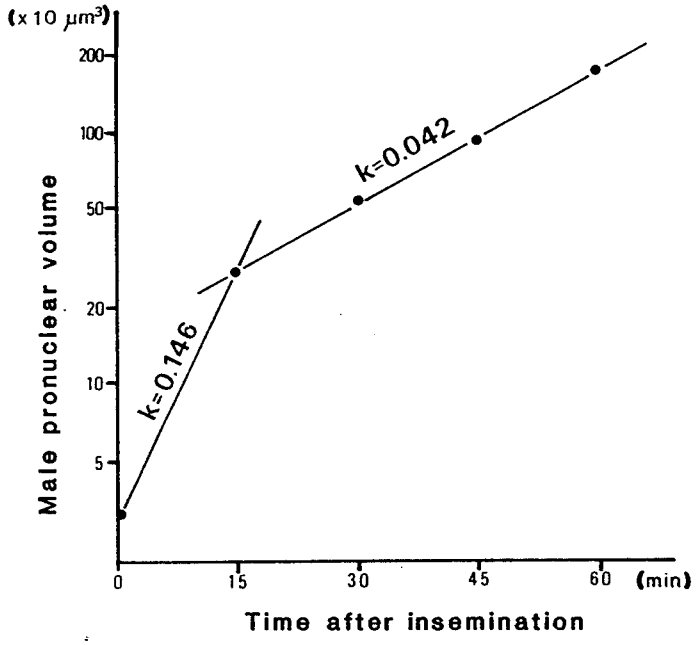

Text-Fig. 9. The development pattern of the male pronucleus in Amphipholis kochii. The instantaneous relative growth rate is indicated as k.

pronucleus is relatively small, and its density is high when compared to that just prior to fusion of pronuclei. The male pronucleus continues to develop, irrespective of meiosis and female pronucleus formation, and attains a diameter of 7.5 μm at the time of pronuclear fusion (60 min postinsemination)(Fig. 36B and Text-Fig. 8). When the volume of the male pronucleus is plotted semi-logarithmically vs time, the developing male pronucleus exhibits two distinct phases of the chromatin dispersion; the first phase (the first dispersion) before the formation of the male pronuclear envelope, 15 min postinsemination, and the second phase (the second dispersion) on and after that (Text-Figs. 8 and 9). The instantaneous relative growth rates of the first and the second dispersion are 0.146 and 0.042, respectively, indicating that the male pronuclear volume increases 14.6% per min during the first dispersion and 4.2% per min during the second dispersion.

The developing male pronucleus remains near the cortical region of the egg until its envelope has completely formed (Fig. 36A). It then gradually moves inward as astral fibers begin to develop (Fig. 36B). This observation is consistent with the suggestion that male pronuclear movement is due to propulsion by the sperm aster (Chambers, 1939; Allen, 1954; Longo and Anderson, 1968). The correspondence between male pronuclear movement and sperm aster formation has also been reported in recent observations based on differential interference microscopy (Hamaguchi and Hiramoto, 1980; Schatten, 1981). The sperm mitochondrion is observable in close proximity to the nucleus at least till the

male pronuclear envelope has completely formed (Figs. 35A-C and E), whereupon it breaks away from the nucleus during the inward movement of the male pronucleus.

Autoradiographic studies on the DNA synthesis revealed that in some eggs silver grains become to be found on the male pronucleus at 45 min postinsemination (Fig. 36D). Within 60 min postinsemination these grains are usually detected on the male pronucleus of all eggs examined. It may be said therefore that the onset of DNA synthesis is irrespective of fusion of male and female pronuclei, as suggested for the echinoid Arbacia punctulata (Longo and Plunkett, 1973).

b. Development of female pronucleus

The chromosomes during meiosis are not associated with membranous elements (Fig. 37A), whereas those after the meiosis become to be surrounded by vacuoles (Fig. 37B). The chromosomes decondense after meiosis and become partly surrounded by the nuclear envelope with nuclear pores (Fig. 37C). This membrane system may be derived from vacuoles previously associated with the chromosomes. The decondensing maternal chromosomes, so called karyomeres, fuse together, producing an irregularly shaped female pronucleus 45 min postinsemination (Figs. 36B and 37D). Finally, the irregular shape disappears and the female pronucleus becomes circular, measuring about 8 μm in diameter (Fig. 38A). During the formation of the female pronucleus, it moves inward to the central portion of the egg. Autoradiographic studies revealed that some developing female pronuclei begin to synthesize DNA at 45 min postinsemination (Fig. 36C and D). Within 60

min postinsemination the female pronucleus in all eggs examined synthesize DNA (Fig. 36E), irrespective of fusion of the female and male pronuclei.

c. Fusion of pronuclei

The male and female pronuclei encounter each other in the central region of the egg. They are distinguishable by their size and electron density: The male pronucleus is smaller and more dense than the female (Figs. 36E and 38A). Occasionally, nuceoli are found in the pronuclei (Fig. 38B). Neither pronucleus possesses nucleoplasmic projections (Fig. 38A), dissimilar to those prominently seen in other animals (cf., Longo, 1973). Fusion of the pronuclei occurs 60 min postinsemination (Text-Fig. 8). This process appears to be brought about by a disintegration of both pronuclear envelopes into vesicles, producing a internuclear bridge between the male and female pronuclei (Fig. 38B). This manner of pronuclear fusion contrasts with observations in echinoids where it occurs as a result of the fusion of inner laminae of pronuclear envelope following the fusion of their outer laminae (Longo and Anderson, 1968). The internuclear bridge becomes prominent and large, as fusion proceeds (Figs. 39A and B). In the early developing zygote nucleus, we were able to identify paternal and maternal chromatins owing to their different densities (Fig. 39A). As the internuclear bridge becomes large, however, the density of the developing zygote nucleus becomes uniform within a short time (Figs. 39B and C), suggesting rapid intermixing of the paternal and maternal chromatins. This

is different from the case of the echinoid where a denser part, probably derived from the paternal chromatins, is found even in the circular zygote nucleus (Longo and Anderson, 1968), suggesting slower intermixing of chromatins. In autoradiographic studies, we are able to find the silver grains on the zygote nucleus, indicating the DNA synthesis on it (Fig. 36F).

3. Male and female pronuclear formation in the eggs treated with the meiosis inhibitors

a. Meiosis and female pronucleus formation in the treated eggs

Table 6 shows the meiosis and the female pronucleus formation in the eggs treated with the meiosis inhibitors. The meiosis, including nuclear division (separation of chromosomes) and cytokinesis (formation of polar bodies) was completely inhibited when colchicine or colcemid was applied to the eggs before the completion of the meiosis. In these meiosis-inhibited eggs, the maternal chromosomes neither decondensed nor formed karyomeres surrounded by the nuclear envelope (Figs. 40A and 41A). On the other hand, when the same treatment was applied to the eggs which had completed the meiosis, the female pronucleus was formed on schedule; the maternal chromosomes deconsensed to form karyomeres, and their fusion yielded the female pronucleus (Fig. 41B). The resulted female pronucleus showed a DNA synthesis within 60 min postinsemination (Fig. 40B), as in the case of the normal eggs.

Although the cytokinesis (the polar body formation) was completely inhibited in cytochalasin B treated eggs, the nuclear

division (separation of the chromosomes) occurred on schedule (Fig. 42A). The female pronucleus was formed on schedule in these cytokinesis-inhibited eggs (Figs. 42B and C). It was however large as compared with the female pronucleus in the normal eggs. This is probably due to the fact that excess chromosomes which must be discarded from the egg during meiosis also participate in the formation of the female pronucleus (Figs. 42B and C). The large female pronucleus synthesized DNA on schedule (Figs. 42C and D).

Table 6. Meiosis and female pronucleus formation in Amphipholis kochii eggs treated with meiosis inhibitors.

Time after insemination (min)	15	30	45	60
Normal events	1st. polar body formation	2nd. polar body formation	Female pronucleus formation	DNA synthesis
Colchicine or colcemid treatment from (min postinsemination)				
-30	-	-	-	-
5	-	-	-	-
15	+	-	-	-
30	+	+	+	+
45	+	+	+	+
Cytochalasin B treatment	-	-	+	+

+; normal events
-; events inhibited

b. Male pronucleus formation in the treated eggs

Table 7 indicates the male pronucleus formation in the eggs treated with the meiosis inhibitors. Penetration of the spermatozoon into the egg cytoplasm occurred normally even in the presence of colchicine or colcemid, as reported in other animal eggs (cf., Schatten and Schatten, 1981). In all eggs, the incorporated sperm nucleus became to decondense at first in its lateral portion (Fig. 43A). The nucleus swelled considerably and became circular (Fig. 43B), showing the first dispersion process as those in the normal eggs (cf., Text-Fig. 8). The same process was detected in the eggs which had been treated as early as 30 min preinsemination. However, further changes in the nucleus (the second dispersion process) were not detectable when the eggs were treated before 5 min postinsemination: The sperm nucleus did not wear the nuclear envelope and showed no remarkable dispersion (Fig. 43C). These nuclei were unable to synthesize DNA (Fig. 40C). When the treatment was made from 15 min postinsemination, at which time the first polar body is extruded from the eggs, the male pronucleus previously formed stopped the growth and showed degeneration of the nuclear envelope; the envelope took an appearance of vesicular aggregations (Fig. 43D). This seems to be a reversed process of the nuclear envelope formation (cf., Figs. 35C and D). Such nucleus completely took off the nuclear envelope within 45 min postinsemination (Fig. 43D). No synthesis of DNA was detected in these nuclei. On the other hand, when the eggs were treated after 30 min postinsemination, at which time the second polar body is eliminated, the preexisting male pronucleus continued to grow on schedule (Fig. 43F) and initiated the

DNA synthesis within 60 min postinsemination (Fig. 40D). This resembles the process observed in the case of the normal eggs. Fusion of the male and female pronuclei was however inhibited in all of treated eggs. This is probably due to the inhibition of male and female pronuclear movements mediated by microtubules, as well demonstrated in echinoid eggs (cf., Schatten and Schatten, 1981).

In contrast to the case of colchicine and colcemid, cytochalasin B had no effect on the male pronucleus formation: The male pronucleus was formed on schedule in the cytochalasin B treated eggs, and the resulted male pronucleus was able to synthesize DNA within 60 min postinsemination (Fig. 42D). Fusion of the pronuclei also occurred in the cytochalasin-treated eggs.

Table 7. Male pronucleus formation in Amphipholis kochii eggs treated with meiosis inhibitors.

Time after insemination (min)	5	15	30	45	60
Normal events	Initiation of chromatin dispersion	Chromatin dispersion with nuclear envelope	Further dispersion	Further dispersion	DNA synthesis
Colchicine or colcemid treatment from (min postinsemination)					
-30	+	±	-	-	-
5	+	±	-	-	-
15	+	+	-	-	-
30	+	+	+	+	+
45	+	+	+	+	+
Cytochalasin B treatment	+	+	+	+	+

+; normal events
-; events inhibited
±; chromatin dispersion occurs but nuclear envelope not formed

IV. DISCUSSION

A. Ultrastructure of the gonads of *Amphipholis kochii* and *Ophiura sarsii*

1. Ultrastructure of the gonadal wall and a possible mechanism for gonad nutrition

The present observation shows that the fine structure of the gonadal wall of the two brittle-stars, *A. kochii* and *O. sarsii*, is similar, except only for the morphology of the flagellated cells present in the visceral peritoneum. The facts observed in the present study therefore seem to be applicable to the general feature of the gonadal wall of the ophiuroids.

To date, there have been no published fine structural observations on the gonadal wall of the ophiuroids, although Davis treated it briefly. According to Davis' unpublished data cited by Atwood (1973), the gonadal walls of the ophiuroids and the asteroids are similar, but the muscle fibers in the outer epithelium of the GCS are lacking in the ophiuroids while being present in the asteroids. The present study confirms these findings. It also describes the different cellular character of the gonadal wall of the ophiuroids and the asteroids: the flagella found on the visceral peritoneum of the former are much smaller in number than those of the latter; the muscle fibers in the inner epithelium of the GCS are circular in the former, but they are longitudinal in the latter (Tangapregassom and Delavault, 1967; Bruslé, 1969; Walker, 1974, 1976 and 1979).

In the echinoids, the nutrients are believed to be reserved mainly in the gonads (Lasker and Giese, 1954; Giese *et al.*, 1959;

Pearse and Giese, 1966). The particular nutrient transport for gametogenesis is therefore not necessary for this echinoderm. On the other hand, it has been suggested that the nutrients are mainly reserved in the pyrolic caeca for the asteroids (Farmanfarmaian et al., 1958; Anderson, 1966; Giese, 1966; Mauzey, 1966; Rao, 1966; Kim, 1968; Crump, 1971; Nimitz, 1971 and 1976; Ferguson, 1975a and b; Jangoux and Van Impe, 1977; Barker, 1979; Harrold and Pearse, 1980) and in the stomach for the holothuroids (Farmanfarmaian, 1963). In these echinoderms the nutrients for gametogenesis must therefore be transported from the reservoir to the gonad. In the ophiuroids, however, we are uncertain where the nutrients are mainly reserved. Schechter and Lucero (1968) have reported though that the cytoplasm of the stomach cells of the ophiuroid Ophiuroiderma panamensis is heavily laden with lipid bodies and represents a very abundant nutritive storehouse. Moreover, our preliminary data proves that the stomach wall of A. kochii becomes thinner as the gametogenesis proceeds. Judging from these observations, it is likely that in the ophiuroids the nutrients are reserved mainly in the stomach and transported to the gonad during the process of gametogenesis.

As for the route for the nutrient transport from the reservoir to the gonads, it has been thought that in the asteroids the coelomic fluid and hemal sinus participate in it (Ferguson, 1964a and b; Walker, 1979; Broertjes et al., 1980a and b). In the ophiuroids, the present autoradiographic observation on the testis that thymidine injected intracoelomically was absorbed into the testis within a short time (Fig. 18A) suggests that nutrients

such as thymidine are transported from the coelomic fluid to the gonad through the gonadal wall. On the other hand, the present electron microscopic study shows that abundant nutritive materials and hemal cells containing many nutritive bodies are found in the genital hemal sinus (Figs. 3A and 5A). This suggests the nutritive transport to the gonad through the genital hemal sinus. These findings allow us to conclude that the coelomic fluid and/or hemal sinus is a route for nutritive transport to the gonad in the ophiuroids, as in the case of the asteroids.

With regard to the problem of how the nutrients transported to the gonads are distributed over the germinal epithelium, the somatic cells found in the germinal epithelium have been noticed by several authors, and it has been suggested that these somatic cells serve as a vehicle for distribution of the nutrients over the germinal epithelium (Walker, 1979 and 1980; Bickell et al., 1980). The present observations that the somatic cells in the ophiuroid gonads (the amoeboid cells) have a phagocytic role (Figs. 4 and 5F) also suggest a qualification of the amoeboid cells as a vehicle of nutritive distribution. Moreover, the present finding of a close contact of the amoeboid cells with the genital hemal sinus (Figs. 3A, D and 5E), through which the nutrients may be transported, proves that these cells play an important role in the distribution of te nutrients over the germinal epithelium.

In conclusion, we can summarize the gonad nutrition of the ophiuroids as follows: the nutrients mainly reserved in the stomach wall are transported to the gonad through the coelomic fluid and/or hemal sinus and are distributed over the germinal

epithelium by the amoeboid cells scattered there.

2. Ultrastructure of the spermatogenesis: The precocious formation of the acrosome and its significance

The present observations show that, irrespective of the difference in their taxonomic families, the entire process of the spermatogenesis of A. kochii and O. sarsii are very similar; the findings obtained may be regarded as indicating the general characteristics of ophiuroid spermatogenesis.

The basic features of ophiuroid spermatogenesis resemble those of other echinoderm spermatogenesis. As reviewed by Bickell et al. (1980), at least three characteristics of the acrosome formation are common to all echinoderms: 1)the acrosome is derived from Golgi apparatus; 2) the acrosome is formed at caudal end of the cell; 3) the vesicle membrane of the acrosome has a region of more osmiophilic characteristics. These three characteristics are also recognized during the ophiuroid spermatogenesis, suggesting that these are very basic feature in the echinoderm spermatogenesis.

The remarkable fact about ophiuroid spermatogenesis is that the early stage of acrosome formation, i.e., the production of the proacrosomal vesicles, is initiated in the spermatogonia, unlike that of many other animals, where it observed first in the spermatids (cf., Welsch and Storch, 1976). The beginning of the acrosome formation in other echinoderms hitherto reported is in the spermatogonia in the holothuroids (Atwood, 1974; Pladerollens and Subirana, 1975), in the primary spermatocytes in the crinoids (Bickell et al., 1980) and in the spermatids in the echinoids

(Longo and Anderson, 1969a). Although the beginning of the acrosome formation in the asteroids is presumed to occur in the spermatids, the exact time of beginning is still uncertain, because only spermiogenesis has been observed for the asteroids (Dan and Shirakami, 1971). Our unpublished observation reveals that in the asteroid Asterina pectinifera the proacrosomal vesicles are already found in the primary spermatocytes. This therefore allows us to conclude that the acrosome formation in the echinoderms is initiated at the latest in the primary spermatocytes, with the exception of the echinoids.

The presence of proacrosomal vesicles in the early stage of spermatogenesis has also been recognized in the mussel Mytilus edulis. It has been suggested that the male germ cells of Mytilus have failed to evolve the necessary machinery for the rapid production of acrosomal materials at a specific later period of spermatogenesis. This is deduced from the fact that well-developed endoplasmic reticula are absent in the spermatids (Longo and Dornfeld, 1967). The present study also shows the absence of developed endoplasmic reticula in the spermatids of A. kochii and O. sarsii. The same property suggested in the germ cells of Mytilus may therefore occur in these echinoderms.

The precocious formation of the acrosome might be related to the short duration of spermatogenesis. This may result in an insufficient production of the acrosomal material during spermiogenesis. The similar phenomenon has also been reported in the mussel, in which the acrosome formation is initiated in the spermatogonia (Longo and Dornfeld, 1967). In this molluscs, the

duration of spermatogenesis is also relatively short (Kelly et al., 1982). In the sea urchin, however, the spermatogenesis is short in length (Holland and Giese, 1965), although the acrosome formation is initiated in the spermatids (Longo and Anderson, 1969a). The contrasting situation between the sea urchin and the brittle-star together with mussel may be explained by the fact that the acrosome of the sea urchin is small when compared with that of the brittle-star and mussel (Dan, 1967). Although the spermatogenesis of the sea urchin is of a short duration, it may be sufficient for the production of such a small acrosome during the spermatid stage.

B. Annual reproductive cycle of Amphipholis kochii

1. Gross features of the annual reproductive cycle

Among echinoderms, detailed studies on the reproductive cycle have been made for echinoids by many authors; little is known about the cycle in asteroids, holothuroids, crinoids and ophiuroids (cf., Holland et al., 1975). In the ophiuroids, several authors briefly reported observations on the gonadal state at a few different times of the year (Smith, 1940; Olsen, 1942; Fell, 1946; Boolootian, 1966). To date, a complete observation of the annual reproductive cycle of the ophiuroids has been restricted to the following species; Gorgonocephalus caryi (Patent, 1969), Amphipholis chiajei (Fenaux, 1970), Ophioderma longicauda (Fenaux, 1972), Ophiura albida, O. texturata (Tyler, 1977), Ophiocoma echinata, O. pumila, O. wendti, O. aethiops, O. alexandri, Ophioderma appressum, O. brevicauduma, O. cinereum,

O. rubicundum (Hendler, 1979), Ophiura ljungmani (Tyler and Gage, 1980), Ophiacantha bidentata (Tyler and Gage, 1982) and Ophiomuseum lymani (Gage and Tyler, 1982).

The characteristics of the gametogenesis in Amphipholis kochii are somewhat different from most of those found in echinoids. It has already been known that, in the sequential changes of the gametogenesis in the echinoids, two distinct stages are recognizable in the annual reproductive cycle (Yoshida, 1952; Fuji, 1960a; Pearse, 1970): In the first stage, the nutrient accumulation accompanied by increases of the gonadal size and in the gonad index takes place; nutrients are reserved in the cytoplasm of the nutritive phagocytes (somatic cells in echinoid gonads) as spherical bodies of several types. In the second stage following the nutritive build-up, gametogenic cells begin to grow consuming the reserves in the nutritive phagocytes. In the annual reproductive cycle of A. kochii, however, we detected none of the two stages mentioned above either by examination of gonad index or by histological observation. This is presumably due to the fact that the gonad of the ophiuroids does not have any nutritive reservoir cells comparable to the nutritive phagocytes of the echinoids (Smith, 1940; Patent, 1976). Unlike the echinoids, the nutrients are thought to be transferred continuously to the gonads in this species. A possible route for nutritive transport to the gonads has been discussed in the previous part (A-1).

Resting period in the annual reproductive cycle of echinoderms has been found by many authors, and its presence is usually

assumed to be a typical pattern in the echinoderms (Boolootian, 1966). In the basket-star Gorgonocephalus caryi, a clear resting period for about three months after spawning was described by Patent (1969). The post-spawning resting period can be also observed in A. kochii. It is however relatively short in length as compared with G. caryi. The resting periods of A. kochii and of the crinoid Comanthus japonica are very similar in that after spawning the gonad passes through a brief phagocytic stage and enters an unsexuable stage (post-spawning resting period) (Holland et al., 1975).

2. Growth pattern of oocytes

The fact that small oocytes are present throughout the year (Text-Fig. 3) suggests a constant production of oocytes through an annual reproductive cycle. This suggestion is justified by the observation that mitotic figures of oogonia are found through all the seasons. Futhermore the assumption explains why the size-frequency polygon does not show a single generation of oocytes. The reduction of the number of medium-sized oocytes is probably caused by the following two events: First, the growth of small oocytes is arrested, whereas that of medium-sized oocytes continues. Second, the medium-sized oocytes are selectively destroyed by somatic cells in the ovary or by autolysis. The cytoplasmic globules found in the premature or mature ovary (Fig. 17D) might originate from these destroyed oocytes.

Ordinary, the ovary of most echinoderms contains more than one oocyte generation. In several species the ovary possesses only single generation of oocytes. This is found in the

asteroids Asterias rubens (Schlieper, 1957) and Patiriella regularis (Crump, 1971), and the crinoids Comanthus japonica (Holland, et al., 1975). The occurrence of oocyte production throughout the year has been up to now poorly known in echinoderms with the exception of the echinoid Stylocidaris affinis, which has a similar size-frequency polygon to that in the present species (Holland, 1967). In S. affinis, oogonia are giving rise to primary oocytes throughout the annual reproductive cycle and, when the small oocytes grow to a diameter of 25-30 um, they are destroyed if large oocytes are present in the same ovary. Breaking down of oocytes in A. kochii appears to occur however only near the breeding season.

Up to the present time, ther are two reports on the oocyte growth rate in echinoderms exist; for the echinoid Strongylocentrotus purpuratus by Gonor (1973b) and for the crinoid Comanthus japonica by Holland et al. (1975). In S. purpuratus, the instantaneous relative growth rate is highest for medium-sized oocytes and not for small ones. In C. japonica, the oocytes grow rapidly at first but slowly later on. The pattern of oocyte growth in A. kochii is apparently diiferent from that of S. purpuratus; in A. kochii the growth rate is highest in small oocytes. In comparison with C. japonica, the pattern in A. kochii differs in the following point: The oocyte growth in A. kochii is clearly divided two successive stages, the first stage and the slow stage, while the oocyte growth rate in C. japonica changes gradually. Such a pattern of oocyte growth as described for A. kochii is not hitherto described in other echinoderms.

3. Annual testicular cycle and its control mechanisms

The present study demonstrates a close correlation between the duration required for the completion of spermatogenesis in the brittle-star A. kochii and the water temperature as an external environment, both under normal and experimental conditions. Seasonal changes in the annual testicular cycle and the factors controlling spermatogenesis are summarized in Text-Fig. 10. Based upon Text-Fig. 10, we suggest the following control mechanisms for spermatogenesis during phases 2 to 4. Phase 2: The sluggish accumulation of the spermatozoa in this phase is probably due to the low spermatocyte production rate. In this phase, the water temperature influences neither the accumulation of the spermatozoa nor the spermatocyte production rate (Tables 2 and 4). The water temperature should be not therefore contribute to the control of spermatogenesis during this phase. Phase 3: Owing

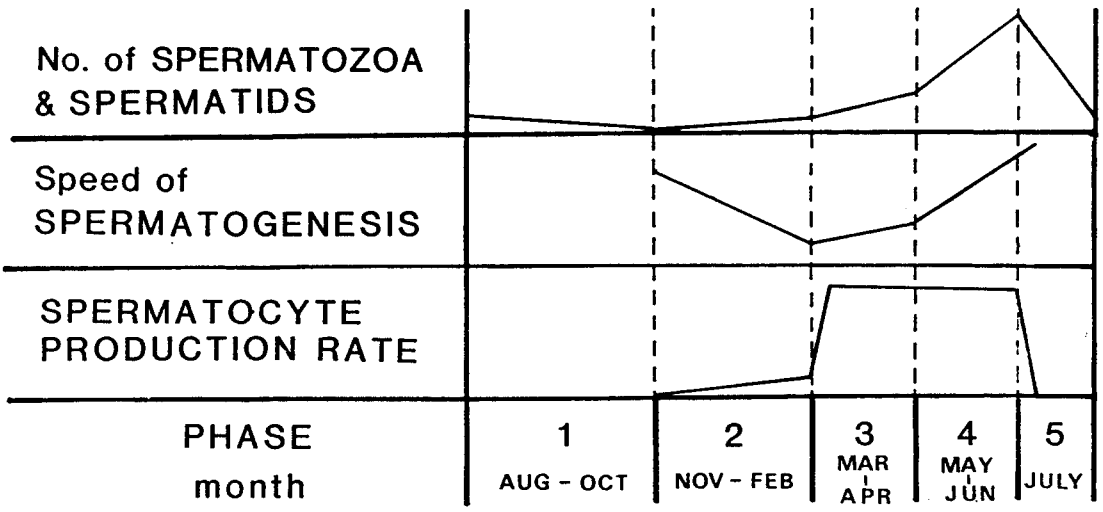

Text-Fig. 10. Seasonal tendencies in the number of the spermatozoa and spermatids, the speed of spermatogenesis and the spermatocyte production rate in Amphipholis kochii, summarized from Text-Fig. 5, Tables 3 and 4.

to the high spermatocyte production rate, the accumulation of the spermatozoa becomes active, but it is slower than that in the next phase. This situation is presumably due to the slow speed of spermatogenesis resulting from the low sea water temperature at this season (Text-Figs. 5 and 6). This explanation is consistent with the following experimental results: 1) the number of the spermatozoa grew larger when the animals were kept during phase 3 at a higher water temperature. 2) it decreased during phase 4 when the animals were kept at a lower temperature (Table 2). The increase in number of the spermatocytes in the animals kept at a lower temperature in phase 4 (Table 2) is therefore probably due to the slow speed of spermatogenesis caused by the low water temperature. Phase 4: The spermatocyte production rate is high and the speed of spermatogenesis is fast owing to the high sea water temperature, resulting in a rapid accumulation of the spermatozoa.

With respect to the sea water temperature as an external factor on the control of the annual reproductive cycle, the testicular cycle of A. kochii can be divided into two distinct periods: the temperature-insensitive period during the season from November to February (phase 2) and the temperature-sensitive period from March to June (phases 3 and 4). The sea water temperature plays an important role as a key factor on spermatogenesis during phases 3 and 4, while other environmental factors such as photoperiod or food supply are likely to be key factor(s) on spermatogenesis during phase 2. Further studies are necessary to know the effect of day length or food supply on spermatogenesis, especially during phase 2.

Concerning the seasonal changes in the speed of spermatogenesis, Holland and Giese (1965) carried out an autoradiographic study on the testis of the echinoid Strongylocentrotus purpuratus, and obtained the result that the duration of spermatogenesis remained constant throughout the annual reproductive cycle. An explanation for Holland and Giese's result, in contrast with that of this study, might be that they measured the duration of spermatogenesis at relatively constant water temperatures throughout the annual cycle.

The possible participation of the somatic cells in the control of the spermatozoa production rate cannot be ignored. By means of an autoradiographic investigation, Holland and Giese (1965) revealed the ingestion of newly-formed spermatozoa by the somatic cells of the testis in the echinoid. The present study also demonstrates that amoeboid cells (somatic cells) in the testis of A. kochii are able to ingest the newly-formed spermatozoa as well as the relict ones by phagocytic action (Fig. 4). Judging from the presence of large clusters of the amoeboid cells during phase 2 (Text-Fig. 5), we might be allowed to assume that the phagocytic activity of the amoeboid cells upon the newly-formed spermatozoa contributes partly to a slow spermatozoa accumulation in phase 2.

The duration of spermatogenesis has been measured in various animal phyla; it is certain that marine invertebrates have a relatively high speed of spermatogenesis in comparison with mammals and insects (see Table 9 in Roosen-Runge, 1977). The present measurement also reveals that the spermatogenesis of the brittle-star is of a relatively short duration. Effect of the

short duration on the mode of the spermatogenesis has been discussed in relation to the beginning of the acrosome formation in the previous part (A-2).

It is very interesting to note that the duration of spermiogenesis appears to be independent of the sea water temperature (Text-Fig. 6). In this respect, it is worth to note that Egami and Hyodo-Taguchi (1967) reported no significant difference in the duration of spermiogenesis in the fish Oryzias latipes at 25°C and 15°C. These observations allow us to suggest that spermiogenesis mainly depends on internal factors, such as hormones (Botticelli et al., 1960; Schoenmakers, 1980; Schoenmakers et al., 1976 and 1977).

C. Gross features of the normal development of Amphipholis kochii eggs

1. The early process

To date, we have had no ophiuroid species available for developmental studies. It seems likely that this situation is mainly due to the lack of an effective method for artificial insemination. Stancyk (1973) succeeded in the establishment of the spawning induction method for Ophiolepis elegans. The embryo of O. elegans, however, does not grow to a typical ophiopluteus but to an abbreviated one. Thus, O. elegans can not be used for developmental studies of a typical ophiuroid species. The present study, however, reveals that for A. kochii the temperature shock method is very effective to induce spawning and obtain a typical ophiopluteus larva. It is therefore clear that A. kochii

is useful for developmental studies of a typical ophiuroid species.

In the ovary of A. kochii, we were unable to find secondary oocytes or ova even in the breeding season. Since the spawned eggs remain in the metaphase of the first meiotic division, oocyte maturation including the break down of the germinal vesicle and the entrance into the meiotic division occurs immediately before the spawning, probably during the time lag between the temperature shock and the spawning. A similar situation for oocyte maturation has been reported in the asteroid, in which oocyte maturation is induced by the neurosecretory system immediately before the spawning (cf., Kanatani, 1973). It is notable that the spawning of the asteroids induced by a gonad stimulating substance (GSS) from the radial nerve also has a time lag of similar duration to that observed after the temperature shock of the present study (Kanatani and Ohguri, 1966). This similarity implies that the temperature shock given for the spawning of A. kochii directly induces the nerve to release the GSS. However, it is still uncertain whether oocyte maturation and the spawning of the ophiuroids are under the control of the neurosecretory system as in the case of the asteroids, although Fontaine (1962) has shown the presence of the neurosecretory cells in the radial nerve of the ophiuroid.

The irregular arrangement of the blastomeres that observed in early cleavage stages of A. kochii egg has also been described in some other ophiuroids, such as Ophiopholis aculeata, Ophiothrix fragilis and Ophiura albida. It has been suggested that the

irregularity of the blastomere arrangement is induced to the hyaline layer which exercises pressure upon the embryonic surface (Olsen, 1942). The fertilization membrane- and hyaline layer-free embryos (denuded embryos) of A. kochii obtained by treating with Ca-Mg-free sea water shows no solid arrangement of the blastomeres (unpublished observation), as is the case of the denuded embryo of the asteroid (Dan-Sohkawa, 1976). It is therefore apparent that the hyaline layer plays important role in the arrangement of the blastomeres in the ophiuroid embryo. The irregular arrangement of the blastomeres has also been found in many mammals which have a thick hyaline layer (Gulyas, 1975).

2. The latter process

The manner of the development of some ophioplutei that has been described in detail is similar to each other, except for the fashion of the hydrocoel formation. The hydrocoel arises from the left anterior coelom in Ophiothrix fragilis (MacBride, 1907) and Ophiocoma nigra (Narasimhamurti, 1933) as is the case of many echinoplutei (cf., Hyman, 1955), but in Ophiopholis aculeata it is formed from the left posterior coelom (Olsen, 1942). In A. kochii, its formation is the same as that in O. aculeata. The difference may indicate that the plane of constriction of the left coelomic pouch varies in different species; this has also been noted by Hyman (1955).

As a rule, the larval spicules of the ophioplutei take a triradiated form as in the echinoplutei (cf., Mortensen, 1921). The tetraradiated spicule present in A. kochii is remarkable when compared with other reported ophioplutei. The triradiated

spicule in other ophioplutei consists of the antero-lateral, postero-lateral and body rods, and the post oral rods are formed in the later stage of embryonic development. In A. kochii, however, the post oral rod is formed at the same stage as that of the earlier three rods. This precocious formation of the post oral rod gives the spicule of A. kochii a tetraradiated shape and may be related to a relatively rapid development of A. kochii as compared with other typical ophioplutei (cf., Hendler, 1975). The simple skeletal system of this larva seems also to reflect the shortness in duration of of the embryonic development. stage.

D. Electron microscopic analysis of the monospermic fertilization process of Amphipholis kochii

1. Normal fertilization process

It has been known for some time that the acrosomal process of the non-echinoid echinoderms is much longer than that of the echinoids (Colwin and Colwin, 1955, 1956; Dan, 1954, 1975; Dan and Hagiwara, 1967). For example, in the ophiuroids Dan (1956) reported that the acrosomal process of Ophioplocus japonicus attained a length of 30 μm, in contrast with the echinoid acrosomal process measuring about 0.5 μm long. This difference has been explained by the inablility of the spermatozoa of the non-echinoids to enter the jelly coat, and therefore, the need of non-echinoids to possess an acrosomal process longer than the thickness of the jelly coat. The present study shows that the acrosomal process of A. kochii is only 5 μm long (Figs. 29B and

30A), much shorter than that of O. japonicus and other non-echinoids hitherto reported. However, the jelly coat of the present species is also very thin (5 μm thick; Fig. 20A), when compared with other non-echinoids, and it seems to correspond to the length of the acrosomal process, confirming the suggestion that in the non-echinoids the length of the acrosomal process is related to the thickness of the jelly coat.

The cortical granules of A. kochii are remarkable in two ways: first, they are arranged in several layers in the egg cortex, whereas they have a monolayer arrangement in many other animals; and, second, they are very large (1.5-2.0 μm in diameter; Fig. 28A) compared with those of other echinoderms (under 1 μm in diameter: cf., Guraya, 1982). With regard to the first point, Holland (1979) has reported that the cortical granules of the ophiuroid O. aculeata exist in multilayers. The present work confirmed this observation in another ophiuroid, A. kochii, suggesting that the multilayer arrangement of the cortical granules is a characteristic of ophiuroids in general. This arrangement of cortical granules in ophiuroids may be related to the thick hyaline layer in the ophiuroid eggs (7-8 μm thick in A. kochii and 2 μm thick in O. aculeata) than in other echinoderms (about 1 μm); the number of cortical granules arranged in a monolayer may not be able to supply sufficient material for formation of a thick hyaline layer. It is possible that the thick hyaline layer in A. kochii is also related to the second remarkable feature, the large size of the cortical granules; that is to say, large cortical granules may be necessary to supply sufficient material for the thick hyaline layer in this species. Thus

the multilayer arrangement and the large size of cortical granules in this species seem to be related to the thickness of the hyaline layer.

An interesting problem is how the contents of the cortical granules are discharged from the egg. In echinoids, two discrepant observations have been made with regard to this problem: a), exocytosis of cortical granules is achieved by a fusion of the cortical granule membrane and the egg plasma membrane at one place (Endo, 1961), or b), it is brought about by membrane vesiculation caused by multiple fusions of the membranes (Anderson, 1968; Millonig, 1969). Discrepant observations have also been made on ophiuroids: Holland (1979) reported that the contents of the cortical granules of Ophiopholis aculeata are discharged by multiple fusions of the membranes, whereas the present study suggests that those of A. kochii are discharged by membrane fusion at only one place of the granule with the egg plasma membrane. As has been suggested in echinoids, these discrepant results may be due to differences in the fixation techniques used. Indeed, a recent quick-freezing and freeze-fracture study (Chandler and Heuser, 1979) has suggested that multiple fusions of membranes during the cortical reaction in echinoids may be an artifact produced during the preparation for electron microscopy. It is, therefore, necessary that a new technique, such as a quick-freezing and freeze-substitution method, should be applied for observing the manner of cortical granule exocytosis.

Previously it was unknown which cortical granule components of ophiuroids contribute to formation of the fertilization mem-

brane and where the vitelline coat material is incorporated into the fertilization membrane. The present observations clearly demonstrate that peripheral fibrous (PF) material of the cortical granules contributes to formation of the fertilization membrane and that the material of the vitelline coat must be incorporated with the outer layer of the fertilization membrane, because the intermediate and inner layers of the fertilization membrane are formed by the addition of cortical granule materials to the inner surface of the previous vitelline coat. Inoue and Hardy (1971) reported that in echinoids the intermediate layer of the fertilization membrane originates from the vitelline coat material. This observation contrasts with the present observation that the materials of the vitelline coat are included only in the outer layer of the fertilization membrane. It is also notable that in the ophiuroid, the materials originated from cortical granules mainly cover the inner surface of the elevated vitelline coat. This situation resembles that in asteroids (Holland, 1980) rather than in echinoids (Inoue and Hardy, 1971; Chandler and Heuser, 1980).

Among echinoderms, a clear hyaline layer is seen only in echinoids and ophiuroids. Many investigations by various methods have demonstrated that the hyaline layer of the echinoids is derived from certain components of the cortical granules (Osanai, 1960; Endo, 1961; McClay and Fink, 1982; Hylander and Summers, 1982; see also review, Guraya, 1982), although some studies have suggested that the hyaline material is a plasma membrane and/or a cell surface protein (McBlaine and Carroll, 1977, 1980). Recently, however, it has been shown by immunohistochemistry that

besides cortical granules as a "first reservoir", the hyaline material is also reserved in a "second reservoir", small randomly distributed cortical vesicles in the unfertilized eggs (Hylander and Summers, 1982). The work of Holland (1979) and the present study have shown that the ophiuroid hyaline layer is also derived from the cortical granule materials. This conclusion does not exclude a possibility that hyaline also exists in a "second reservoir" of unfertilized egg. Further investigations by other techniques of the approache seem necessary to clarify the origin of the hyaline material in ophiuroids.

No electron microscopic observations during the entire fertilization process of the brittle-stars have previously been made, although electron microscopic investigations, partly concerned with ophiuroid fertilization, are contained in reports of the acrosome reaction (Hylander and Summers, 1975) and the cortical reaction (Holland, 1979). The present study demonstrates for the first time by means of electron microscopy that the basic processes of the early fertilization process of the ophiuroid, including the sperm penetration, are similar to those of other echinoderms. It is, however, premature to compare the latter fertilization processes in the ophiuroids with that of all other echinoderms, since detailed electron microscopic observations have been reported only for the echinoid Arbacia punctulata (Longo and Anderson, 1968). In comparison with A. punctulata, the fertilizing spermatozoon and the male pronucleus of the ophiuroid undergo morphological changes similar to those of the echinoid in spite of differences in their meiotic states at the

time of insemination. In connection with this, Wilson (1925) suggested a relationship between the meiotic state of the egg at insemination and the manner of the male and female pronuclei at the time of association; the zygote nuclear stage, at which the actual fusion of the male and female pronuclei occurs, is observed only in eggs that are inseminated after meiosis had been completed, such as echinoid eggs. Longo (1973) confirmed this observation by means of electron microscopic observations. The present study, however, clearly demonstrates that actual fusion of both pronuclei in the ophiuroid occurs even when the eggs are inseminated at the metaphase of the first meiotic division. The relation suggested by Wilson cannot, therefore, be applied to the ophiuroid. It is not clear whether the relation established by Wilson (1925) and reexamined by Longo (1973) occurs in all echinoderms or whether the ophiuroid is an exception. Thus, further observations are needed on other echinoderms, such as asteroids, holothuroids and crinoids.

Several authors have demonstrated that male pronucleus formation has a relationship to the stages of meiosis in the egg or of the female pronucleus formation (Das and Barker, 1976; Moriya and Katagiri, 1976; Usui and Yanagimachi, 1976; Da-Yuan and Longo, 1983; see also review by Longo and Kunkle, 1978). For example, Hirai *et al.* (1981) have shown that in the asteroid the decondensation of the sperm nucleus does not occur during meiosis, but occurs in conjunction with maternal chromosome dispersion after meiosis. Longo and Anderson (1970) have reported that in the surf clam the formation of the male pronuclear envelope is not completed until egg meiosis has been finished and the

formation of the female pronucleus has begun, although the sperm chromatin has been dispersed before the pronuclear envelope formation. These observations suggest the presence of the same factor controlling the formations of both pronuclei. The present study reveals that the male pronuclear envelope is formed at the time when the first polar body is eliminated and that the male pronucleus with a complete envelope develops constantly, irrespective of meiosis and the formation of the female pronucleus. Sperm nuclear decondensation in advance of the completion of meiosis have also been reported for the mussel (Longo and Anderson, 1969b). These observations, in contrast to those of Longo and Anderson (1970) and Hirai et al. (1981), suggest the presence of different factors responsible for the paternal and maternal chromatin dispersion or for the formation of the male and female pronuclei. Otherwise, when the same factor exists for both pronuclei formation, a mechanism which controls the time lag between the male and the female pronuclear formations should be present in the brittle-star or mussel eggs. Control mechanisms for the male and female pronuclear formations will be disccused in detail in the next section (D-2).

2. Control factor for male pronucleus formation and its relationship to meiosis and female pronucleus formation

The present study concerning the normal monospermic fertilization process of A. kochii shows that the development of the male pronucleus has superficially no relationship to meiosis and to the female pronucleus formation (cf., Text-Fig. 8). The study using the meiosis inhibitors (colchicine and colcemid)

demonstrates however intrinsical interrelationship between the male pronucleus formation and the meiosis or the female pronucleus formation, as suggested for other species (cf., Longo and Kunkle, 1978).

As described in RESULTS (D-3), the male pronucleus formation consists of two steps, the first dispersion step before the nuclear envelope formation and the second dispersion step on and after that. The first step is not affected by the meiosis inhibitors while the second step is highly sensitive to the drugs, suggesting the presence of at least two factors for the development of male pronucleus. The factor for the first dispersion seems to have been established at least in the spawned egg at the first meiotic metaphase. In other words, the first dispersion of sperm nucleus may be an semi-automatic step in the spawned eggs. Many investigations however shows that the dispersion of incorporated sperm nucleus requiers the materials from the germinal vesicle (Katagiri, 1980; Hylander et al., 1981; Schuetz and Longo, 1981; Longo and Schuetz, 1982; Da-Yuan and Longo, 1983; see also review by Longo and Kunkle, 1978). Therefore, it is necessary to examine whether the first dispersion of the sperm nucleus occurs in the eggs with the intact germinal vesicle.

Chemical or physical nature of the factor for the first dispersion of the sperm nucleus is unclear, but judging from the present TEM observations it is likely that the factor is not associated with membranes, unlike the factor for the second dispersion of the nucleus as discussed in the next paragraph. It is of interest to note that in mammals the sperm nuclear

dispersion is initiated with such reducing agents as dithiothreitol or 2-mercaptoethanol. Based upon this fact the sperm nuclear dispersion in mammals has been thought to be caused by cleavage of disulphide (-S-S-) bonding in sperm nuclear proteins which make sperm chromatins compact (Mahi and Yanagimachi, 1975). It is therefore plausible that the factor for the first dispersion of the sperm nucleus in A. kochii also acts as a cleaver of disulphide bonding in the sperm nuclear proteins, although further experiments, such as in vitro induction of sperm chromatin dispersion, are necessary.

As for the factor for the second dispersion of sperm nucleus, it should be noted that this dispersion stopped when colchicine or colcemid was added before the completion of meiosis while it continued when the drugs were added after meiosis (Table 7). These observations suggest that the factor is not sensitive to the action of these drugs but is correlated with meiosis itself. In other words, the factor has an intimate relation to events of meiosis. Since the male pronucleus formation occurs in the presence of cytochalasin B which inhibits the cytokinesis of meiosis (Table 7), the factor is related not to the cytokinesis but to the nuclear devision of meiosis. It is also notable that the second dispersion never continued without the sperm nuclear envelope (Table 7), suggesting that the second dispersion of sperm nucleus strongly depends on the presence of the nuclear envelope; perhaps the factor is associated with membranes and controls it through intermediation of the nuclear envelope. Importance of membrane system for swelling of sperm nucleus has also been demonstrated by recent investigations attempting in

vitro formation of the male pronucleus (Lohka and Masui, 1983 and 1984; Iwao and Katagiri, 1984). In addition, it has been revealed by the *in vitro* studies that the initial dispersion of sperm nucleus does not need the presence of membranes (Lohka and Masui, 1983 and 1984). These *in vitro* findings are fairly consistent with the present *in vivo* observations that the initial dispersion of the sperm nucleus (the first dispersion) occurs in the absence of membranes whereas further swelling (the second dispersion) requires the membranes.

Concerning the relationship between the male and the female pronuclear formations, the present study using monospermic conditions demonstrates that the two events are closely related to each other. This has been suggested from observations on the polyspermic fertilization of various animals (Das and Barker, 1976; Moriya and Katagiri, 1976; Usui and Yanagimachi, 1976; Da-Yuan and Longo, 1983). We were unble to find the complete formation of one pronucleus without the formation of the other (Tables 6 and 7). This seems to suggest the presence of the same or very closely related factors controlling both the male and female pronucleus formation. On the other hand, the male pronucleus formation in advance of the female pronucleus formation is also certain in the normal fertilization process (Text-Fig. 8). Therefore, when the same factor for both proncelei formation exists, mechanisms controlling this time lag between the male and the female pronucleus formation should be present in *A. kochii* eggs. One of such mechanisms is that the female pronucleus formation is selectively inhibited during meiosis from the

action of the factor responsible for both pronuclei formation. This inhibition may be accomplised by the prevention of the nuclear envelope formation around the maternal chromosomes; the control factor may be unable to act on these naked maternal chromosomes, as it could not act on the naked paternal chromosomes.

V. SUMMARY

The present study has dealt with the reproduction and embryonic development of two brittle-stars, Amphipholis kochii Lutken and Ophiura sarsii Lütken: Fine structure of the gonads, especially of the gonadal wall and spermatogenesis, the annual reproductive cycle of the gametogenesis, the development of the embryos and larvae, and the monospermic fertilization process of the brittle-stars have been examined.

1. The gonadal walls of the brittle-stars, A. kochii and O. sarsii, are very similar to each other, except for the morphology of the flagellated cells present in the visceral peritoneum. The basic structure of the gonadal wall of the ophiuroids is more similar to that of the asteroids than that of other echinoderms, except for the density of the flagella on the visceral peritoneum and for the arrangement of the muscle fibers. It is suggested that nutrients reserved in the stomach wall are transported to the gonad through the coelomic fluid and/or hemal sinus and that the transported nutrients are distributed over the germinal epithelium by amoeboid cells.

2. Basic processes of the spermatogenesis of the brittle-stars, A. kochii and O. sarsii, are very similar to each other, suggesting that the present findings can be regarded as a general feature of the ophiuroid spermatogensis. The remarkable point in the ophiuroid spermatogenesis is that the formation of the pro-acrosomal vesicles is initiated in the spermatogonia, unlike that in many animals, where it occurs in the spermatids. The significance of the precocious formation of the acrosome in the

ophiuroids has been discussed in relation to the fact that the duration of the spermatogenesis in the ophiuroids is very short as compared with that of other animals.

3. The annual reproductive cycle of A. kochii was studied by the gonad index method and by histological observations. The present species shows a well defined annual reproductive cycle. The spawning period is in June and July at Abuta and takes place once a year. The growth pattern of oocytes was studied by the frequency polygon method and by the instantaneous relative growth rate. Oocytes are produced in all seasons. As maturation proceeds, the number of medium-sized oocytes is reduced, probably by means of the phagocytic activity of amoeboid cells (somatic cells) in the gonads. Following the post-spawning resting period of about one month, the growth pattern of the largest oocytes clearly shows two successive stages, the fast and the slow growth stage.

4. An autoradiographic study was applied for analysis of the seasonal changes in the number of spermatogenic cells, the duration of spermatogenesis and the spermatocyte production rate. The annual testicular cycle can be divided into five phases; spermatogenesis occurs during phases 2 to 4 (November to June). Spermatogenesis during phases 3 and 4 (March to June) was sensitive to the sea water temperature as an external environment, while that during phase 2 (November to February) was insensitive to it: The sea water temperature directly controls the speed of the latter phase of spermatogenesis (from spermatocyte to spermatozoon), but it is not able to control the spermatocyte

production rate. It is therefore suggested that the water temperature plays an important role in spermatogenesis during phases 3 and 4 by controlling the speed of the latter phase of spermatogenesis, and that other environmental factor(s) controlling the spermatocyte production rate are likely to be important to spermatogenesis during phase 2.

5. The embryonic development of A. kochii egg, from fertilization through metamorphosis, was observed in a laboratory culture. Eggs spawned by a sudden change of sea water temperature remain in the meiotic metaphase until being fertilized. The cleavage in the radial type often shows irregularity in the arrangement of the blastomeres. The larval spicule takes a tetraradiated form. The fully-grown ophiopluteus has 8 arms with a very simple skeletal system. The left posterior coelom is divided into a hydrocoel and a somatocoel. The shrinkage of the anterior part of the larva and degeneration of the larval arms except for the postero-lateral arms are observable at the beginning of metamorphosis.

6. The normal, monospermic fertilization process of A. kochii was described with electron microscopy. The observations concerned the acrosome reaction of the spermatozoon, penetration of the spermatozoon into the egg cytoplasm, egg cortical reaction together with the fertilization membrane and hyaline layer formation, male and female pronuclei formation and their fusion. The acrosomal process of this species is short, about 5 um long. The thickness of the jelly coat is correspondently thin, confirming the notion that the length of the acrosomal process of the non-echinoids corresponds to the thickness of the jelly coat.

The contents of the cortical granules are clearly distinguished into two components: peripheral fibrous (PF) material and central fibrous (CF) material. The vitelline coat and some PF materials form the fertilization membrane, and CF materials together with some PF materials form the hyaline layer. The incorporated sperm nucleus becomes the male pronucleus through the two successive stages, the first dispersion stage before the nuclear envelope formation and the second dispersion stage on and after that. Dispersion of the sperm nucleus, formation of the male pronuclear envelope, and the growth of the male pronucleus occur irrespective of meiosis and the female pronucleus formation in the normal fertilization process. In spite of the different maturation state of eggs at insemination, the fertilization process of the ophiuroid, including the pronuclear formation and association of pronuclei, is generally similar to that of the echinoid, indicating that Wilson's hypothesis on the manner of pronuclear association in relation with karyological state of the mature egg may not apply to ophiuroids.

7. The control mechanism for the male pronucleus formation and its relationship to meiosis or the female pronucleus formation were analysed by means of the electron microscopic observations on the eggs treated with the meiosis inhibitors (colchicine, colcemid or cytochalasin B). The first dispersion of the incorporated sperm nucleus was not affected by the drugs. On the other hand, the second dispersion of sperm nucleus was inhibited when the eggs were treated with colchicine or colcemid before the completion of meiosis, while it occurred on schedule

when the eggs were treated after the meiosis. The same results were obtained in the female pronucleus formation. Cytochalasin B had no effects on the pronuclei formation. It is suggested that the male pronucleus formation is controlled by at least two factors, one is for the first dispersion of the sperm nucleus and another is for the second dispersion of the nucleus: The former is a soluble component and has no relationship to meiosis, whereas the latter is associated with the membrane system (probably nuclear envelope) and has a relationship to nuclear division of meiosis. Formations of the male and female pronuclei are also related to each other, and the presence of the same or closely-linked factors for both pronuclear formation was suggested.

VI. ACKNOWLEDGMENTS

The author wishes to express his sincere appreciation to Professor F. Iwata for continuous guidance throughout the present study and improvement of the manuscript. He also thanks Professors T. Aoto, M. Yamada and T.S. Yamamoto for critical reading of the manuscript. Thanks are also due to Dr. M. Wakahara for guidance of autoradiographic techniques, Dr. K. Konishi for help in collecting the samples of Amphipholis kochii, the late Professor T. Igarashi and Mr. Y. Arashida of the Usujiri Fisheries Laboratory for help in collecting the samples of Ophiura sarsii, and Mr. Y. Takakuwa for technical assistance in electron microscopy.

VII. REFERENCES

Afzelius, B.A., 1956. The ultrastructure of the cortical granules and their products in the sea urchin egg as studied with the electron microscope. Exp. Cell Res., **10**: 257-285.

Afzelius, B.A., 1978. Fine structure of the garfish spermatozoon. J. Ultrastruct. Res., **64**: 309-314.

Allen, R.D., 1954. Fertilization and activation of sea urchin eggs in glass capillaries. Exp. Cell Res., **6**: 403-424.

Anderson, E., 1968. Oocyte differentiation in the sea urchin, Arbacia punctulata, with particular reference to the origin of cortical granules and their participation in the cortical reaction. J. Cell Biol., **37**: 514-539.

Anderson, J.M., 1966. Aspects of nutritional physiology. In: Physiology of Echinodermata (R.A. Boolootian, ed.), pp. 329-357. Interscientific Publishers, New York.

Andrews, P.M., 1976. Microplicae: Characteristic ridge-like folds of the plasmalemma. J. Cell Biol., **68**: 420-429.

Atwood, D.G., 1973. Ultrastructure of the gonadal wall of the sea cucumber, Leptosynapta clarki (Echinodermata: Holothuroidea). Z. Zellforsch., **141**: 319-330.

Atwood, D.G., 1974. Fine structure of spermatogonia, spermatocytes, and spermatids of the sea cucumber Cucumaria lubrica and Leptosynapta clarki (Echinodermata: Holothuroidea). Can. J. Zool., **52**: 1389-1396.

Austin, C.R., 1968. Ultrastructure of Fertilization. Holt, Reinhart and Winston, New York.

Barker, M.F., 1979. Breeding and recruitment in a population of the New Zealand starfish Stichaster australis (Verrill). J. Exp. Mar. Biol. Ecol., **41**: 195-211.

Bickell, L., F.S. Chia and B.J. Crawford, 1980. A fine structural study of the tsticular wall and spermatogenesis in the crinoid, Florometra serratissima (Echinodermata). J. Morph., **166**: 109-126.

Boolootian, R.A., 1966. Reproductive physiology. In: Physiology of Echinodermata (R.A. Boolootian, ed.), pp. 561-613. Interscientific Publischers, New York.

Botticelli, C.R., F.L. Hisaw, Jr. and H.H. Wotiz, 1960. Estradiol-17β and progesterone in ovaries of starfish (Pisaster ochraceous). Proc. Soc. Exp. Biol. Med., **103**: 875-877.

Bowmer, T., 1982. Reproduction in Amphiura filiformis (Echinodermata: Ophiuroidea): Seasonality in gonad development. Mar. Biol., **69**: 281-290.

Brody, S., 1945. Bioenergetics and Growth. p. 1023. Reinholdt Publishing Co., New York.

Broertjes, J.J.S., G. Postuma, P. Den Breejen and P.A. Voogt, 1980a. Evidence for an alternative transport route for the use of vitellogenesis in the sea-star Asterias rubens (L.). J. Mar. Biol. Ass. U.K., **60**: 157-162.

Broertjes, J.J.S., G. Postuma, G. Beijnink, and P.A. Voogt, 1980b. The admission of nutrients from the digestive system into the haemal channels in the sea-star Asterias rubens (L.). J. Mar. Biol. Ass. U.K., **60**: 883-890.

Bruslé, J., 1969. Ultrastructural aspects of the innervation of the gonads in the starfish Asterina gibbosa P. Z. Zellforsch., **98**: 88-97. (In French with English summary)

Chambers, E.L., 1939. Movement of the egg nucleus in relation to the sperm aster in the echinoderm egg. J. Exp. Biol., **16**: 409-424.

Chandler, D.E. and J. Heuser, 1979. Membrane fusion during secretion: Cortical granule exocytosis in sea urchin eggs as studied by quick-freezing and freeze-fracture. J. Cell Biol., **83**: 91-108.

Chandler, D.E. and J. Heuser, 1980. The vitelline layer of the sea urchin egg and its modification during fertilization: A freeze-fracture study using quick-freezing and deep-etching. J. Cell Biol., **84**: 618-632.

Chatlynne, L.G., 1969. A histochemical study of oogenesis in the sea urchin, Strongylocentrotus purpuratus. Biol. Bull., **136**: 137-184.

Cochran, R.C. and F. Engelmann, 1975. Environmental regulation of the annual reproductive season of Strongylocentrotus purpuratus (Stimpson). Biol. Bull., **148**: 393-401.

Colwin, A.L. and L.H. Colwin, 1955. Sperm entry and the acrosome filament (Holothuria atra and Asterias amurensis). J. Morph., **97**: 543-568.

Colwin, L.H. and A.L. Colwin, 1956. The acrosome filament and sperm entry in Thyone briareus (Holothuria) and Asterias. Biol. Bull., **110**: 243-257.

Colwin, L.H. and A.L. Colwin, 1961a. Changes in the spermatozoon during fertilization in Hydroides hexagonus (Annelida). I. Passage of the acrosomal region through the vitelline membrane. J. Biophys. Biochem. Cytol., **10**: 231-254.

Colwin, A.L. and L.H. Colwin, 1961b. Changes in the spermatozoon during fertilization in Hydroides hexagonus (Annelida). II. Incorporation with the egg. J. Biophys. Biochem. Cytol., **10**: 255-274.

Colwin, A.L. and L.H. Colwin, 1963a. Role of the gamete membranes in fertilization in Saccoglossus kowalevskii (Enteropneusta). I. The acrosome region and its changes in early stage of fertilization. J. Cell Biol., **19**: 477-500.

Colwin, L.H. and A.L. Colwin, 1963b. Role of the gamete membranes in fertilization in Saccoglossus kowalevskii (Enteropneusta). II. Zygote formation by gamete membrane fusion. J. Cell Biol., **19**: 501-518.

Colwin, L.H. and A.L. Colwin, 1967. Membrane fusion in relation to sperm-egg association. In: Fertilization, Vol. 1 (C.B. Metz and A. Monroy, eds.), pp. 295-367. Academic Press, New York.

Colwin, A.L., L.H. Colwin and R.G. Summers, 1975. The acrosome region and the beginning of fertilization in the holothurian, Thyone briareus. In: The Functional Anatomy of the Spermatozoon (B.A. Afzelius, ed.), pp. 27-38. Pergamon Press, Oxford.

Crump, R.G., 1971. Annual reproductive cycles in three geographically separated populations of Patiriella regularis (Verrill), a common New Zealand asteroid. J. Exp. Mar. Biol. Ecol., **7**: 137-162.

Da-Yuan, C. and F.J. Longo, 1983. Sperm nuclear dispersion coordinate with meiotic maturation in fertilized Spisula solidissima eggs. Develop. Biol., **99**: 217-224.

Dan, J.C., 1954. Studies on the acrosome. II. Acrosome reaction in starfish spermatozoa. Biol. Bull., **107**: 203-218.

Dan, J.C., 1956. The acrosome reaction. Int. Rev. Cytol., **5**: 365-393.

Dan, J.C., 1967. Acrosome reaction and lysins. In: Fertilization, Vol. 1 (C.B. Metz and A. Monroy, eds.), pp. 237-293. Academic Press, New York.

Dan, J.C., 1975. The acrosome reaction. In: Eggs and Spermatozoa (The Zoological Society of Japan, ed.), pp. 89-119. Gakkai Publishing Center, Tokyo. (In Japanese)

Dan, J.C. and Y. Hagiwara, 1967. Studies on the acrosome. IX. Course of acrosome reaction in the starfish. J. Ultrastruct. Res., **18**: 562-579.

Dan, J.C. and A. Shirakami, 1971. Studies on the acrosome. X. Differentiation of the starfish acrosome. Develop. Growth and Differ., **13**: 37-52.

Dan-Sohkawa, M., 1976. A "normal" development of denuded eggs of the starfish, Asterina pectinifera. Develop., Growth and Differ., **18**: 439-445.

Das, H.K. and C. Barker, 1976. Mitotic chromosome condensation in the sperm nucleus during post fertilization maturation division in Urechis eggs. J. Cell. Biol., **68**: 155-159.

Egami, N. and Y. Hyodo-Taguchi, 1967. An autoradiographic examination of rate of spermatogenesis at different temperatures in the fish, Oryzias latipes. Exp. Cell Res., **47**: 665-667.

Endo, Y., 1961. Changes in the cortical layer of sea urchin eggs at fertilization as studied with the electron microscope. I. Clypeaster japonicus. Exp. Cell Res., **25**: 383-397.

Epel, D, A.M. Weaver and D. Mazia, 1970. Methods for removal of the vitelline membrane of sea urchin eggs. I. Use of Dithiothreitol. Exp. Cell Res., **61**: 64-68.

Farmanfarmaian, A., 1963. Transport of nutrients in echinoderms. Proc. XVI Int. Congr. Zool., Washington, D.C., **1**: 118.

Farmanfarmaian, A., A.C. Giese, R.A. Boolootian and J. Bennett, 1958. Annual reproductive cycles in four species of west coast starfishes. J. Exp. Zool., **138**: 355-367.

Fell, H.B., 1946. The embryology of the viviparous ophiuroid Amphipholis squamata Delle Chiajei. Trans. Roy. Soc. New Zealand, **75**: 419-464.

Fenaux, L., 1963. Note préliminaire sur le développement larvaire de Amphiura chiajei (Forbes). Vie et Millieu, **14**: 91-96.

Fenaux, L., 1969. Le developpement larvaire chez Ophioderma longicauda (Rezius). Cah. Biol. Mar., **10**: 59-62.

Fenaux, L., 1970. Maturation of the gonads and seasonal cycle of the planktonic larvae of the ophiuroid Amphiura chiajei Forbes. Biol. Bull., **138**: 262-271.

Fenaux, L., 1972. Seasonal variations in the gonads of Ophioderma longicauda (Retzius), Ophiuroidea. Int. Rev., Ges. Hydrobiol., **57**: 257-262. (In French with English summary)

Ferguson, J.C., 1964a. Nutrient transport in starfish. I. Properties of the coelomic fluid. Biol. Bull., **126**: 33-53.

Ferguson, J.C., 1964b. Nutrient transport in starfish. II. Uptake of nutrients by isolated organ. Biol. Bull., **126**: 391-406.

Ferguson, J.C., 1975a. The role of free amino acids in nitogen storage during the annual cycle of a starfish. Comp. Biochem. Physiol., **51A**: 341-350.

Ferguson, J.C., 1975b. Fatty acid and carbohydrate storage in the annual reproductive cycle of Echinaster. Comp. Biochem. Physiol., **52A**: 585-590.

Fontaine, A.R., 1962. Neurosecretion in the ophiuroid Ophiopholis aculeata. Science, **138**: 908-909.

Franzen, A., 1970. Phylogenetic aspects of the morphology of spermatozoa and spermiogenesis. In: Comparative Spermatology (B. Baccetti, ed.), pp. 29-46. Academic Press, New York.

Fuji, A., 1960a. Studies on the biology of the sea urchin. I. Superficial and histological gonadal changes in gametogenic process of two sea urchins, Strongylocentrotus nudus and S. intermedius. Bull. Fac. Fish. Hokkaido Univ., **11**: 1-14.

Fuji, A., 1960b. Studies on the biology of the sea urchin. III. Reproductive cycle of two sea urchins, S. nudus and S. intermedius, in southern Hokkaido. Bull. Fac. Fish., Hokkaido Univ., **11**: 49-57.

Gage, J.D. and P.A. Tyler, 1982. Growth and reproduction of the deep-sea brittle-star Ophiomuseum lymani Wylville Thomson. Oceanol. Acta, **5**: 73-83.

Giese, A.C., 1966. On the biochemical constitution of some echinoderms. In: Physiology of Echinodermata (R. Boolootian, ed.), pp. 757-796. Interscientific Publishers, New York.

Giese, A.C., L. Greenfield, H. Huang, A. Farmanfarmaian, R. Boolootian and R. Lasker, 1959. Organic productivity in the reproductive cycle of the purple sea urchin. Biol. Bull., **116**: 49-58.

Gonor, J.J., 1973a. Reproductive cycle in Oregon populations of the echinoids, Strongylocentrotus purpuratus (Stimpson). I. Annual gonadal growth and ovarian gametogenetic cycles. J. Exp. Mar. Biol. Ecol., **12**: 45-64.

Gonor, J.J., 1973b. Reproductive cycles in Oregon populations of the echinoid, Strongylocentrotus purpuratus (Stimpson). II. Seasonal changes in oocyte growth and in abundance of gametogenic stages in the ovary. J. Exp. Mar. Biol. Ecol., **12**: 65-78.

Gulyas, B.J., 1975. A reexamination of cleavage patterns in eutherian mammalian eggs: Rotation of blastomere pairs during second cleavage in the rabbit. J. Exp. Zool., **193**: 235-248.

Guraya, S.S., 1982. Recent progress in the structure, origin, composition, and function of cortical granules in animal eggs. Int. Rev. Cytol., **78**: 257-360.

Hagiwara, Y., J.C. Dan and A. Saito, 1967. Studies on the acrosome. VIII. The intact starfish acrosome. J. Ultrastruct. Res., **18**: 551-561.

Hamaguchi, M.S. and T. Hiramoto, 1980. Fertilization process in the heart-urchin, Clypeaster japonicus observed with a differential interference microscope. Develop. Growth and Differ., **22**: 517-530.

Harrold, C. and J.S. Pearse, 1980. Allocation of pyloric caecum reserves in fed and starved sea stars, Pisaster giganteus (Stimpson): Somatic maintenance comes before reproduction. J. Exp. Mar. Biol. Ecol., **48**: 169-183.

Hendler, G., 1975. Adaptational significance of the patterns of ophiuroid development. Amer. Zool., **15**: 691-715.

Hendler, G., 1977. Development of Amphioplus abditus (Verrill) (Echinodermata: Ophiuroidea). I. Larval biology. Biol. Bull., **152**: 51-63.

Hendler, G., 1978. Development of Amphioplus abditus (Verrill) (Echinodermata: Ophiuroidea). II. Description and discussion of ophiuroid skeletal ontogeny and homologies. Biol. Bull., **154**: 79-95.

Hendler, G., 1979. Reproductive periodicity of ophiuroids (Echinodermata: Ophiuroidea) on the Atlantic and Pacific coasts of Panama. In: Reproductive Ecology of Marine Invertebrates (S.E. Stancyk, ed.), pp. 145-146. University of South Carolina Press, Columbia, South Carolina.

Hinegardner, R.T., 1969. Growth and development of the laboratory cultured sea urchin. Biol. Bull., **137**: 465-475.

Hirai, S., Y. Nagahama, T. Kishimoto and H. Kanatani, 1981. Cytoplasmic maturity revealed by the structural changes in incorporated spermatozoon during the course of starfish oocyte maturation. Develop., Growth and Differ., **23**: 465-478.

Hirao, Y. and R. Yanagimachi, 1979. Development of pronuclei in polyspermic eggs of the golden hamster. Zool. Mag., **88**: 24-33. (In Japanese with English summary)

Holland, N.D., 1967. Gametogenesis during the annual reproductive cycle in a cidaroid sea urchin (Stylocidaris affinis). Biol. Bull., **133**: 578-590.

Holland, N.D., 1979. Electron microscopic study of the cortical reaction of an ophiuroid echinoderms. Tissue and Cell, **11**: 445-455.

Holland, N.D., 1980. Electron microscopic study of the cortical reaction in eggs of the starfish (Patiria miniata). Cell Tiss. Res., **205**: 67-76.

Holland, N.D. and A.C. Giese, 1965. An autoradiographic investigation of the gonads of the purple sea urchin (Strongylocentrotus purpuratus). Biol. Bull., **128**: 241-258.

Holland, N.D., J.D. Grimmer and H. Kubota, 1975. Gonadal development during the annual reproductive cycle of Comanthus japonica (Echinodermata: Crinoidea). Biol. Bull., **148**: 219-242.

Houk, M.S. and R.T. Hinegardner, 1981. Cytoplasmic inclusions specific to the sea urchin germ line. Develop. Biol., **86**: 94-99.

Hunter, R.H.F., 1967. Polyspermic fertilization in pigs during the lucteal phase of the oestrous cycle. J. Exp. Zool., **165**: 451-460.

Hylander, B.L., J. Anstrom and R.G. Summers, 1981. Premature sperm incorporation into the primary oocyte of the polychaete Pectinaria: Male pronuclear formation and oocyte maturation. Develop. Biol., **82**: 382-387.

Hylander, B.L. and R.G. Summers, 1975. An ultrastructural investigation of the spermatozoa of two ophiuroids, Ophiocoma echinata and Ophiocoma wendti: Acrosomal morphology and reaction. Cell Tiss. Res., **158**: 151-168.

Hylander, B.L. and R.G. Summers, 1982. An ultrastructural immunocytochemical localization of hyaline in the sea urchin egg. Develop. Biol., **93**: 368-380.

Hyman, L.H., 1955. Echinodermata. The Invertebrates, Vol. 4. McGraw-Hill Book Com., New York.

Inoue, S. and J.P. Hardy, 1971. Fine structure of the fertilization membranes of sea urchin embryo. Exp. Cell Res., **68**: 259-272.

Inoue, S., J.P. Hardy, G.H. Cousineau and A.K. Bal, 1967. Fertilization membranes structure analysis with the surface replica method. Exp. Cell Res., **48**: 248-251.

Iwao, Y. and Ch. Katagiri, 1984. In vitro induction of sperm nucleus decondensation by cytosol from mature toad eggs. J. Exp. Zool., **230**: 115-124.

Jangoux, M. and E. Van Impe, 1977. The annual pyrolic cycle of Asterias rubens L. (Echinodermata: Asteroidea). J. Exp. Mar. Biol. Ecol., **30**: 165-184.

Kanatani, H., 1973. Maturation-inducing substance in starfishes. Int. Rev. Cytol., **35**: 253-298.

Kanatani, H. and M. Ohguri, 1966. Mechanism of starfish spawning. I. Distribution of active substance responsible for maturation of oocytes and spawning of gametes. Biol. Bull., **131**: 104-114.

Katagiri, Ch., 1980. Appearance of pronucleus-inducing activity during hormonally induced meiotic maturation in toad oocytes. Develop., Growth and Differ., **22**: 237-245.

Kelly, R.N., M.J. Ashwood-Smith and D.V. Ellis, 1982. Duration and timing of spermatogenesis in a stock of the mussel Mytilus californianus. J. Mar. Biol. Ass. U.K., **62**: 509-519.

Kidd, P., 1978. The jelly and vitelline coats of the sea urchin egg: New ultrastructural features. J. Ultrastruct. Res., **64**: 204-215.

Kim, Y.S., 1968. Histological observations on the annual change in the gonad of the starfish Asterias amurensis Lutken. Bull. Fac. Fish. Hokkaido Univ., **19**: 97-108.

Lasker, B. and A.C. Giese, 1954. Nutrition of the sea urchin, Strongylocentrotus purpuratus. Biol. Bull., **106**: 328-340.

Lessios, H.A., 1981. Reproductive periodicity of the echinoids Diadema and Echinometra on the two coasts of Panama. J. Exp. Mar. Biol. Ecol., **50**: 47-61.

Lohka, M.J. and Y. Masui, 1983. Formation in vitro sperm pronuclei and miotic chromosomes induced by amphibian ooplasmic components. Nature, **220**: 719-721.

Lohka, M.J. and Y. Masui, 1984. Roles of cytosol and cytoplasmic particles in nuclear envelope assembly and sperm pronuclear formation in cell-free preparations from amphibian eggs. J. Cell Biol., **98**: 1222-1230.

Longo, F.J., 1973. Fertilization: A comparative ultrastructural review. Biol. Reprod., **9**: 149-215.

Longo, F.J. and E. Anderson, 1968. The fine structure of pronuclear development and fusion in the sea urchin, Arbacia punctulata. J. Cell Biol., **39**: 339-368.

Longo, F.J. and E. Anderson, 1969a. Sperm differentiation in the sea urchins Arbacia punctulata and Strongylocentrotus purpuratus. J. Ultrastruct. Res., 27: 462-480.

Longo, F.J. and E. Anderson, 1969b. Cytological aspects of fertilization in the lamellibranch, Mytilus edulis. II. Development of the male pronucleus and the association of the maternally and paternally derived chromosomes. J. Exp. Zool., 172: 97-120.

Longo, F.J. and E. Anderson, 1970. An ultrastructural analysis of fertilization in the surf clam, Spisula solidissima. II. Development of the male pronucleus and the association of the maternally and paternally derived chromosomes. J. Ultrastruct. Res., 33: 515-527.

Longo, F.J. and E.J. Dornfeld, 1967. The fine structure of spermatid differentiation in the mussel, Mytilus edulis. J. Ultrastruct. Res., 20: 462-480.

Longo, F.J. and M. Kunkle, 1978. Transformation of sperm nuclei upon insemination. Curr. Top. Develop. Biol., 12: 149-184.

Longo, F.J. and W. Plunkett, 1973. The onset of DNA synthesis and its relation to morphogenetic events of the pronuclei in activated eggs of the sea urchin, Arbacia punctulata. Develop. Biol., 30: 56-67.

Longo, F.J. and A.W. Schuetz, 1982. Male pronuclear development in starfish oocytes treated with 1-methyladenine. Biol. Bull., 163: 453-464.

Lönning, S., 1976. Reproductive cycle and ultrastructure of yolk development in some echinoderms from the Bergen area, western Norway. Sarsia, 62: 47-72.

Luft, J.H., 1961. Improvements in epoxy resin embedding methods. J. Biophys. Biochem. Cytol., 9: 409-414.

Luft, J.H., 1971a. Ruthenium red and violet. I. Chemistry, purification, methods of use for electron microscopy and mechanism of action. Anat. Rec., 171: 347-368.

Luft, J.H., 1971b. Ruthenium red and violet. II. Fine structural localization in animal tissues. Anat. Rec., 171: 369-416.

Mabuchi, Y. and I. Mabuchi, 1973. Acrosomal ATPase in starfish and bivalve mollusc spermatozoa. Exp. Cell Res., 82: 271-279.

MacBride, E.W., 1907. The development of Ophiothrix fragilis. Quart. J. Microsc. Sci., 51: 557-606.

Mahi, C. and R. Yanagimachi, 1975. Initiation of nuclear decondensation of mammalian spermatozoa *in vitro*. J. Reprod. Fert., **44**: 393-396.

Mauzey, K.P., 1966. Feeding behavior and reproductive cycles in *Pisaster ochraceus*. Biol. Bull., **131**: 127-144.

Mazia, D., G. Schatten and W. Sale, 1975. Adhesion of cell to surfaces coated with polylysine. J. Cell Biol., **66**: 198-200.

McBlaine, P.J. and E.J. Carroll, 1977. Hyaline layer formation in sea urchin eggs does not require cortical granule exocytosis. J. Cell Biol., **75**: 169a.

McBlaine, P.J. and E.J. Carroll, 1980. Sea urchin egg hyaline layer: Evidence for the localization of hyaline on the fertilized egg surface. Develop. Biol., **75**: 137-147.

McClay, D.R. and R.D. Fink, 1982. Sea urchin hyaline: Appearance and function in development. Develop. Biol., **92**: 285-293.

Miller, K.R., C.S. Prescott, T.L. Jacobs and H.L. Lassignal, 1983. Artifacts associated with quick-freezing and freeze-drying. J. Ultrastruct. Res., **82**: 123-133.

Millonig, G., 1969. Fine structure of the cortical reaction in the sea urchin egg: After normal fertilization and after electric induction. J. Submicrosc. Cytol., **1**: 69-84.

Mladenov, P.V., 1979. Unusual lecithotropic development of the Caribbean brittle star *Ophiothrix oerstedi*. Mar. Biol., **55**: 55-62.

Moriya, M. and Ch. Katagiri, 1976. Microinjection of toad sperm into oocytes undergoing maturation division. Develop., Growth and Differ., **18**: 349-356.

Mortensen, Th., 1913. On the development of some British echinoderms. J. Mar. Biol., Ass. U.K., **10**: 1-18.

Mortensen, Th., 1920. Notes on the development and the larval forms of some Scandinavian echinoderms. Vidensk. Medd. Naturhist. Foren., Kobenhavn, **71**: 133-160.

Mortensen, Th., 1921. Studies on the development and larval forms of echinoderms. G.E.C. Gad., Copenhagen.

Mortensen, Th., 1931. Contributions to the study of the development and larval forms of echinoderms. I. II. K. Dansk. Vidensk. Selsk. (9), 4: 1-39.

Mortensen, Th., 1937. Contributions to the study of the development and larval forms of echinoderms. III. K. Dansk. Vidensk. Selsk. (9), **7(1)**: 1-65.

Mortensen, Th., 1938. Contributions to the study of the development and larval forms of echinoderms. IV. K. Dansk. Vidensk. Selsk. (9), **7(3)**: 1-59.

Narasimhamurti, N., 1933. The development of Ophiocoma nigra. Quart. J. Microsc. Sci., **76**: 63-88.

Nimitz, Sr. M. Aquinas, 1971. Histochemical study of gut nutrient reserves in relation to reproduction and nutrition in the sea stars, Pisaster ochraceus and Patiria miniata. Biol. Bull., **140**: 461-481.

Nimitz, Sr. M. Aquinas, 1976. Histochemical changes in gonadal nutrient reserves correlated with nutrition in the sea stars, Pisaster ochraceus and Patiria miniata. Biol. Bull., **151**: 357-369.

Oguro, Ch, T. Shosaku and M. Komatsu, 1982. Development of the brittle-star, Amphipholis japonica Matsumoto. Int. Echinoderm Conference, Tampa Bay, pp.491-496.

Olsen, H., 1942. The development of the brittle-star Ophiopholis aculeata (O. Fr. Muller), with a short report on the outer hyaline layer. Bergens Mus. Arbok. Naturvid., **6**: 1-107.

Osanai, K., 1960. Development of the sea urchin egg with inhibited breakdown of the cortical granules. Sci. Rep. Tohoku Univ., Ser. IV, Biol., **26**: 77-87.

Patent, D.H., 1969. The reproductive cycle of Gorgonocephalus caryi (Echinodermata; Ophiuroidea). Biol. Bull., **136**: 241-252.

Patent, D.H., 1970. The embryology of the basket star Gorgonocephalus caryi (Echinodermata: Ophiuroidea). Mar. Biol., **6**: 262-267.

Patent, D.H., 1976. Gonadal histology of the basket star, Gorgonocephalus eucnemis. Thal. Jugo., **12**: 269-276.

Pearse, J.S., 1965. Reproductive periodicities in several contrasting populations of Odontaster validus Koehler, a common antarctic asteroid. Biology of Antarctic seas. II. Antarctic Res., **5**: 39-85.

Pearse, J.S., 1969a. Reproductive periodicities of Indo-Pacific invertebrates in the Gulf of Suez. I. The echinoids Prionocidaris baculosa (Lamarck) and Lovenia elongata (Gray). Bull. Mar. Sci., **19**: 323-350.

Pearse, J.S., 1969b. Reproductive periodicities of Indo-pacific invertebrates in the Gulf of Suez. II. The echinoid Echinometra mathaei (De Blainville). Bull. Mar. Sci., **19**: 580-613.

Pearse, J.S., 1970. Reproductive periodicities of Indo-Pacific invertebrates in the Gulf of Suez. III. The echinoid Diadema setosum (Leske). Bull. Mar. Sci., **20**: 697-720.

Pearse, J.S., 1972. A monthly reproductive rhythm in the diadematid sea urchin Centrostephanus coronatus Verrill. J. Exp. Mar. Biol. Ecol., **8**: 697-720.

Pearse, J.S., 1975. Lunar reproductive rhythms in sea urchins: A review. J. Interdiscipl. Cycle Res., **6**: 47-52.

Pearse, J.S., 1981. Synchronization of gametogenesis in the sea urchins Strongylocentrotus purpuratus and S. franciscanus. In: Advances in Invertebrate Reproduction (W.H. Clark, Jr. and T.S. Adams, eds.), pp. 53-68. Elsevier North Holland Inc., New York.

Pearse, J.S. and D.J. Eernisse, 1982. Photoperiodic regulation of gametogenesis and gonadal growth in the sea star Pisaster ochraceus. Mar. Biol., **67**: 121-125.

Pearse, J.S. and A.C. Giese, 1966. Food, reproduction and organic constitution of the common antarctic echinoid Sterechinus neumayeri (Meissner). Biol. Bull., **130**: 387-401.

Pearse, J.S. and B.F. Phillips, 1968. Continuous reproduction in the Indo-pacific sea urchin Echinometra mathaei at Rottnest Island, western Australia. Aust. J. Mar. Freshwater Res., **19**: 161-172.

Pladellorens, E.S. and J.A. Subirana, 1975. Spermiogenesis in the sea cucumber Holothuria tubulosa. J. Ultrastruct. Res., **52**: 235-242.

Rambourg, A., W. Hernandez and C.P. Leblond, 1969. Detection of complex carbohydrates in the Golgi apparatus of rat cells. J. Cell Biol., **40**: 395-414.

Rao, K.S., 1966. Reproductive nutritional cycles of Oreaster hedemanni Lutken. J. Mar. Biol. Ass. India, **8**: 254-272.

Reynolds, E.S., 1963. The use of lead citrate at high pH as an electron-opaque stain in electron microscopy. J. Cell Biol., **17**: 208-212.

Roosen-Runge, E.C., 1977. Spermatogonia and kinetics of spermatogenesis. In: The Process of Spermatogenesis in Animals, pp. 133-144. Cambridge Univ. Press, London.

Runnström, J., 1966. The vitelline membrane and cortical particles in sea urchin eggs and their function in maturation and fertilization. Adv. Morphogen., **5**: 221-325.

Schatten, G., 1981. Sperm incorporation, the pronuclear migrations, and their relation to the establishment of the first embryonic axis: Time-lapse video microscopy of the movements during fertilization of the sea urchin Lytechinus variegatus. Develop. Biol., **86**: 426-437.

Schatten, G. and D. Mazia, 1976. The penetration of the spermatozoon through the sea urchin egg surface at fertilization. Exp. Cell Res., **98**: 325-337.

Schatten, G. and H. Schatten, 1981. Effects of motility inhibitors during sea urchin fertilization. Exp. Cell Res., **135**: 311-330.

Schechter, J. and J. Lucero, 1968. A light and electron microscopic investigation of the digestive system of the ophiuroid Ophiuroiderma panamensis (brittle-star). J. Morph., **124**: 451-482.

Schlieper, C., 1957. Comparative study of Asterina rubens and Mytilus edulis from the North Sea (30 per 1,000 S) and the Western Baltic Sea (15 per 1,000 S). Ann. Biol., **33**: 117-127.

Schoenmakers, H.J.N., 1980. The variation of 3β-hydroxysteroid dehydrogenase activity of the ovaries and pyloric caeca of the starfish Asterias rubens during the annual reproductive cycle. Gen. Comp. Physiol., **138**: 27-30.

Schoenmakers, H.J.N., P.H.J.M. Colenbrander and J. Pente, 1977. Ultrastructural evidence for the existence of steroid synthesizing cells in the ovary of the starfish, Asterias rubens (Echinodermata). Cell Tiss. Res., **182**: 275-279.

Schoenmakers, H.J.N., J.G.D. Lambert and P.A. Voogt, 1976. The steroid synthesizing capacity of the gonads fo Asterias rubens. Gen. Com. Endocrinol., **29**: 256.

Schuetz, A.W. and F.J. Longo, 1981. Hormone-cytoplasmic interactions controlling sperm nuclear decondensation and male pronuclear development in starfish oocytes. J. Exp. Zool., **215**: 107-111.

Smith, J.E., 1940. The reproductive system and associated organs of the brittle-star Ophiothrix fragilis. Quart. J. Micro. Sci., **82**: 267-309.

Stancyk, S.E., 1973. Development of Ophiolepis elegans (Echinodermata: Ophiuroidea) and its implications in the estuarine environment. Mar. Biol., **21**: 7-12.

Summers, R.G., B.L. Hylander, L.H. Colwin and A.L. Colwin, 1975. The functional anatomy of the echinoderm spermatozoon and its interaction with the egg at fertilization. Amer. Zool., **15**: 523-551.

Tangapregassom, A.M. and R. Delavault, 1967. Analyse, en microscopie photonique et electronique, des structures peripheriques des gonades chez deux etoiles de mer: Asterina gibbosa Pennant et Echinaster sepositus Gray. Cah. Biol. Mar., **8**: 153-159.

Thorson, G., 1934. On the reproduction and larval stages of the brittle-stars Ophiocten sericeum (Forbes) and Ophiura robusta (Ayres) in east Greenland. Medd. OM Brønl. Bd. 100, Nr. 4.

Tilney, L.G., 1976. The polymerization of actin. II. How nonfilamentous actin becomes nonrandomly distributed in sperm: Evidence for the association of this actin with membrane. J. Cell Biol., **69**: 51-72.

Tilney, L.G., 1978. Polymerization of actin. V. A new organelle, the actomere, that initiates the assembly of actin filaments in Thyone sperm. J. Cell Biol., **77**: 551-564.

Tilney, L.G., S. Hatano, H. Ishikawa and M.S. Mooseker, 1973. The polymerization of actin: Its role in the generation of the acrosomal process of certain echinoderm sperm. J. Cell Biol., **59**: 109-126.

Tilney, L.G., D.P. Kiehart, C. Sardet and M. Tilney, 1978. Polymerization of actin. IV. Role of Ca^{++} and H^{+} in the assembly of actin and in membrane fusion in the acrosomal reaction of echinoderm sperm. J. Cell Biol., **77**: 536-550.

Tyler, P.A., 1977. Seasonal variation and ecology of gametogenesis in the genus Ophiura (Ophiuroidea: Echinodermata) from the Briostol Channel. J. Exp. Mar. Biol. Ecol., **30**: 185-197.

Tyler, P.A. and J.D. Gage, 1980. Reproduction and growth of the deep-sea brittle-star Ophiura ljungmani (Cyman). Oceanol. Acta, **3**: 177-185.

Tyler, P.A. and J.D. Gage, 1982. Reproductive biology of Ophiacantha bidentata (Echinodermata: Ophiuroidea) from the Rockall Through. J. Mar. Biol. Ass. U.K., **62**: 45-55.

Usui, N. and R. Yanagimachi, 1976. Behavior of hamster sperm nuclei incorporated into eggs at various stages of maturation, fertilization, and early development. The appearance and disappearance of factors involved in sperm chromatin decondensation in egg cytoplasm. J. Ultrastruct. Res., **57**: 276-288.

Walker, C.W., 1974. Studies on the reproductive system of sea stars. I. The morphology and histology of the gonad of Asterias vulgaris. Biol. Bull., **147**: 661-677.

Walker, C.W., 1976. Studies on the reproductive system of sea stars. III. Horse-star, Hippasterina phrygiana. Thal. Yugo., 12: 361-369.

Walker, C.W., 1979. Ultrastructure of the somatic portion of the gonads in asteroids, with emphasis on flagellated-collar cells and nutrient transport. J. Morph., 162: 127-162.

Walker, C.W., 1980. Spermatogenic columns, somatic cells, and the microenvironment of germinal cells in the testes of asteroids. J. Morph., 166: 81-107.

Welsch, U. and V. Storch, 1976. Comparative Animal Cytology and Histology, pp. 321-332. Sidwic and Jackson Limited, London.

Wilson, E.B., 1925. The Cell in Development and Heredity. Macmillan, New York.

Woodley, J.D., 1975. The behaviour of some amphiurid brittle-stars. J. Exp. Mar. Biol. Ecol., 18: 29-46.

Yoshida, M., 1952. Some observations on the maturation of the sea urchin, Diadema setosum. Annot. Zool. Jap., 25: 265-271.

Explanation of Plate 1

Fig. 1. Photographs (A, B) and histological cross sections (C-E) of Amphipholis kochii. **A:** The ventral view, partly dissected to show the attachment and arrangement of the testes. Scale, 5 mm. **B:** The testes isolated from one interradial part. Scale, 1mm. **C:** The testis, showing a zonation of spermatogonia (SG), spermatocytes (SC) and spermatozoa together with spermatids (STZ). Scale, 100 μm. **D:** High magnification of the testis in Fig. 1C. From the testicular wall to the inside, spermatogonia (SG), spermatocytes (SC) and spermatozoa together with spermatids (STZ) form zones. Scale, 50 μm. **E:** The amoeboid cell cluster in the sperm mass. Scale, 50 μm.

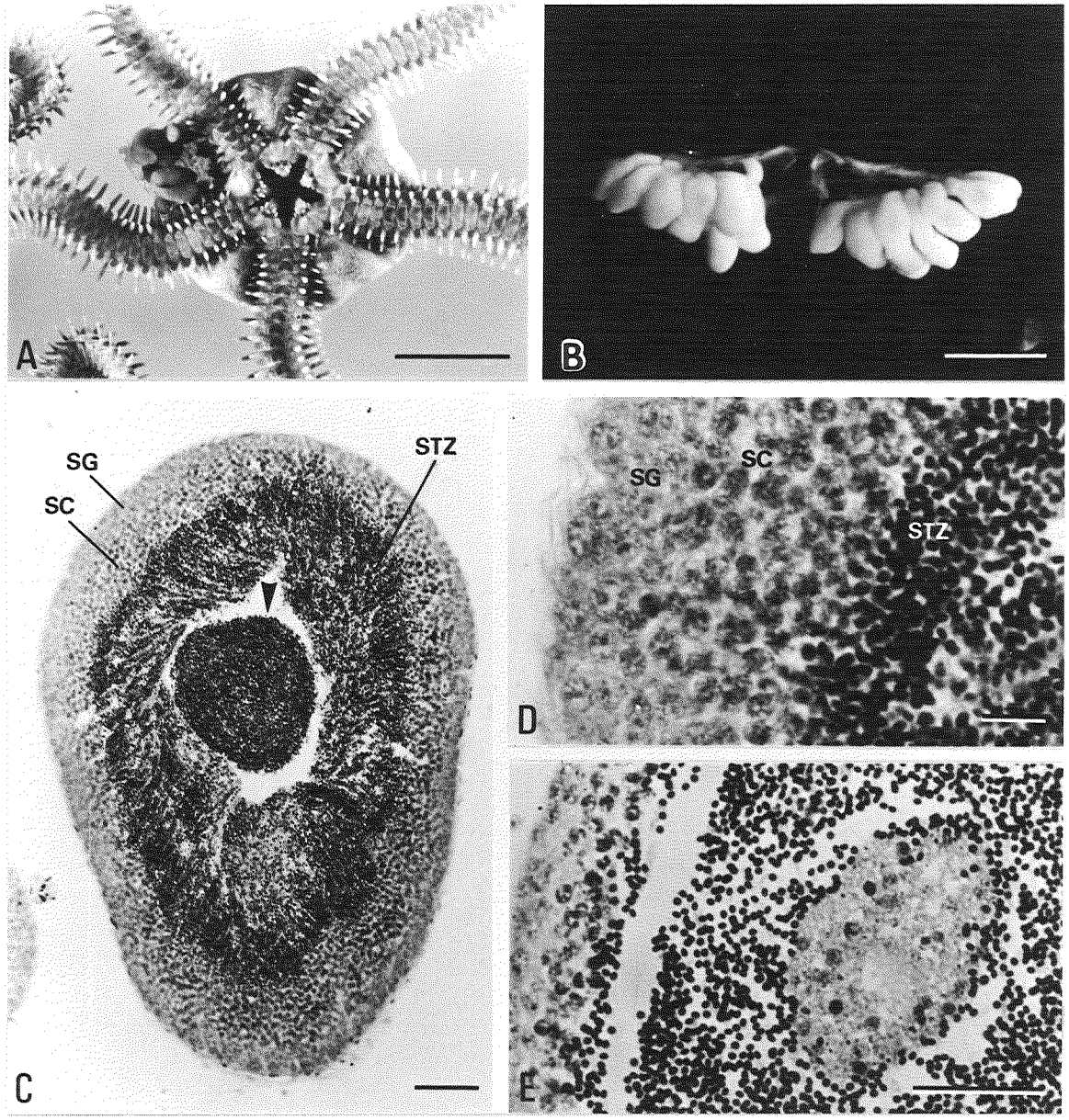
A
B
SG
SC
STZ
C
SG
SC
STZ
D
E

Explanation of Plate 2

Fig. 2. Histological sections of the ovaries of Amphipholis kochii. Scale, 0.1 μm (A), 10 μm (B). **A:** Longitudinal section. Small oocytes are found at the basal portion of the ovary. In the lumen, some residual bodies are still present (arrowhead). **B:** High magnification of the basal region of the ovary, showing the oogonia (OG) and genital rachis (GR).

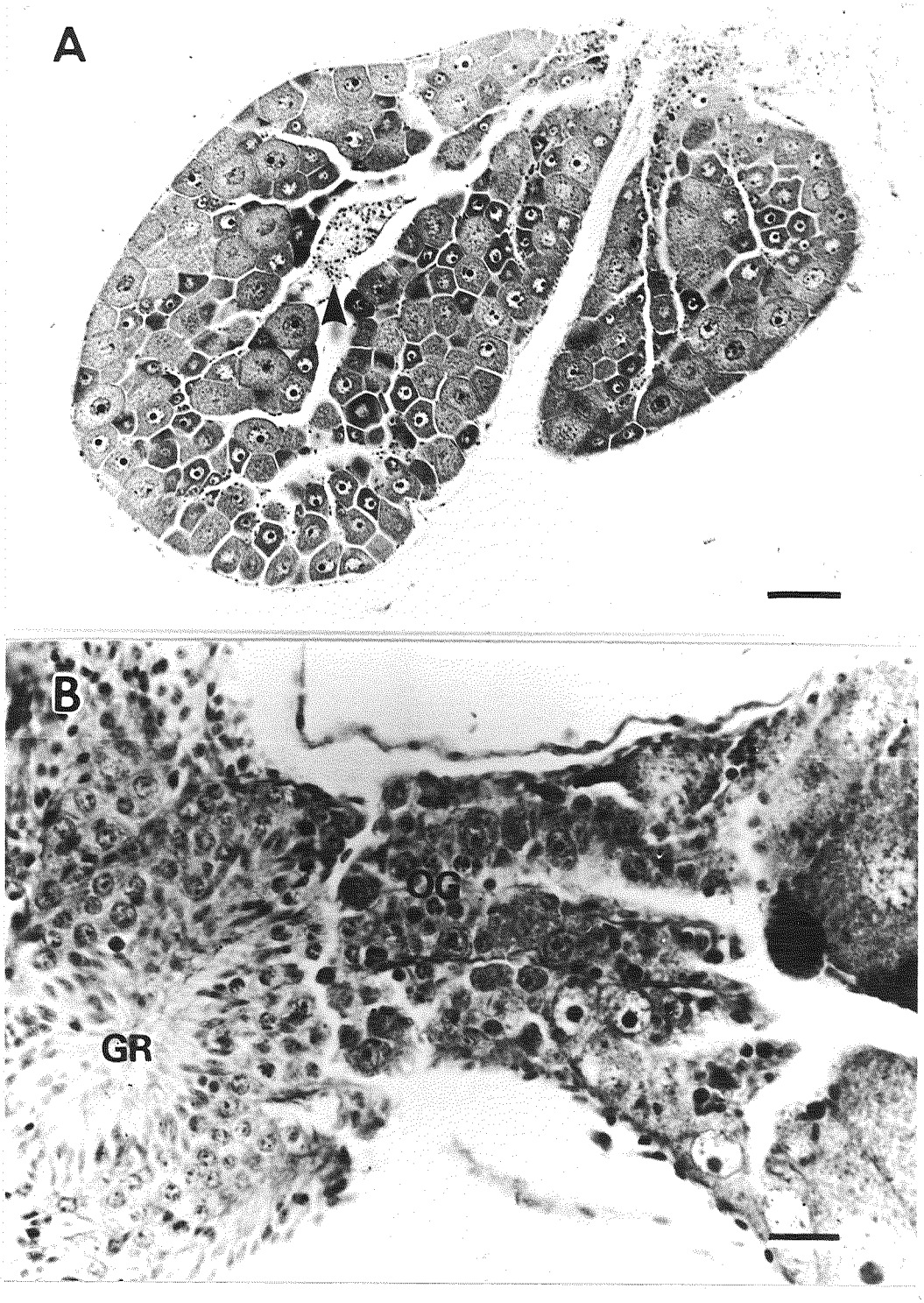
A
B
OG
GR

Explanation of Plate 3

Fig. 3. TEM of the gonadal wall of Amphipholis kochii. Scale, 1 μm. **A:** Transverse section of the gonadal wall. Arrowheads show the cytoplasm of the amoeboid cell in close contact with the genital hemal sinus (GHS). The asterisk indicates the cytoplasm of the cells scattered freely in the connective tissue layer (CTL). BL, basal lamina; CF, collagen fiber; CM, circular muscle fiber; F, flagellum; GCS, genital coelomic sinus; GE, germinal epithelium; HC, hemal cell; IE, inner epithelium of GCS; IS, inner sac; LM, longitudinal muscle fiber; N, nucleus; NE, nerve process; OE, outer epithelium of GCS; OS, outer sac; VP, visceral peritoneum. **B:** The flagellum (F) on the visceral peritoneum. Note that it possesses no collar-like projections around it. **C:** Longitudinal section of the inner epithelium of the genital coelomic sinus, showing the nerve process (NE) and circular muscle fiber (CM). **D:** The amoeboid cell (AC) which comes in contact with the genital hemal sinus (GHS). GE, germinal epithelium; IE, inner epithelium of the genital coelomic sinus.

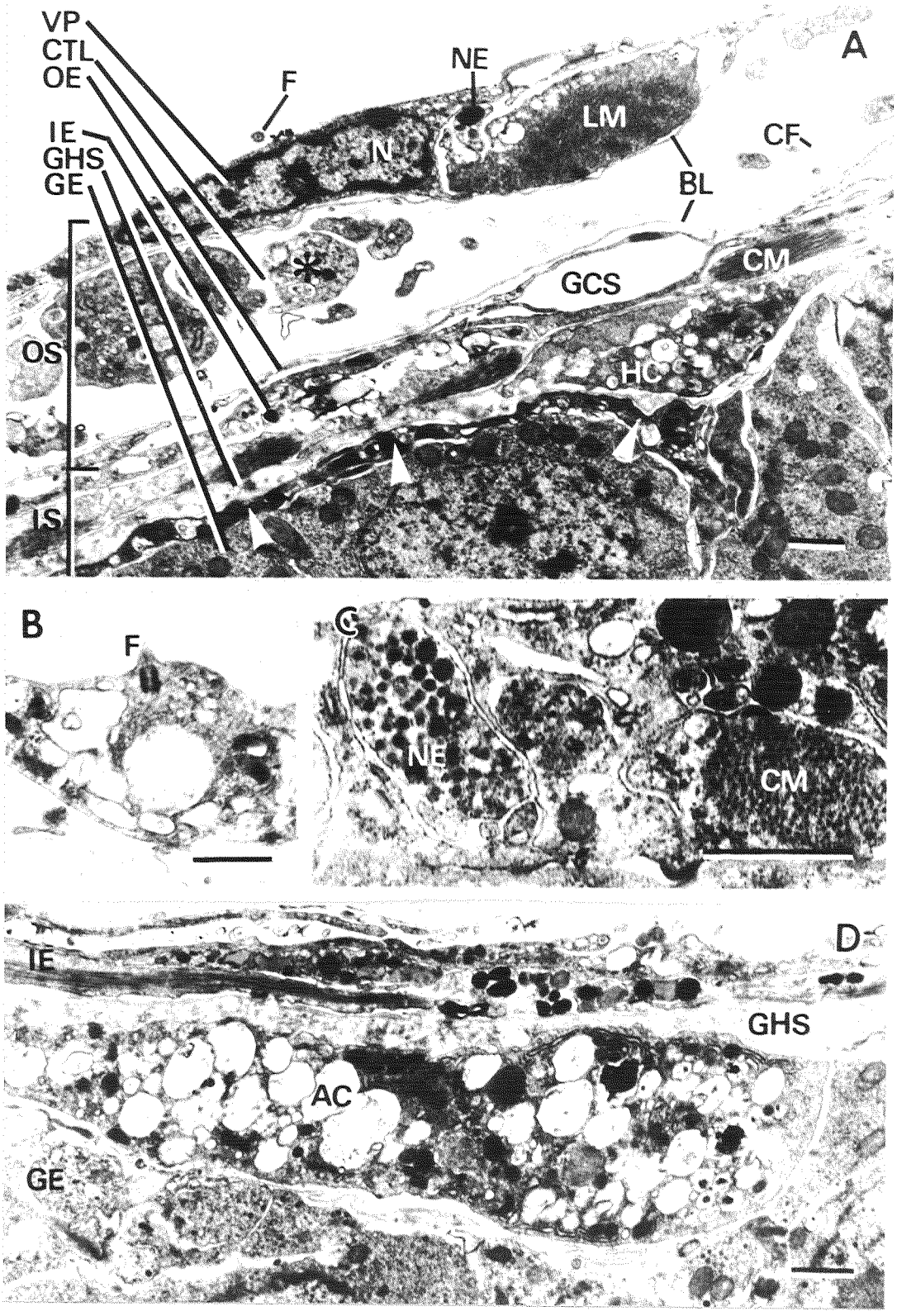
VP
CTL
OE
IE
GHS
GE
OS
IS
F
NE
LM
N
CF
BL
GCS
CM
HC
A
B
F
C
NE
CM
D
IE
GHS
AC
GE

Explanation of Plate 4

Fig. 4. TEM of the amoeboid cells of Amphipholis kochii forming a cluster in the sperm mass. Note the mature spermatozoa (arrows) ingested by the amoeboid cells by a phagocytic activity. In the cytoplasm of the amoeboid cells many residual bodies which are probably derived from degenerate spermatozoa are also seen (arrowheads). Scale, 5 μm.

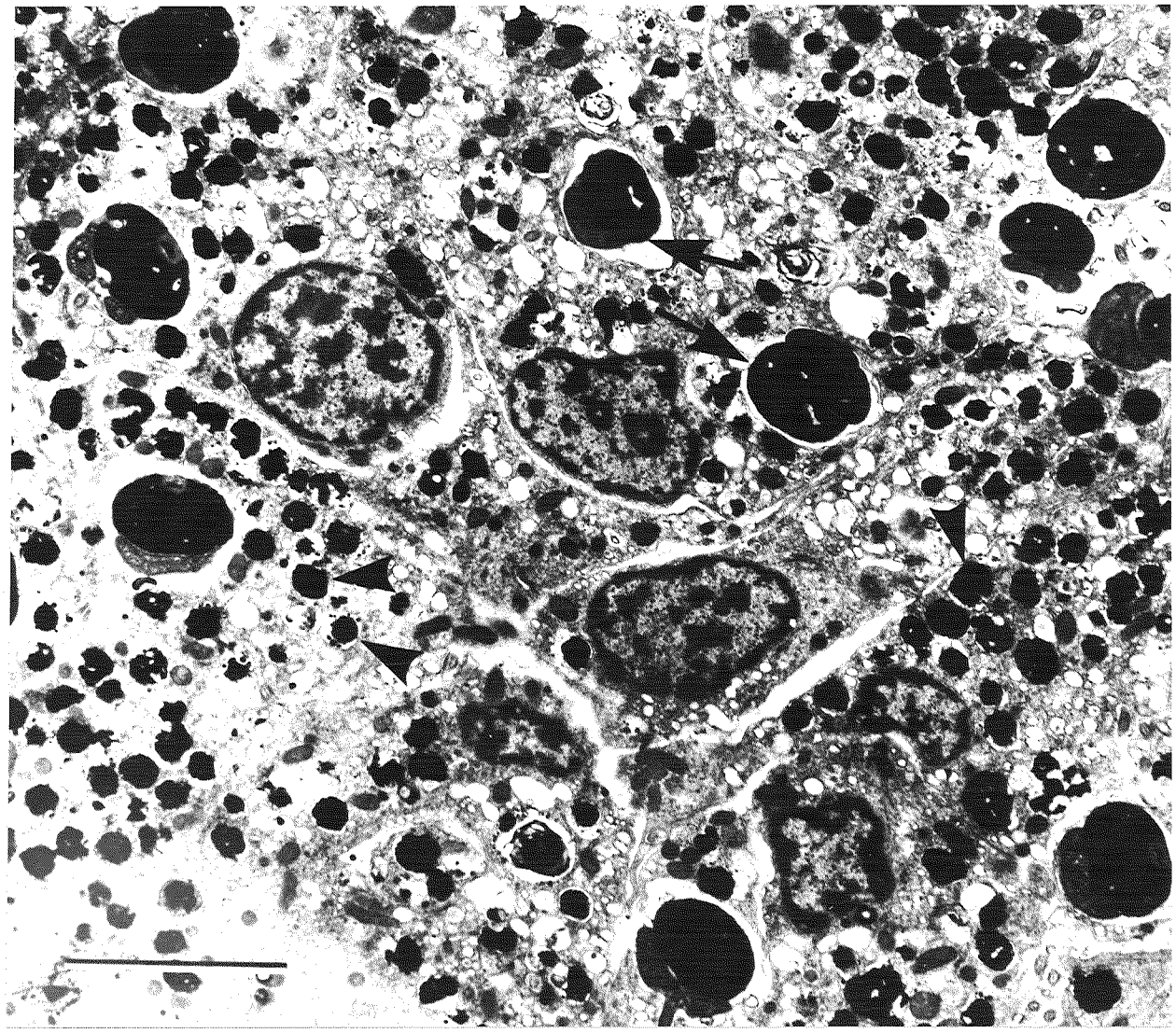

Explanation of Plate 5

Fig. 5. TEM of the gonadal wall of Ophiura sarsii. Scale, 1 μm. **A:** Transverse section of the gonadal wall. BL, basal lamina; CF, collagen fiber; CTL, connective tissue layer; F, flagellum; GCS, genital coelomic sinus; GE, germinal epithelium; GHS, genital hemal sinus; HC, hemal cell; IE, inner epithelium of GCS; IS, inner sac; N, nucleus; NE, nerve process; OE, outer epithelium of GCS; OS, outer sac; VP, visceral peritoneum. **B:** The flagellum (F) with collar-like projections (arrowheads) around it. **C:** Longitudinal section of the gonadal wall, showing the longitudinal muscle fiber (LM) in the visceral peritoneum (VP). GCS, genital coelomic sinus; GE, germinal epithelium. **D:** Longitudinal section of the inner sac, showing the circular muscle fiber (CM) in the inner epithelium (IE) of the genital coelomic sinus (GCS). GE, germinal epithelium. **E:** The amoeboid cell (AC) in close contact with the genital hemal sinus (GHS). GCS, genital coelomic sinus, IE, inner epithelium of GCS. **F:** The amoeboid cell found among the gametogenic (spermatogenic) cells. Note that the spermatozoon (arrowhead) is ingested by the amoeboid cell with phagocytic action.

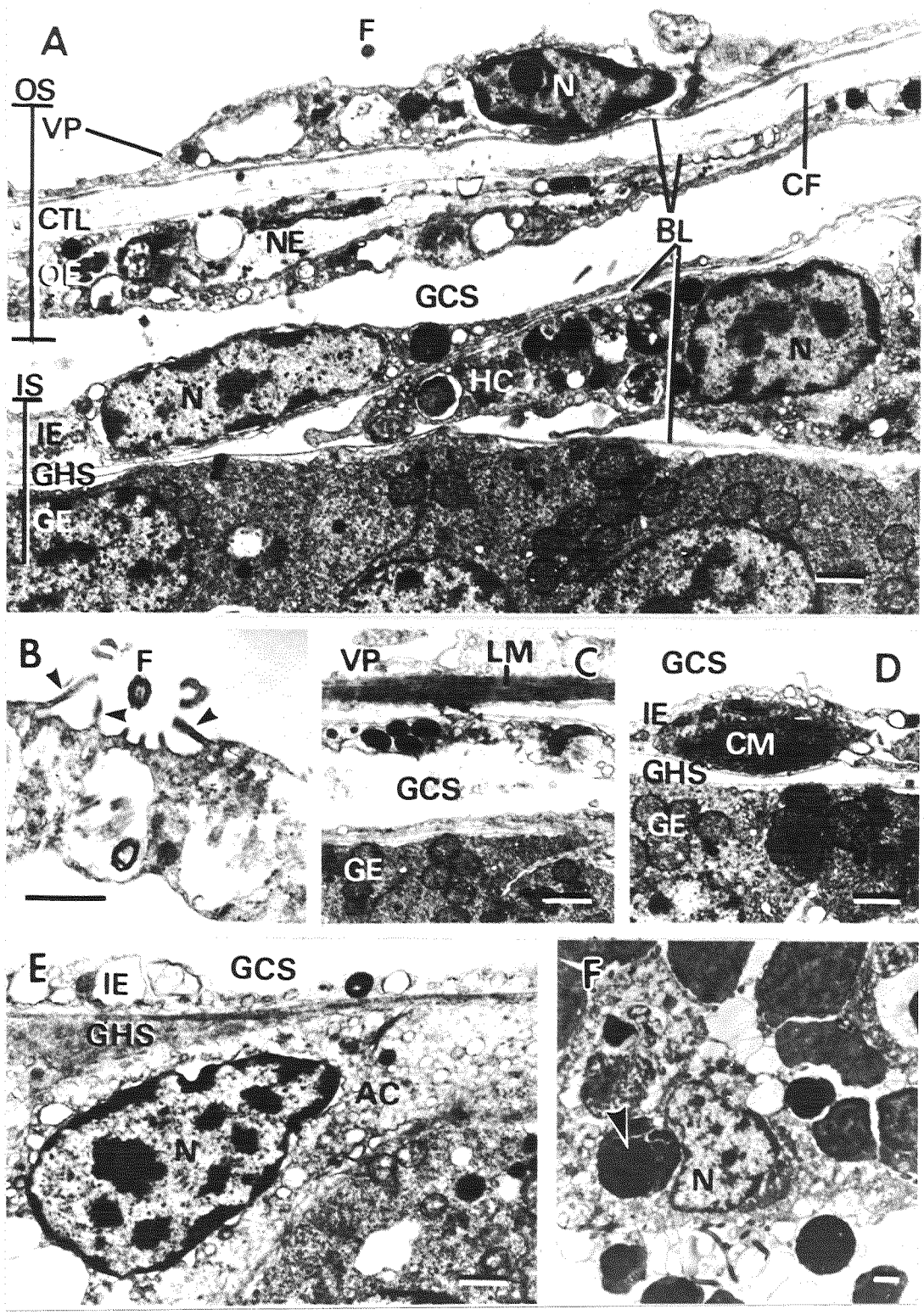
A
F
OS
VP
N
CF
CTL
NE
BL
OE
GCS
N
IS
N
HC
IE
GHS
GE
B
F
VP
LM
C
GCS
D
IE
CM
GHS
GE
GCS
GE
E
IE
GCS
GHS
AC
N
F
N

Explanation of Plate 6

Fig. 6. TEM of the spermatogonia in Amphipholis kochii. Scale 1 µm. **A:** The spermatogonium possesses large nucleus (N) with nucleolus (NO), small tubular or ovoid mitochondria (M), Golgi apparatus (G) near the proximal (PC) and distal (DC) centrioles and the electron dense materials (arrowheads) either near or in contact with the nuclear envelope. **B:** Peripheral cytoplasm of the spermatogonium, showing the rootlet associated with the distal centriole (DC). G, Golgi apparatus; PC, proximal centriole. **C:** The spermatogonium in which proacrosomal vesicles are produced by Golgi apparatus (outlined region). **D:** High magnification of the region outlined in Fig. 6C, showing the proacrosomal vesicle (arrowhead) produced by Golgi apparatus (G).

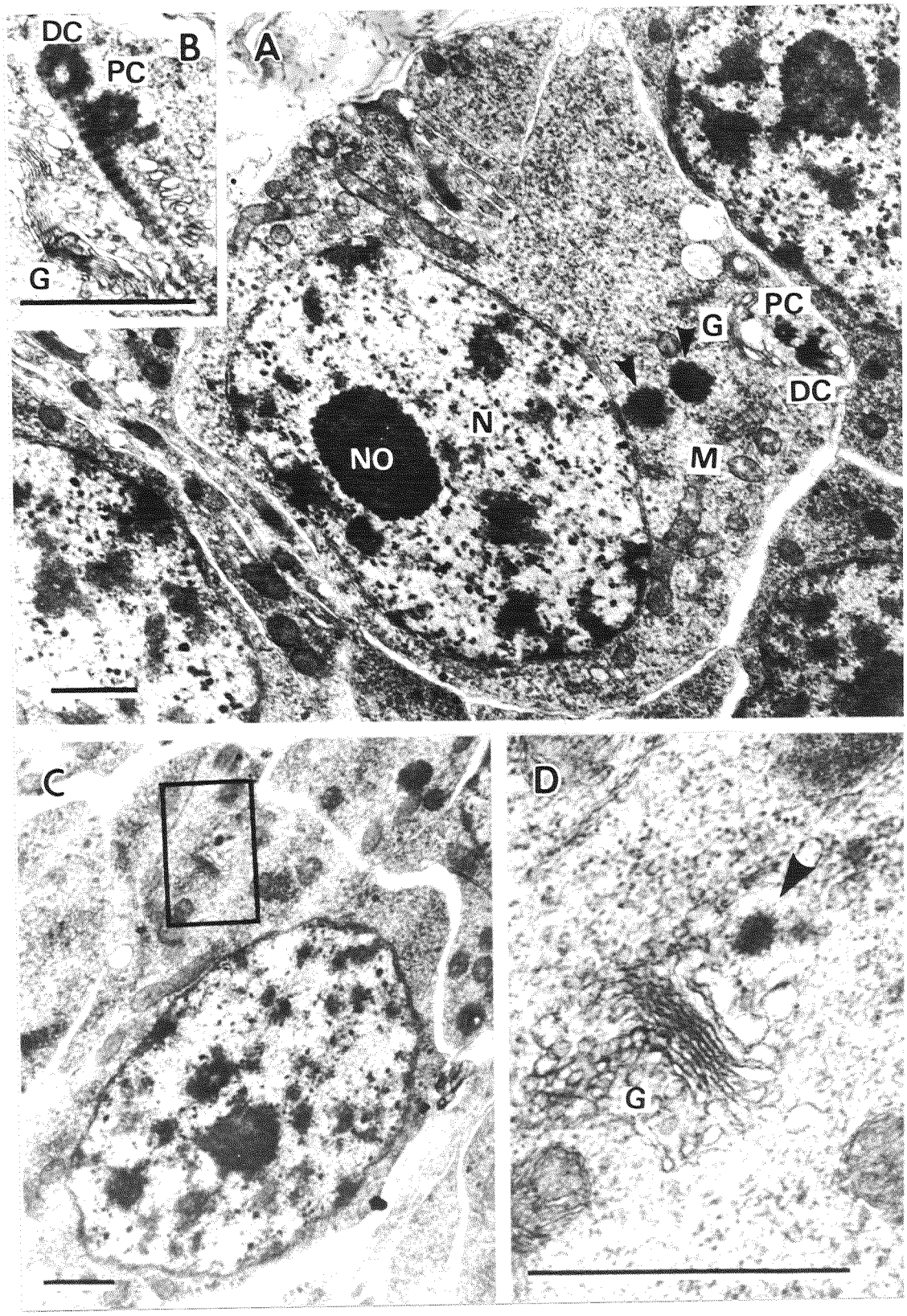
DC
PC
B
G
A
G
PC
DC
N
NO
M
C
D
G

Explanation of Plate 7

Fig. 7. TEM of the spermatogonia in Amphipholis kochii. Scale, 1 μm. **A:** The spermatogonium, showing endoplasmic reticulum (ER) and prominent nucleolus (NO). **B:** High magnification of the region outlined in Fig. 7A. Arrowhead indicates the proacrosomal vesicle produced by Golgi apparatus (G). Desmosome-like junction (DJ) is also seen between the spermatogonia.

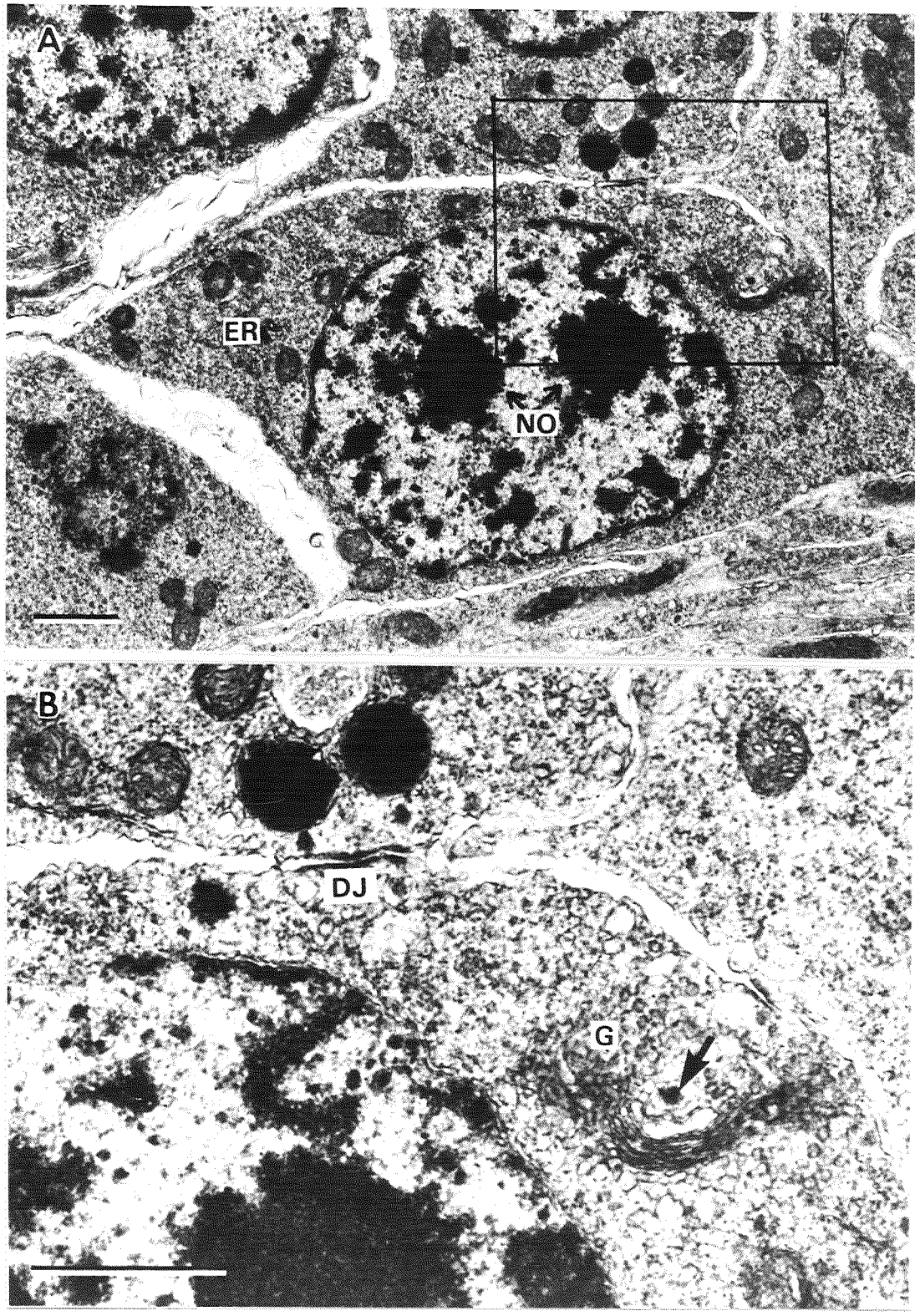
A
ER
NO
G
B
DJ
G

Explanation of Plate 8

Fig. 8. TEM of the spermatocytes in Amphipholis kochii. Scale, 1 μm (A), 0.5 μm (B). **A:** The spermatocyte, having more condensed nucleus (N) than that of the spermatogonium. Mitochondria (M) and Golgi apparatus (G) near the centriole (C) are seen in the cytoplasm. **B:** High magnification of the region outlined in Fig. 8A, showing the proacrosomal vesicles (arrowheads) formed by Golgi apparatus (G) near the centriole (C).

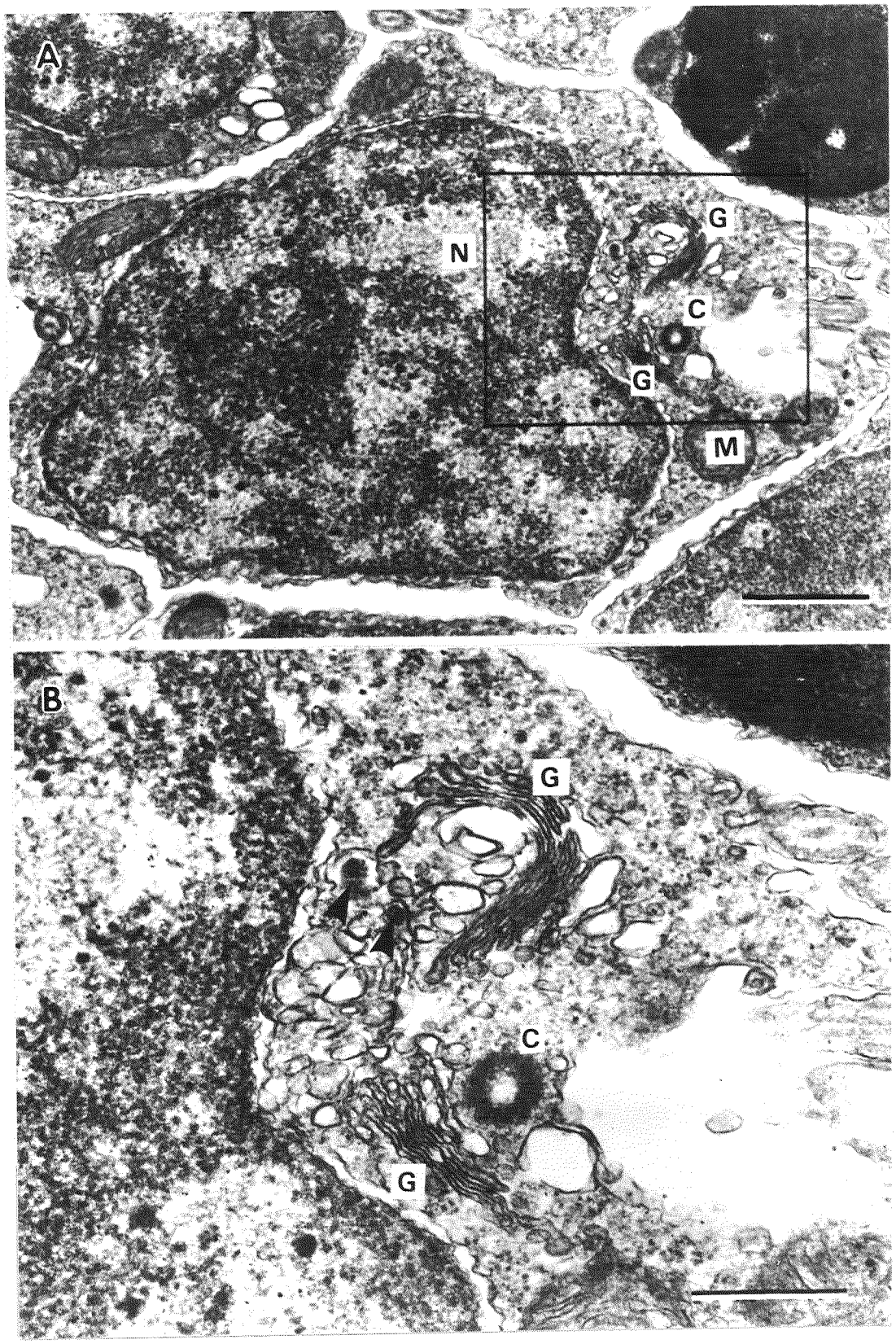
A
N
G
C
G
M
B
G
C
G

Explanation of Plate 9

Fig. 9. TEM of the spermatids (A-D) and spermatozoa (E, F) in Amphipholis kochii. Scale, 1 μm. **A:** The early spermatid, showing a circular acrosomal vesicle (AR) located at the posterior portion of the cell and the proximal (PC) and distal (DC) centrioles which remain perpendicular to each other. G, Golgi apparatus; M, mitochondrion; N, nucleus. **B:** The sper matid more advanced than that in Fig. 9A. The acrosomal vesicle (AR) is transported to the anterior portion of the cell. A shallow indentation (arrowhead) of the nucleus (N) is seen beneath the acrosome. Golgi apparatus (G) and the proximal (PC) and distal (DC) centrioles are still seen in the posterior cytoplasm. **C:** The spermatid more developed than that in Fig. 9B, showing the deep cup-shaped acrosomal fossa (arrowhead) at the apex of the nucleus (N). **D:** The late spermatid. The cytoplasm is confined to the posterior portion of the cell, where mitochondria (M) gather to form sperm mitochondrion. Note the acrosomal vesicle (AR) different in shape. Nuclear vacuoles (NV) are seen in the condensed nucleus. The flagellum (arrowhead) originated from the distal centriole (DC) extends at an angle of about 30° from the antero-posterior axis of the sperm. **E:** Slightly oblique section of the mature spermatozoon. Arrowhead shows the proximal centriole lying at an angle of about 30° from the axis of the distal centriole (DC). M, mitochondrion. **F:** Longitudinal section of the mature spermatozoon and transverse section of the sperm tail. White arrowhead indicates the centriolar fossa and black arrowheads show the lateral expansion of the flagellar membrane. AR, acrosomal vesicle; M, mitochondrion; NV, nuclear vacuole.

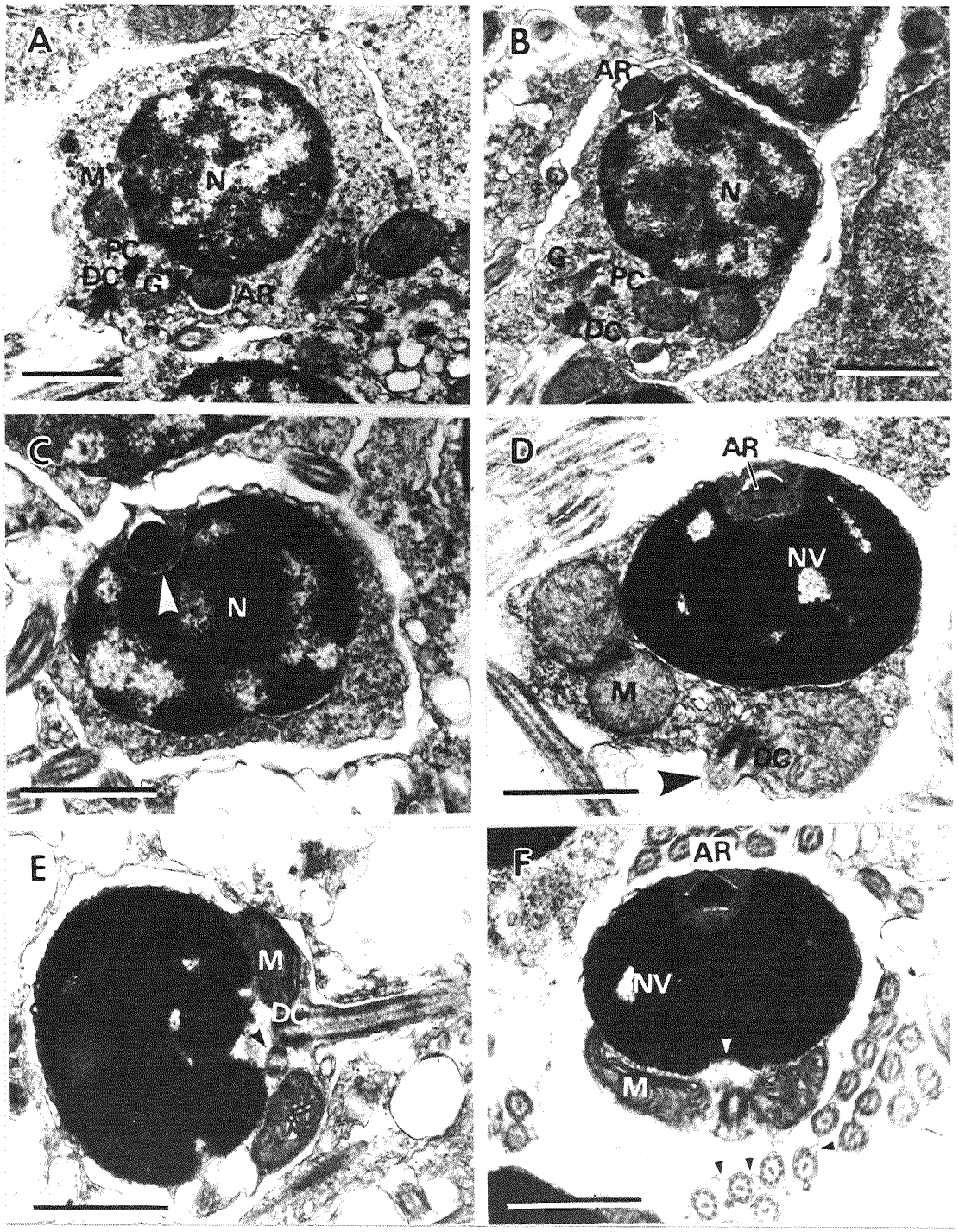
A
M
N
PC
DC
G
AR
B
AR
N
G
PC
DC
C
N
D
AR
NV
M
DC
E
M
DC
F
AR
NV
M

Explanation of Plate 10

Fig. 10. TEM of the centriolar satellite complex (A, B) and the early spermatids (C) of Amphipholis kochii. Scale, 0.1 μm (A, B), 1 μm (C). **A:** Transverse section of the centriolar satellite region. Nine spoke-like satellites emanate from the dense matrix of the distal centriole. **B:** Transverse section through the proximal tip of the central microtubules (arrowheads) of the flagellum. Nine Y-shaped connectives are seen. **C:** The spermatids jointed by intercellular bridges (arrowheads).

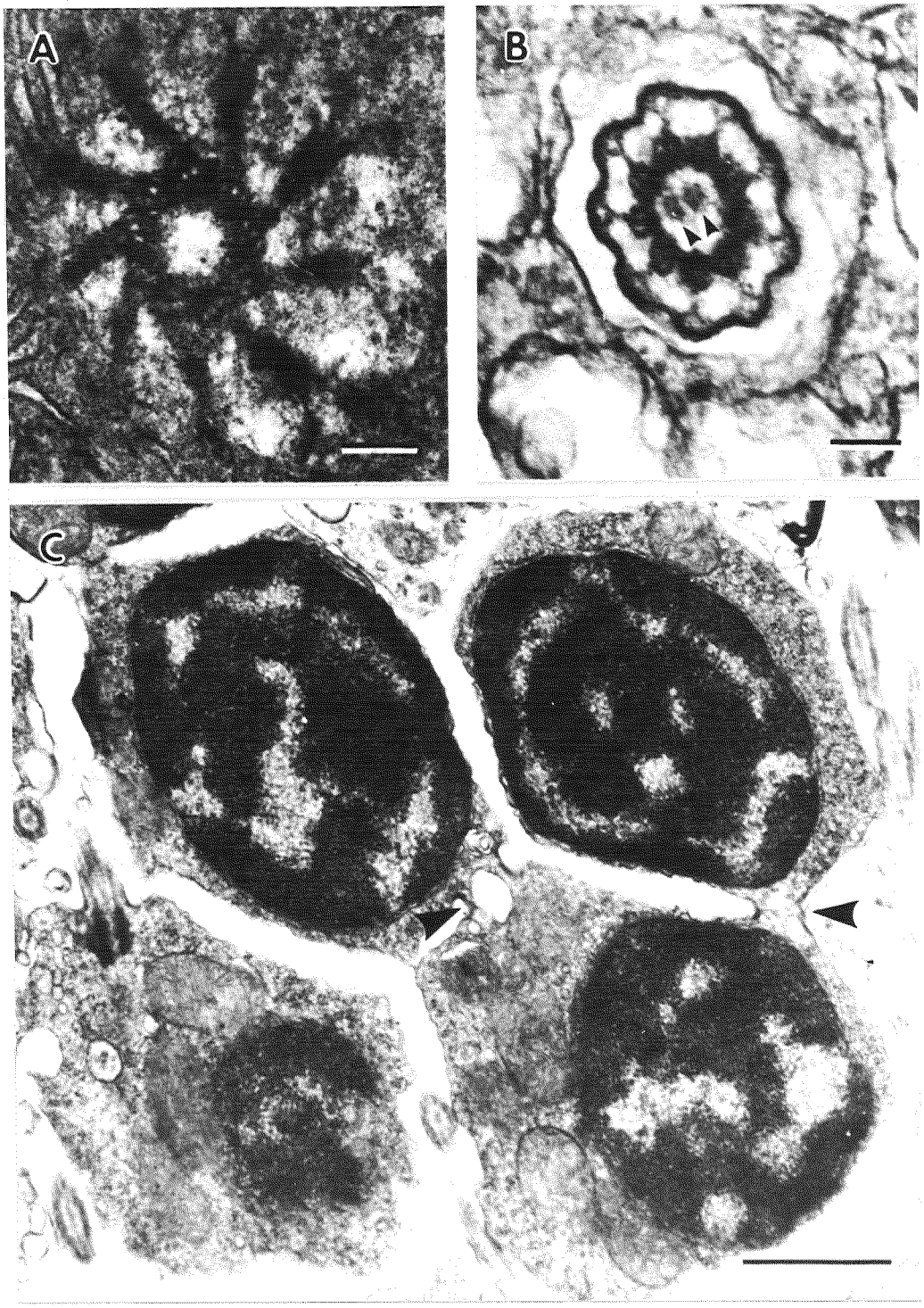
A
B
C

Explanation of Plate 11

Fig. 11. TEM of the acrosomal vesicles during spermiogenesis in Amphipholis kochii. Scale, 0.1 μm. **A:** The acrosomal vesicle (AR) during its formation by fusion of the proacrosomal vesicles (arrowheads) produced by Golgi apparatus (G). N, nucleus. **B:** High magnification of the acrosomal vesicle transported to the anterior portion of the cell. The membrane of the acrosomal vesicle is dense at the basal half (arrowheads). Arrow shows fibrous materials between the acrosomal vesicle and nucleus. **C:** High magnification of the acrosomal vesicle (AR) more developed than that in Fig. 11B. Fibrous materials between the acrosomal vesicle and nucleus form periacrosomal layer (P). Arrowheads indicate that the vesicle membrane is dense at the basal half. **D:** High magnification of the mature acrosomal vesicle. The fully-formed acrosomal vesicle is hat-shaped and condensed at the crown. Note the periacrosomal materials (P) organized as a fibrous tuft beneath the base of the acrosomal vesicle (double-arrowhead). Single-arrowheads show the denser part of the vesicle membrane.

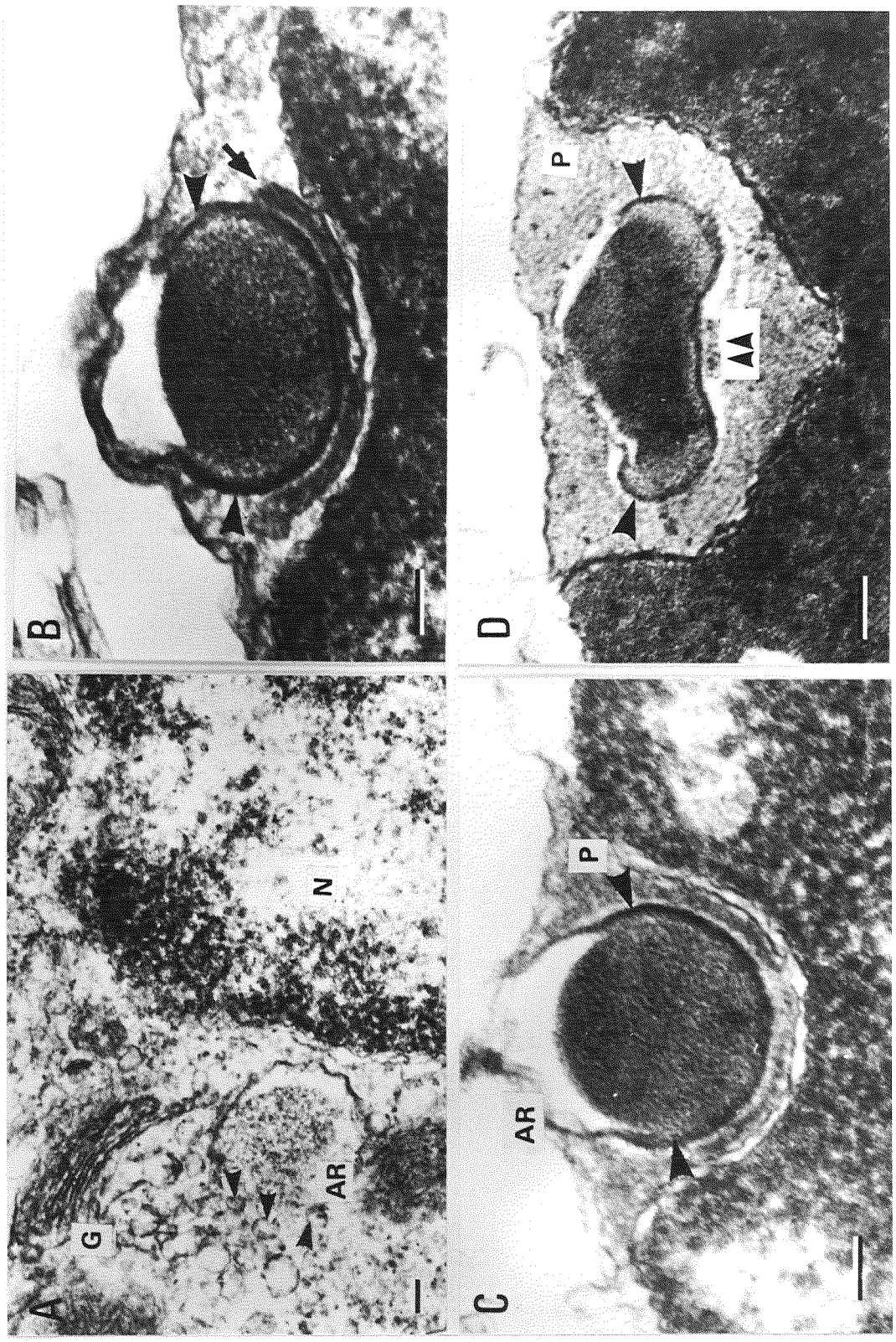
A
G
N
AR
B
C
AR
P
D
P

Explanation of Plate 12

Fig. 12. TEM of the spermatogonia in Ophiura sarsii. Scale, 1 μm (A, B), 0.5 μm (C-E). **A:** The spermatogonium has large nucleus (N) with nucleolus (NO). Note the proacrosomal vesicles (arrowheads) produced by Golgi apparatus (G). Mitochondria (M) and desmosome-like junction (DJ) are also seen. **B:** Arrowheads indicate the dense materials specific to the germ line cells. G, Golgi apparatus; M, mitochondrion; N, nucleus; NO, nucleolus. **C:** The proximal (PC) and distal (DC) centrioles near Golgi apparatus (G). **D:** The rootlet found in the peripheral cytoplasm of the spermatogonium. **E:** High magnification of the Golgi region of the spermatogonium in Fig. 12A, showing the proacrosomal vesicles (arrowheads) produced by Golgi apparatus (G).

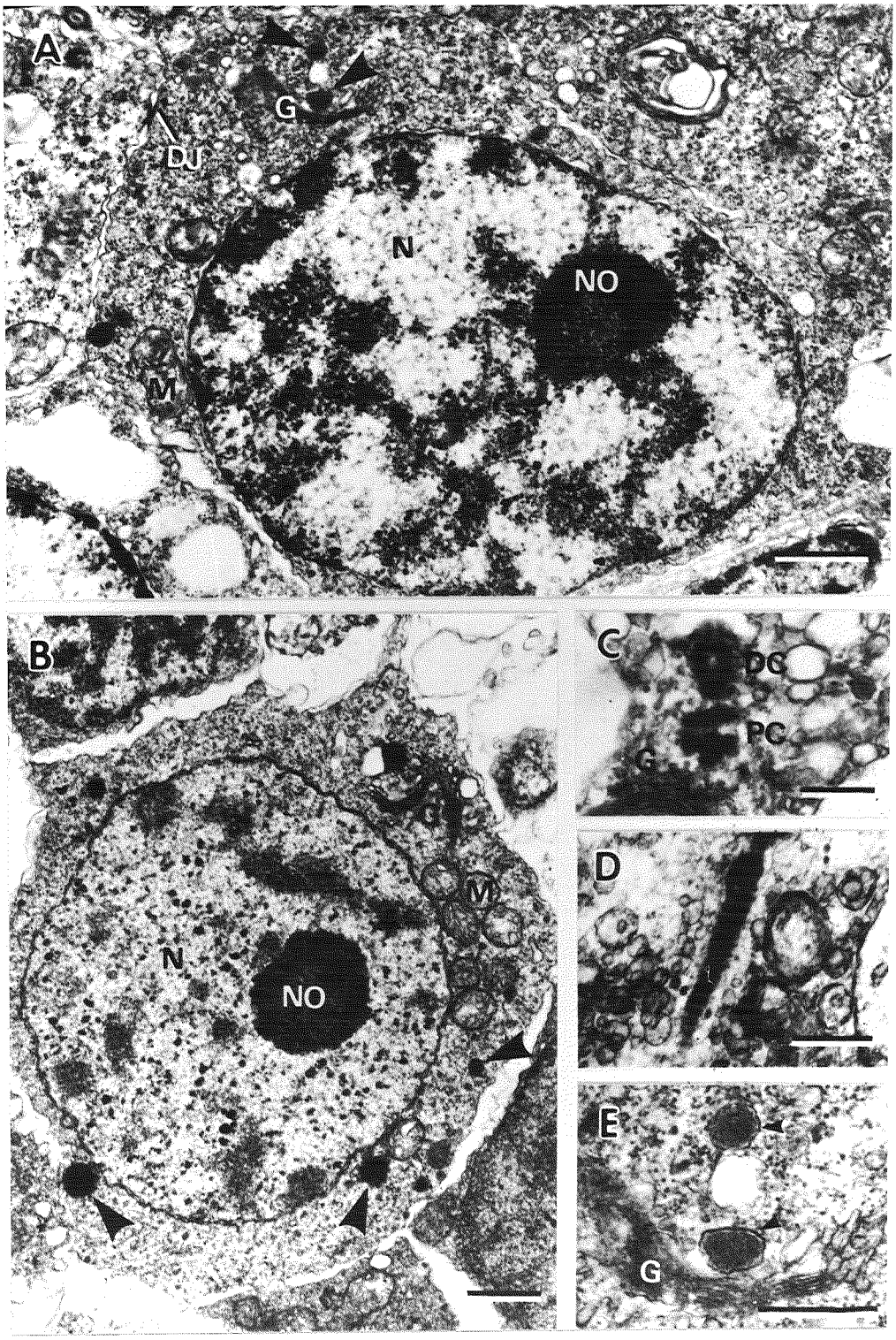
A
G
DJ
N
NO
M
B
N
NO
M
C
DC
PC
D
E
G

Explanation of Plate 13

Fig. 13. TEM of the spermatocytes in Ophiura sarsii. Scale, 1 μm (A, C), 0.5 μm (B). **A:** The spermatocyte has more condensed nucleus (N) than that of the spermatogonium. Note the proacrosomal vesicle (arrowhead) produced by Golgi apparatus (G). DJ, desmosome-like junction; M, mitochondrion. **B:** The Golgi region of the primary spermatocyte, showing the proacrosomal vesicles (arrowheads) formed by Golgi apparatus (G). N, nucleus. **C:** The primary spermatocyte with flagellum (F). Arrowhead indicates the rootlet associated with the distal centriole (DC). The proximal centriole (PC) near the Golgi apparatus (G) is also seen. M, mitochondrion; N, nucleus.

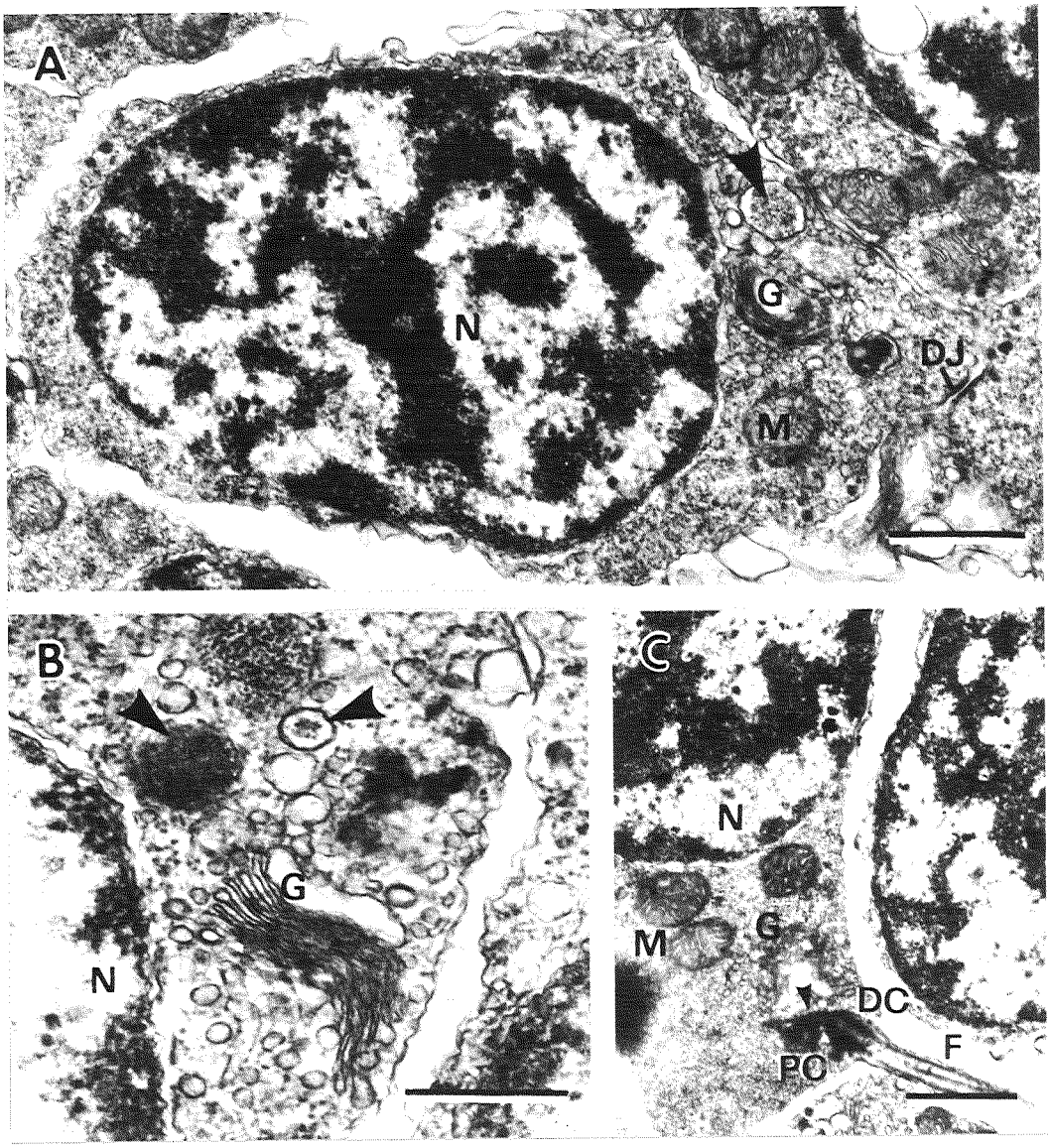
A
N
G
DJ
M
B
G
N
C
N
M
G
DC
PC
F

Explanation of Plate 14

Fig. 14. TEM of the spermatids in Ophiura sarsii. Scale, 1 μm (A-C, H), 0.5 μm (D-G). **A:** The early spermatid, in which circular nucleus (N), mitochondria (M), flagellum (F) and acrosomal vesicle (AR) produced by Golgi apparatus (G) near the proximal (PC) and distal (DC) centrioles are seen. **B:** More developed spermatid than that of Fig. 14A. Arrowhead shows the indentation of the nucleus (N). Note the transportation of the acrosomal vesicle (AR) to the anterior portion of the cell. M, mitochondrion. **C:** The late spermatid. The nucleus (N) is condensed leaving the nuclear vacuoles (NV). The acrosomal vesicle (AR) has been transported to the anterior portion but other organella such as mitochondria (M) and Golgi apparatus (G) remain at the posterior portion. Arrowhead indicates that the acrosomal fossa is deeper at its center. **D:** The proacrosomal vesicles in the early spermatid, showing their fusion (arrowhead). G, Golgi apparatus. **E:** The acrosomal vesicle in the early spermatid. Note that the contents differentiate into two regions and that the plate-like structure is associated with the vesicle membrane (arrowhead). **F:** High magnification of the acrosomal region in Fig. 14B. Arrowheads show fibrous materials which are the precursors of the periacrosomal layer. N, nucleus. **G:** High magnification of the acrosomal region in Fig. 14C. The periacrosomal layer (P) has been formed. N, nucleus. **H:** The spermatids jointed by the intercellular bridge (arrowhead).

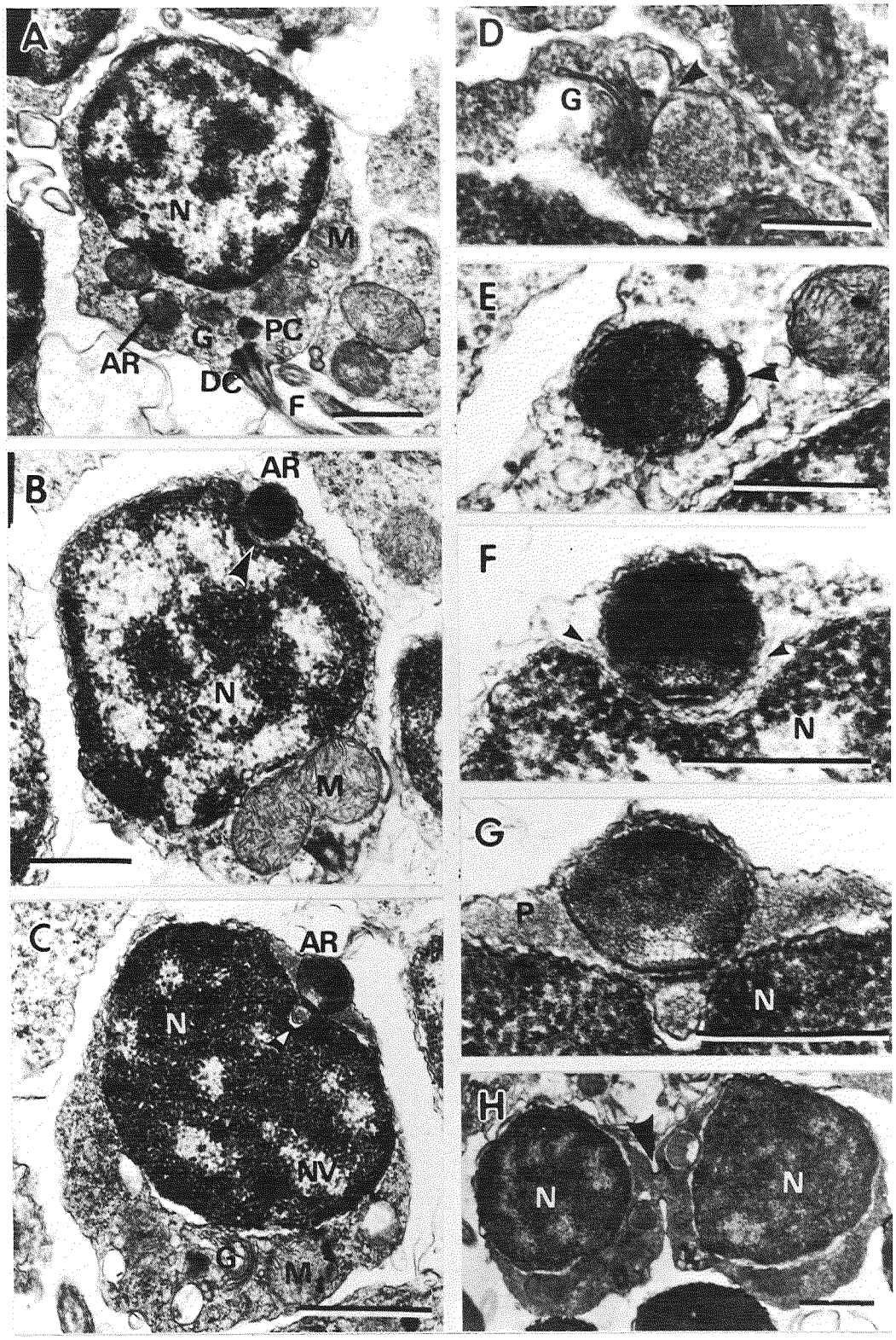
A
N
M
AR
G
PC
DC
F
B
AR
N
M
C
AR
N
NV
G
M
D
G
E
F
N
G
P
N
H
N
N

Explanation of Plate 15

Fig. 15. TEM of the spermatozoa in Ophiura sarsii. Scale, 0.5 μm (A, B), 0.1 μm (C-F). **A:** Longitudinal section, showing the acrosomal vesicle (AR), periacrosomal layer (P), nucleus (N) with nuclear vacuoles (NV) and mitochondrion (M). Arrowhead shows the acrosomal fossa which is deeper at its center. **B:** Slightly oblique section, showing the caudal portion of the spermatozoon. The nucleus (N) is slightly indented at its posterior end (white arrowhead). Black arrowheads show the centriolar satellite complex associated with the distal centriole (DC). The proximal centriole (PC) lies about 30° from the axis of the distal one. F, flagellum; M, mitochondrion. **C:** High magnification of the acrosomal region of Fig. 15A. The plate-like structure is found beneth the acrosomal vesicle (arrowhead). P, periacrosomal layer. **D:** The transverse section through the distal centriole, showing the nine spoke-like satellites. **E:** Transverse section through the proximal tip of the central microtubules of the flagellum, showing the nine Y-shaped connectives. **F:** Transverse section of the flagellum. The lateral expansions of the flagellar membrane are seen (arrowheads).

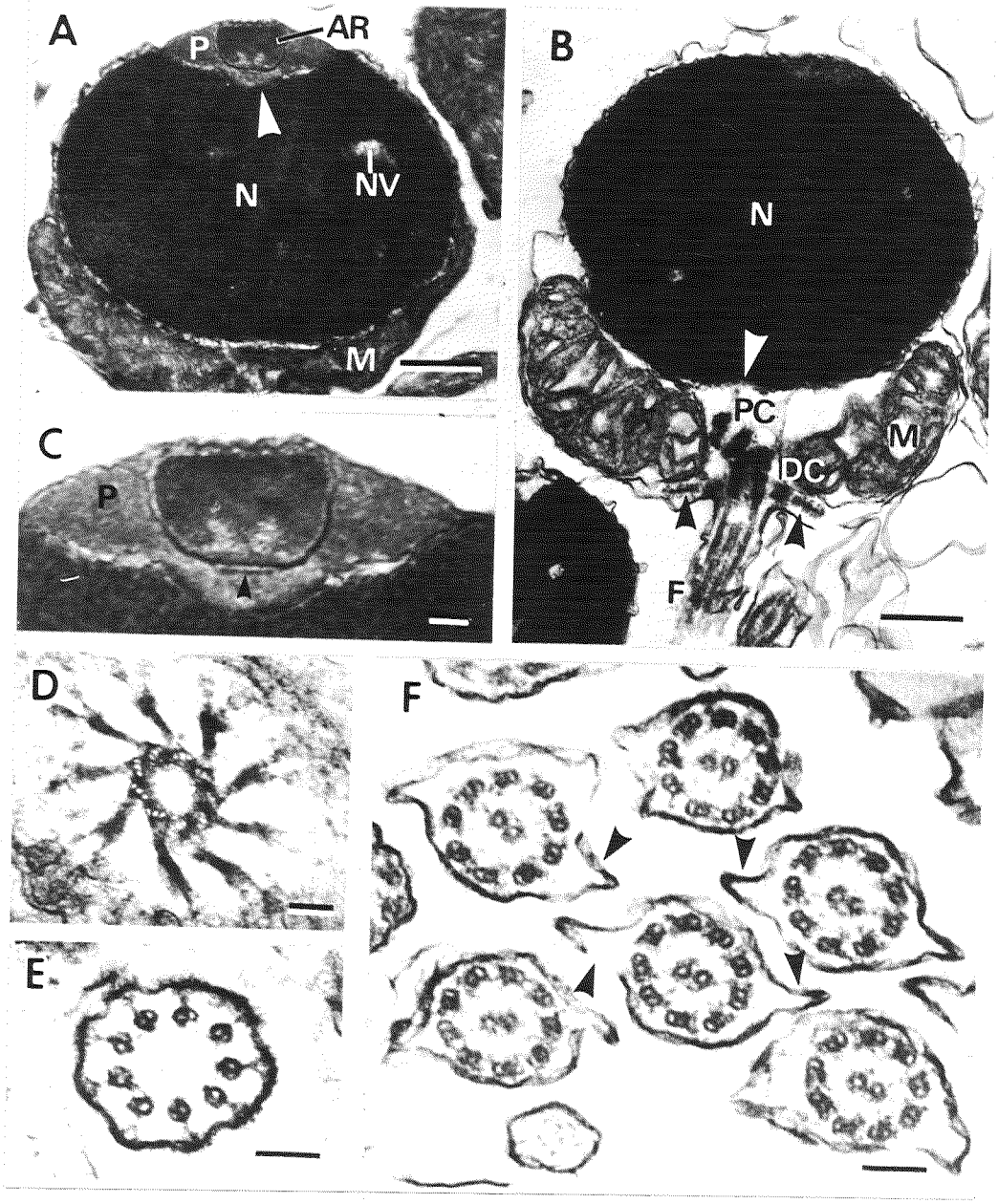
A
P
AR
N
NV
M
B
N
PC
M
DC
F
C
P
D
E
F

Explanation of Plate 16

Fig. 16. Histological sections of the gonad in stage 0 (unsexuable) and the testes in each gonadal stage of *Amphipholis kochii*. Scale, 100 μm (A-D), 200 μm (E, F). **A:** Stage 0. Arrowhead shows the post-spawning debris. **B:** Stage 1. **C:** Stage 2. **D:** Stage 3. **E:** Stage 4. **F:** Stage 5.

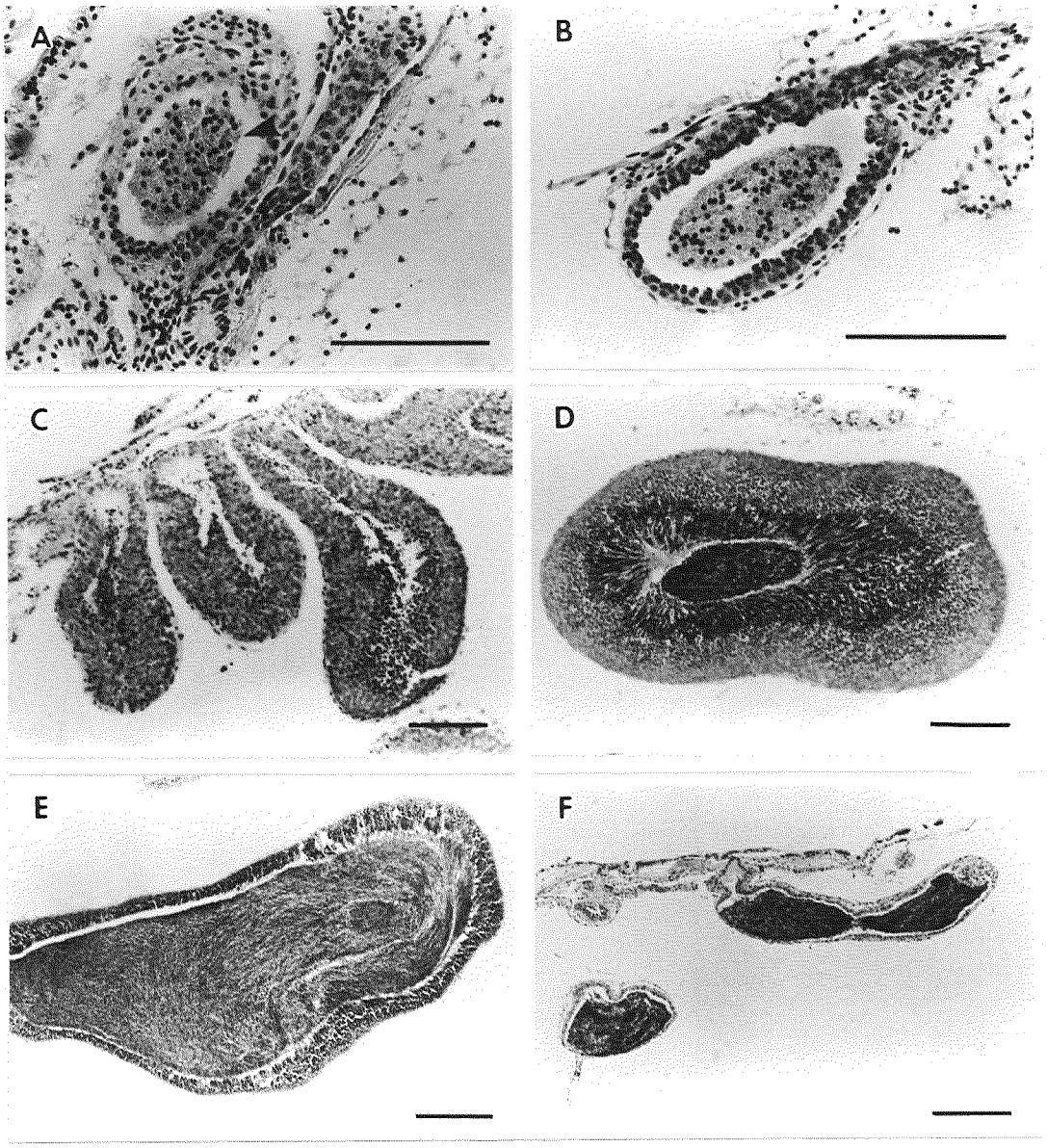
A
B
C
D
E
F

Explanation of Plate 17

Fig. 17. Histological sections of the ovaries of five gonadal stages in Amphipholis kochii. Scale, 100 µm (A, B, D), 200 µm (C, E, F). **A:** Stage 1. **B:** Stage 2. **C:** Stage 3. **D:** Cytoplasmic globules (arrowheads) in ovary of stage 3. **E:** Stage 4. **F:** Stage 5.

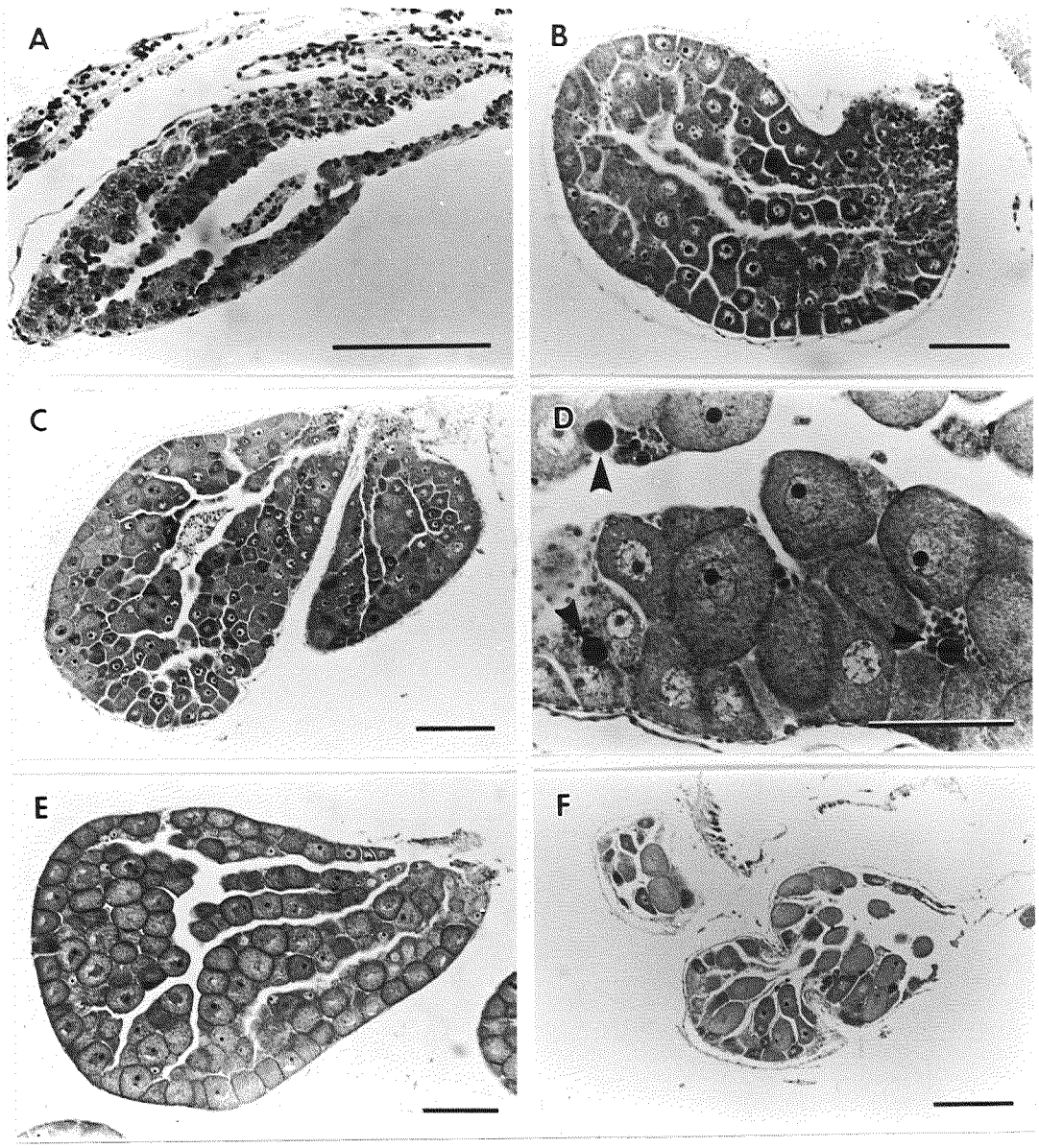
A
B
C
D
E
F

Explanation of Plate 18

Fig. 18. Autoradiograms from the testes of Amphipholis kochii injected with ^{3}H-thymidine. Animals were collected at various seasons and reared under experimental conditions. Testes in March reared at 5°C (A-C); Testis in November reared at 16°C (D). Scale, 10 μm. **A:** 1 hour after injection. The silver grains are heavily developed over the spermatogonia (SG) and spermatocytes (SC) but none over the spermatids (arrowheads) and spermatozoa (arrows). **B:** 14 days after injection. Grains are found in the spermatids (arrowheads) but not in the spermatozoa. **C:** 18 days after injection. The spermatozoa (arrows) have been labeled. **D:** 10 days after injection. The labeled spermatozoa (arrows) have been ingested in the cytoplasm of the amoeboid cells forming a cluster.

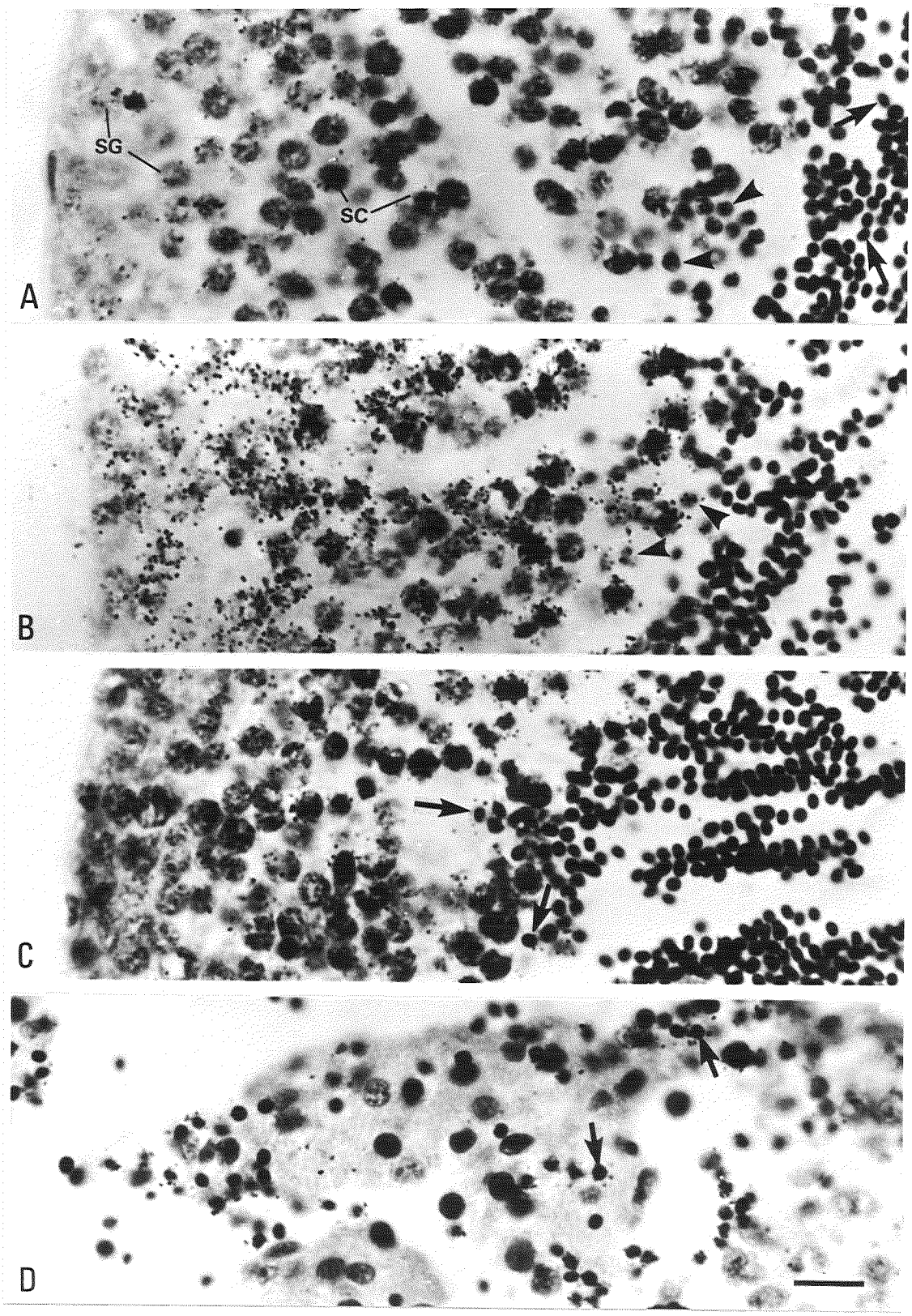
SG
SC
A
B
C
D

Explanation of Plate 19

Fig. 19. Shedding posture of *Amphipholis kochii* induced by the temperature shock. Scale, 5 mm.

Plate 19

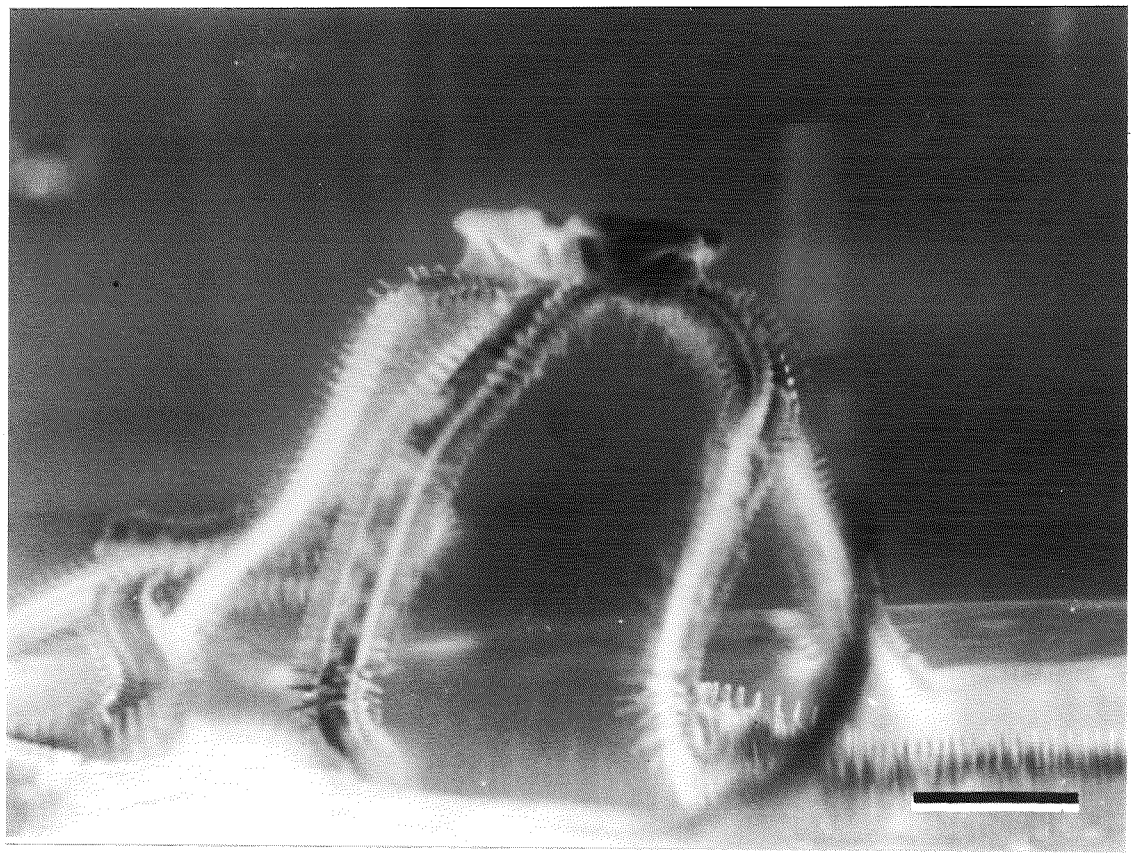

Explanation of Plate 20

Fig. 20. LM of eggs and early embryos of Amphipholis kochii. Scale, 20 μm. **A:** Unfertilized egg in the sea water containing India ink in order to show the jelly coat. Arrowhead indicates the spindle of the first meiotic metaphase. Lateral View. **B:** Fertilized egg surrounded by the fertilization membrane (FM) and the hyaline layer (HL). The swelling of the hyaline layer at the animal pole (arrowhead) is the elimination site of the first polar body. Lateral view. **C:** High magnification of the animal polar region of the fertilized egg, showing the first and second polar bodies (arrowhead). **D:** 2-cell stage embryo. Lateral view. **E:** Regular 4-cell stage embryo. Animal polar view. **F:** Irregular 4-cell stage embryo. Animal polar view. Note the irregular arrangement of the blastomeres. **G:** Regular 8-cell stage embryo. Lateral view. **H:** Irregular 8-cell stage embryo. Lateral view. **I:** Blastula having a narrow blastocoel (BC). **J:** Swimming blastula. Primary mesenchyme (P) immigrates to the blastocoel. The posterior pole of the hyaline layer is thick (arrowhead). **K:** Swimming blastula slightly compressed to show vacuoles in the animal polar wall (arrowheads). Primary mesenchyme occupies almost the whole space of the blastocoel. **L:** Gastrula. Arrowhead indicates the archenteron.

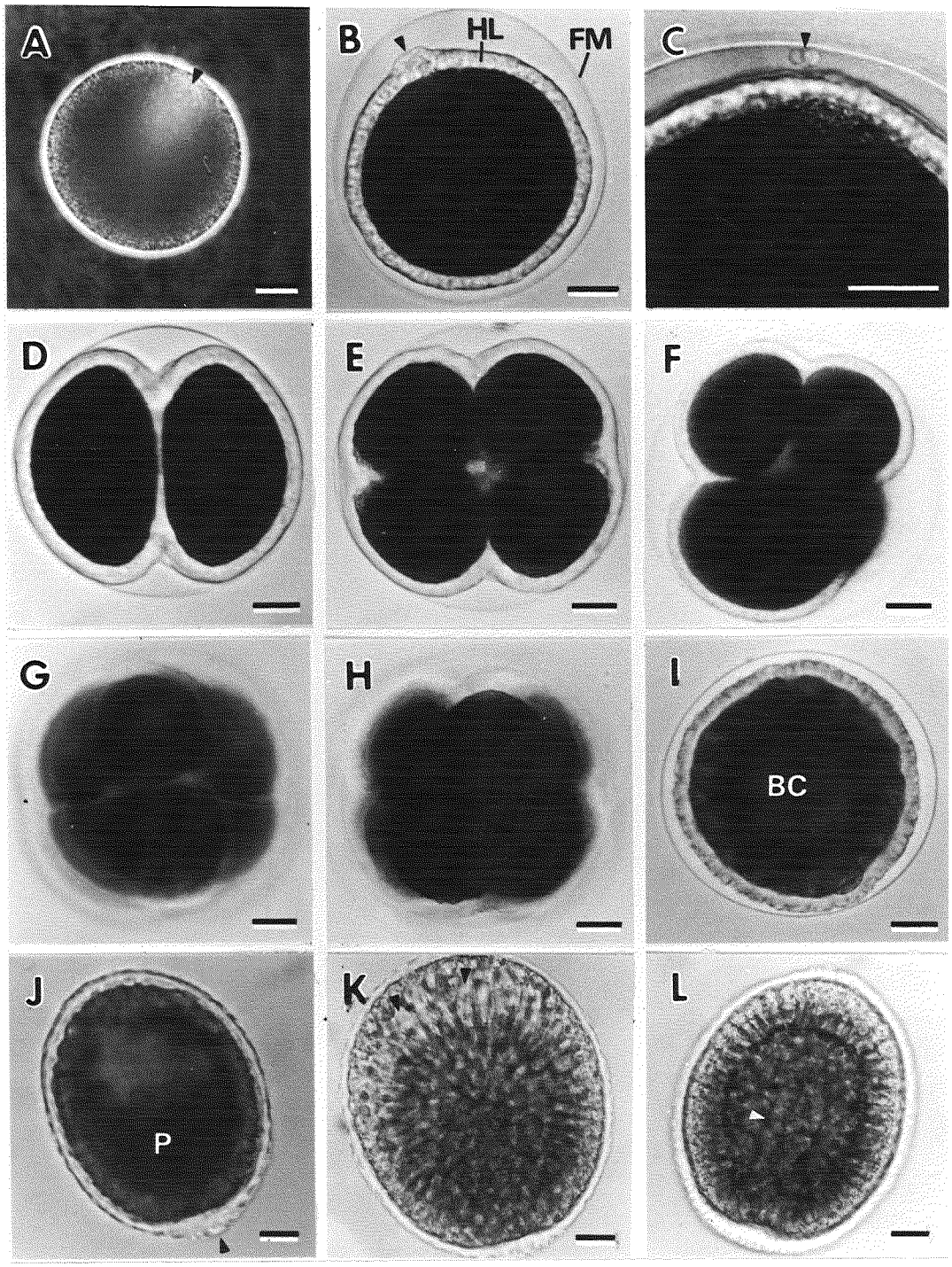
A
B
HL
FM
C
D
E
F
G
H
I
BC
J
P
K
L

Explanation of Plate 21

Fig. 21. LM of successive changes in the early fertilization process of Amphipholis kochii. Fig. 21A is taken within 5-10 sec postinsemination and the subsequent photographs (B-F) are taken at intervals of about 1 sec. The spermatozoon (arrowhead) invades the egg cytoplasm through the transparent fertilization cone. Scale, 5 μm.

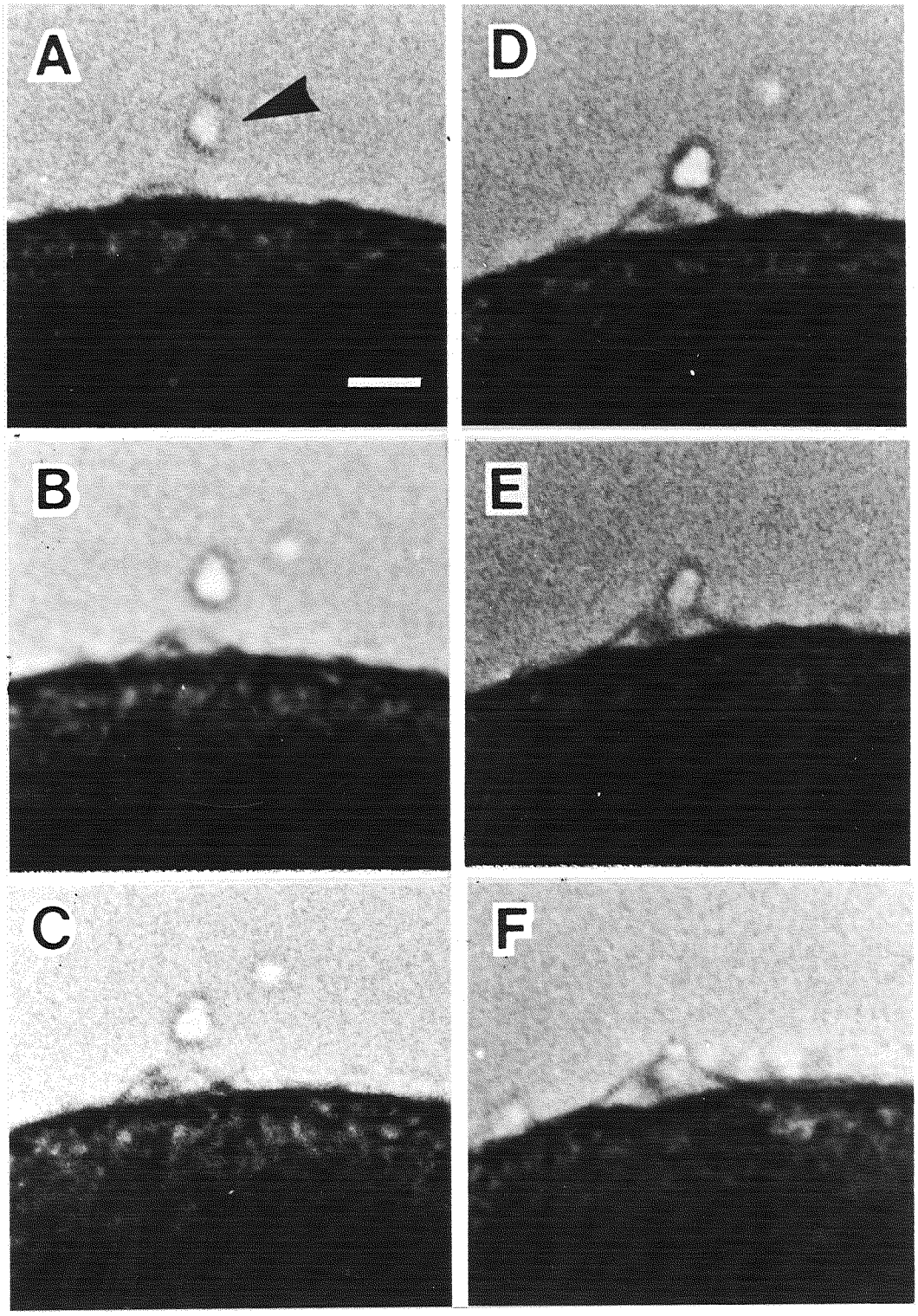
A
D
B
E
C
F

Explanation of Plate 22

Fig. 22. LM of *Amphipholis kochii* egg during fertilization. The spermatozoon entering the egg is indicated by a large arrowhead. The other spermatozoa (small arrowheads) are attached to the jelly surface and are unable to enter the jelly coat (J). The discharged cortical granules (CG) and developing fertilization membrane (FM) are also seen. Note that the jelly coat begins to dissolve at the region of sperm entry. Scale, 10 μm.

Plate 22

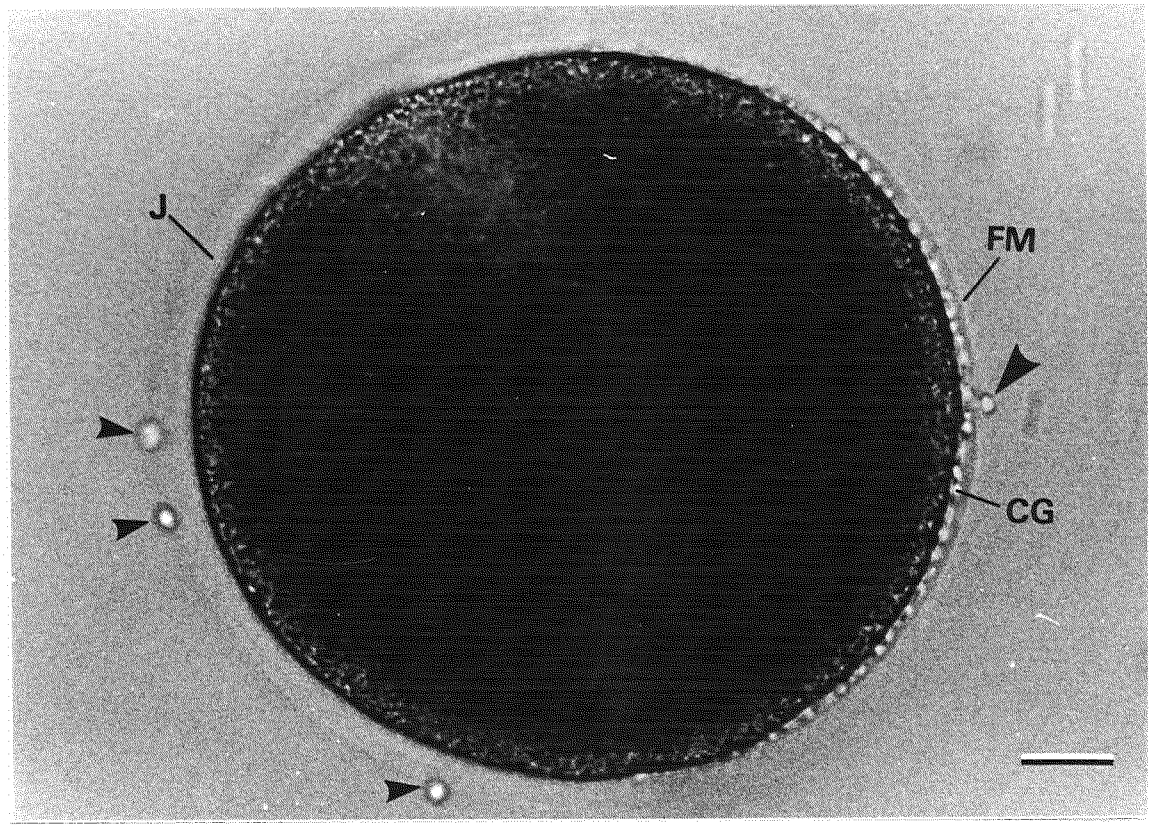

Explanation of Plate 23

Fig. 23. LM of the larvae of Amphipholis kochii. Scale, 10 μm (B), 20 μm (A, C), 50 μm (D, F, H), 100 μm (E, G, I). **A:** Gastrula compressed to show the tetraradiated spicules (arrowheads). **B:** High magnification of the tetraradiated spicule showing the rudiments of the four larval skeletal rods (arrowheads). **C:** Early 2-armed ophiopluteus. Large arrowheads indicate the rudiments of the postero-lateral arms. Apparent coelomic pouches (small arrowheads) are found between the stomach (S) and esophagus (E). The intestine is out of focus. Ventral view. **D:** Early 4-armed ophiopluteus. The antero-lateral arms are indicated by arrowheads. The left coelomic pouch separates into an anterior coelom (LA) and a posterior one (LP). The larval digestive system is well developed into the esophagus (E), stomach (S) and intestine (I). Dorsal view. **E:** 6-armed ophiopluteus. The third arms, post oral arms (arrowheads), are seen. Ventral view. **F:** 6-armed ophiopluteus, in which the right coelomic pouch separates into an anterior coelom (RA) and a posterior one (RP). The left posterior coelom has already been formed at this stage (LP). Dorsal view. **G:** 8-armed ophiopluteus. The fourth arms, postero-dorsal arms (arrowheads), are prominent. Dorsal view. **H:** Ophiopluteus with 5-lobed hydrocoel (arrowhead). The esophagus (E) and stomach (S) are also indicated. **I:** Ophiopluteus during metamorphosis. Arrowheads indicate the podia of a young brittle-star. Dorsal view.

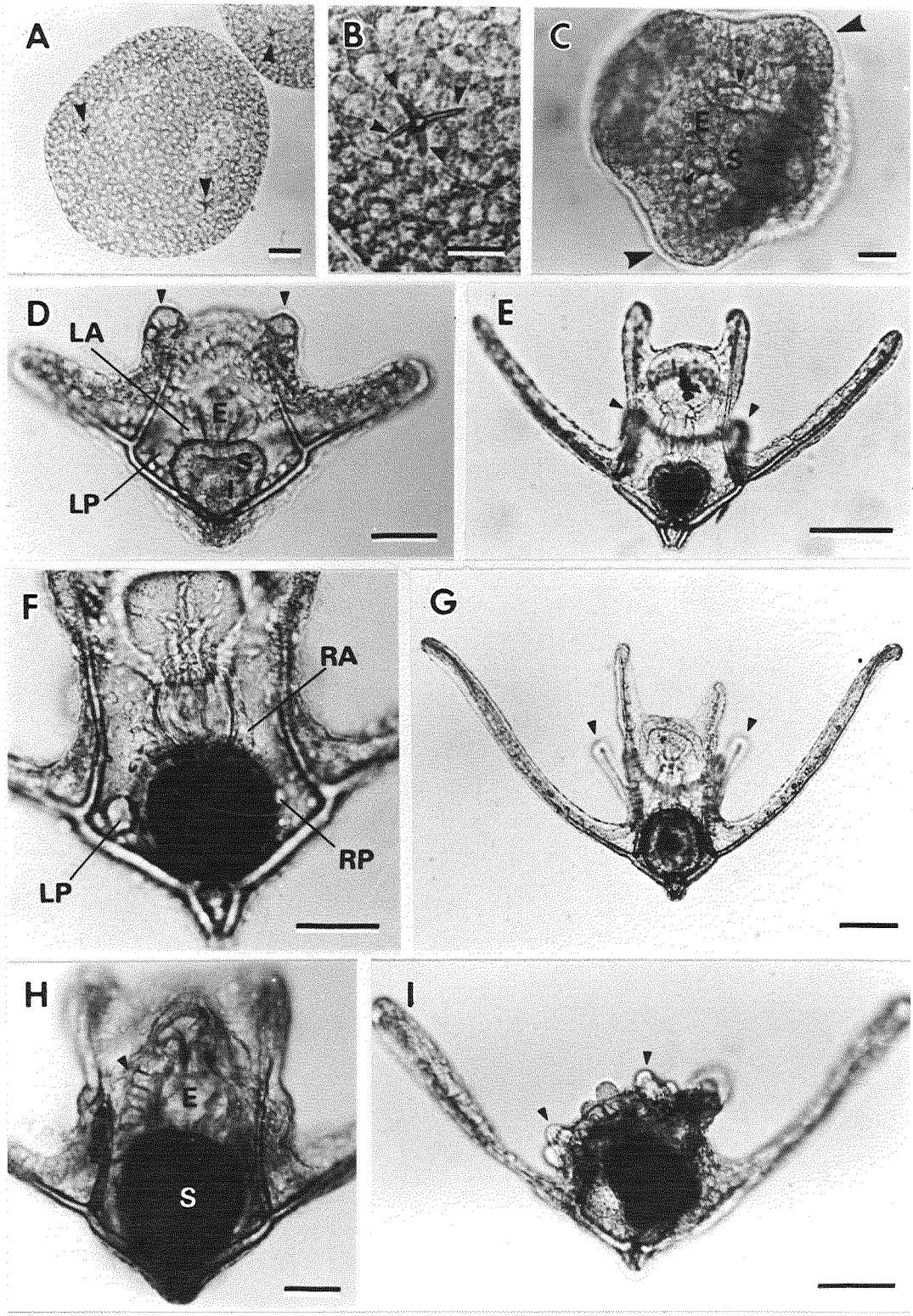
A
B
C
E
S
D
LA
E
S
LP
E
F
RA
RP
LP
G
H
E
S
I

Explanation of Plate 24

Fig. 24. Histological longitudinal sections of the embryos and larvae of Amphipholis kochii. Scale, 20 μm. **A:** Blastula. Primary mesenchyme (P) occupies the blastocoel. Arrowheads show the vacuoles in the animal polar wall. **B:** Early gastrula, showing invagination at the vegetal pole (arrowhead). **C:** Late gastrula. Archenteron is formed. Arrowheads point out two pockets in the archenteron, which are the origin of the coelomic pouches. **D:** 8-armed ophiopluteus. The left posterior coelom segregates into hydrocoel (HC) and somatocoel (SC). AC, axocoel; E, esophagus; I, intestine, RP, right posterior coelom; S, stomach. **E:** Late 8-armed ophiopluteus. The hydrocoel (HC) develops along the esophagus (E) and becomes a 5-lobed shape. The somatocoel (SC) grows at the side of the stomach (S). I, intestine.

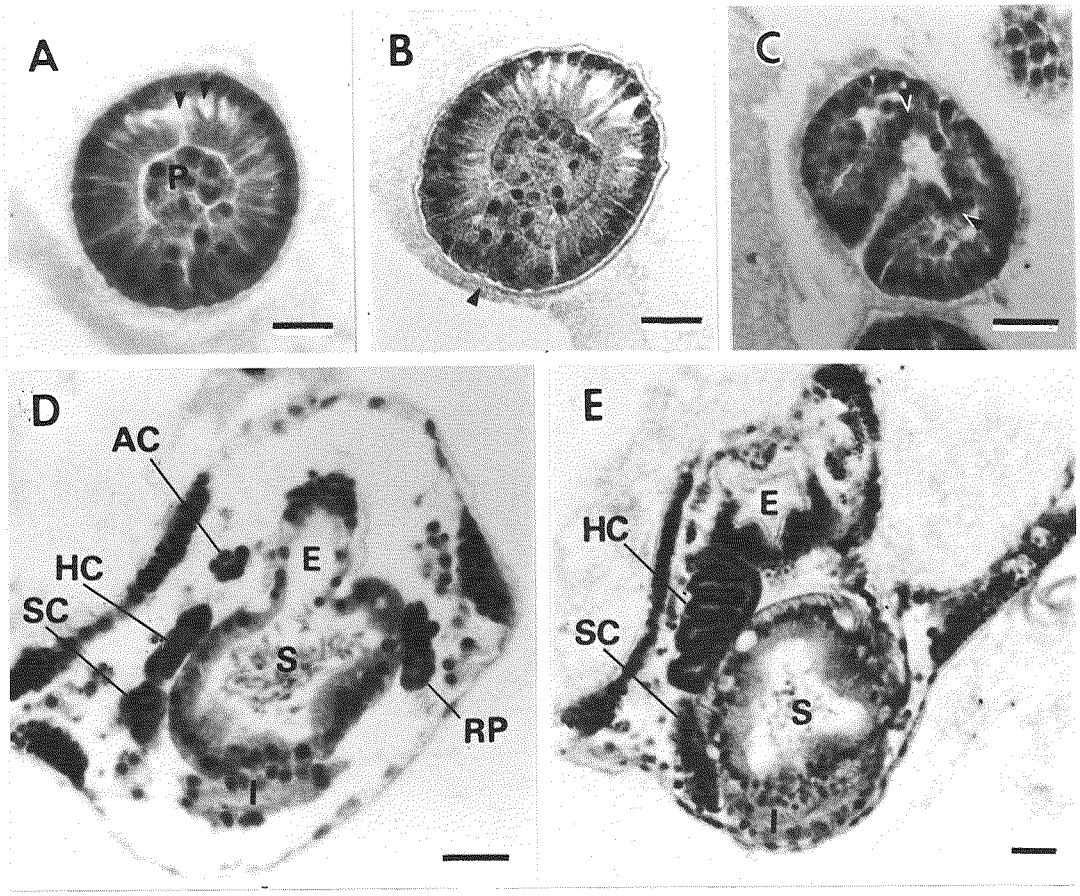
A
P
B
C
D
AC
HC
SC
E
S
RP
E
HC
SC
E
S

Explanation of Plate 25

Fig. 25. SEM (A) and surface replica (B) of the unfertilized eggs of Amphipholis kochii. Scale, 20 μm (A), 0.5 μm (C). **A**: GA-fixed egg surface, showing aggregations of the jelly coat (arrowheads). **B**: GA-fixed jelly coat. The jelly coat is consists of fine fibers which bear many nodules on their surfaces. The ice covering the jelly is dried slightly in order to show the jelly coat fibers clearly.

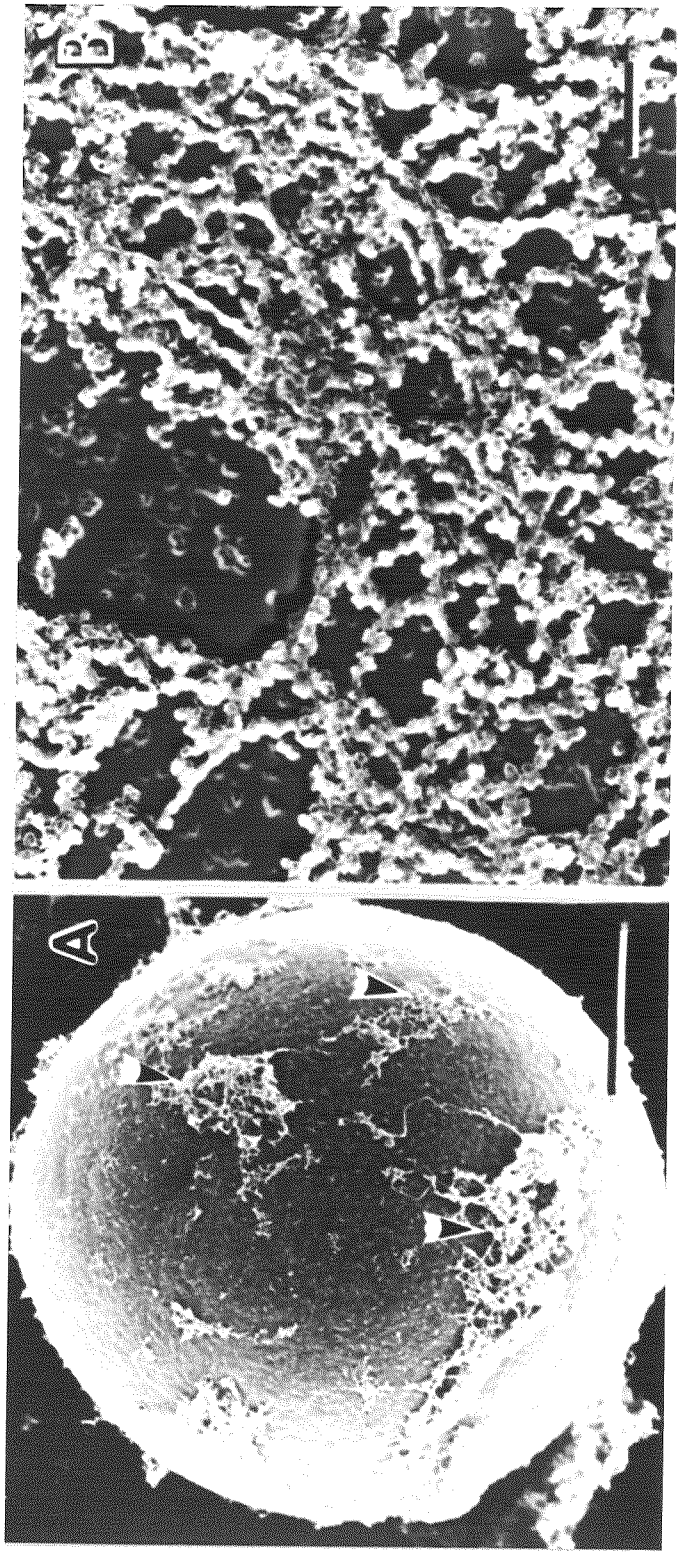
B
A

Explanation of Plate 26

Fig. 26. Surface replicas of the unfertilized eggs in Amphipholis kochii. Scale, 1 μm. **A:** Untreated egg, showing a dense network of vitelline coat fibers. In the upper part of the figure where the network is missing, the underlying egg plasma membrane surface which bears the microplicae (arrowheads) can be seen. **B:** Dithiothreitol-treated egg. The network of the vitelline coat fibers has been completely removed. Many microplicae are seen on the surface of the egg plasma membrane.

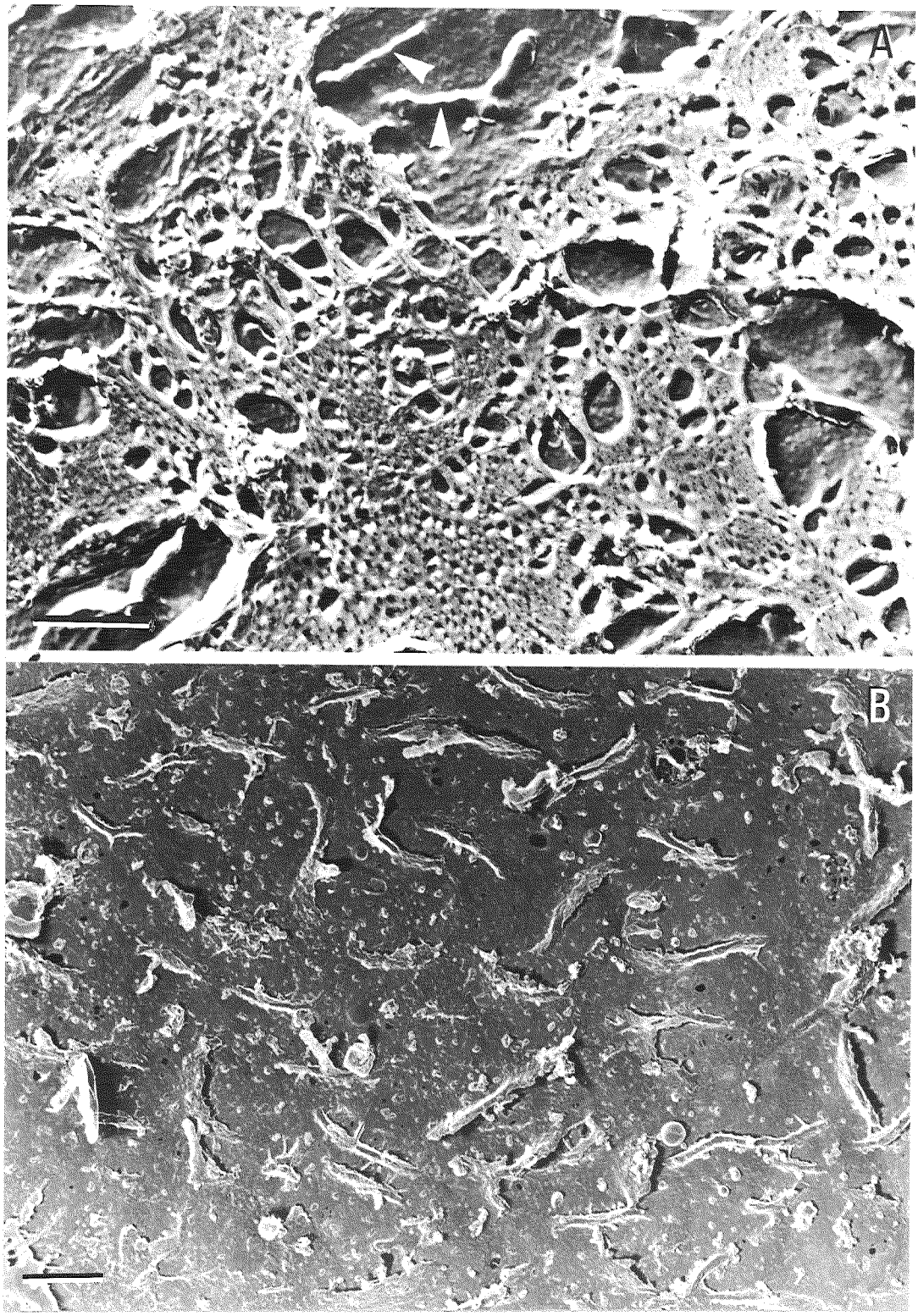
A
B

Explanation of Plate 27

Fig. 27. TEM of the vitelline coats in Amphipholis kochii. Scale, 0.5 μm. **A:** Uranyl acetate and lead citrate stain. The vitelline coat (VC) is very thin. **B:** Ruthenium Red stain. The vitelline coat (VC) is deeply stained.

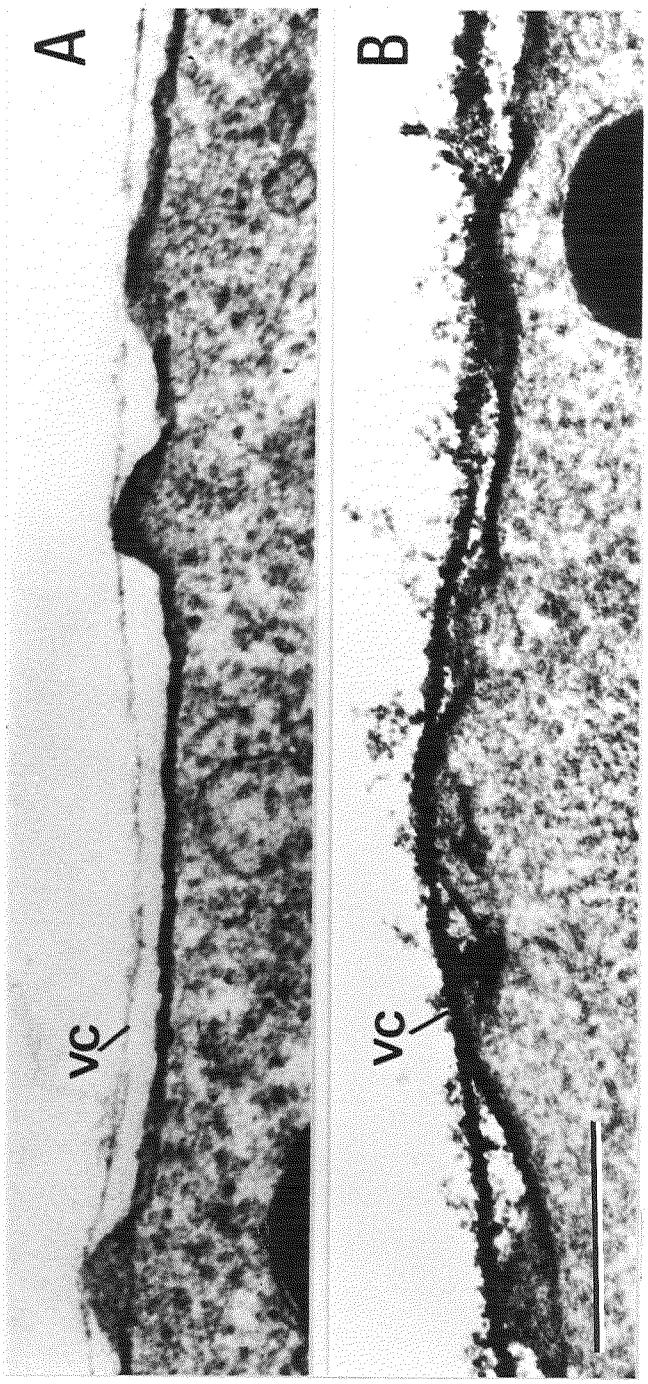
A
VC
B
VC

Explanation of Plate 28

Fig. 28. TEM of the unfertilized eggs in Amphipholis kochii. Scale, 1 μm (A), 0.5 μm (B, C). **A:** Cortical region, showing the multilayer arrangement of cortical granules (CG). Y, yolk granule. **B:** High magnification of the cortical granule. This consists of peripheral fibrous (PF) and central fibrous (CF) materials. The CF materials show two electron densities. Arrowheads indicate sections of the microplicae. Y, yolk granule. **C:** The cortical granules stained by the PA-CrA-silver technique. Silver deposits are dense on the peripheral fibrous (PF) material but slight if at all on the central fibrous (CF) material. Y, yolk granule.

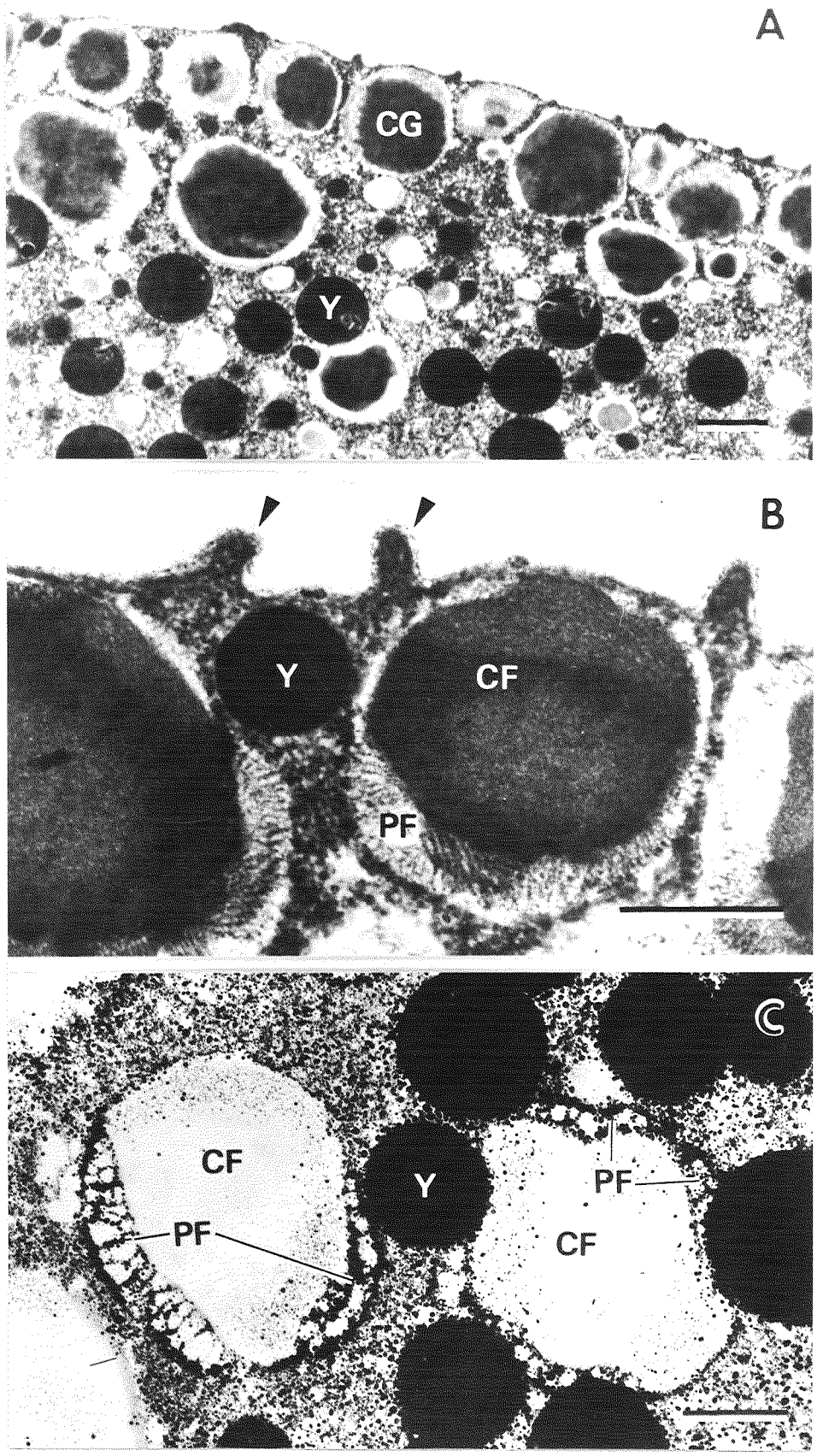
A
CG
Y
B
Y
CF
PF
C
CF
Y
PF
PF
CF

Explanation of Plate 29

Fig. 29. The spermatozoa of Amphipholis kochii before (A, C), during (D, E) and after (B, F) the cortical reaction. Scale, 1 μm (A-C), 0.1 μm (D-F). **A:** SEM of the intact spermatozoon. **B:** SEM of the acrosome-reacted spermatozoon, showing the acrosomal process (arrowhead). **C:** TEM of the intact spermatozoon. Arrowhead shows the acrosomal vesicle. N, nucleus; M, mitochondrion. **C:** TEM of the initial stage of the acrosome reaction. The acrosomal vesicle has opened (arrowhead) by fusion of the vesicle membrane and overlying sperm plasma membrane. **E:** TEM of the acrosomal region during the acrosome reaction. The opening site of the acrosomal vesicle becomes large and the basal membrane of the acrosomal vesicle bulges out anteriorly. **F:** TEM of the acrosome-reacted spermatozoon, showing the acrosomal process (large arrowhead). Small arrowheads indicate fibrous structures in the acrosomal fossa.

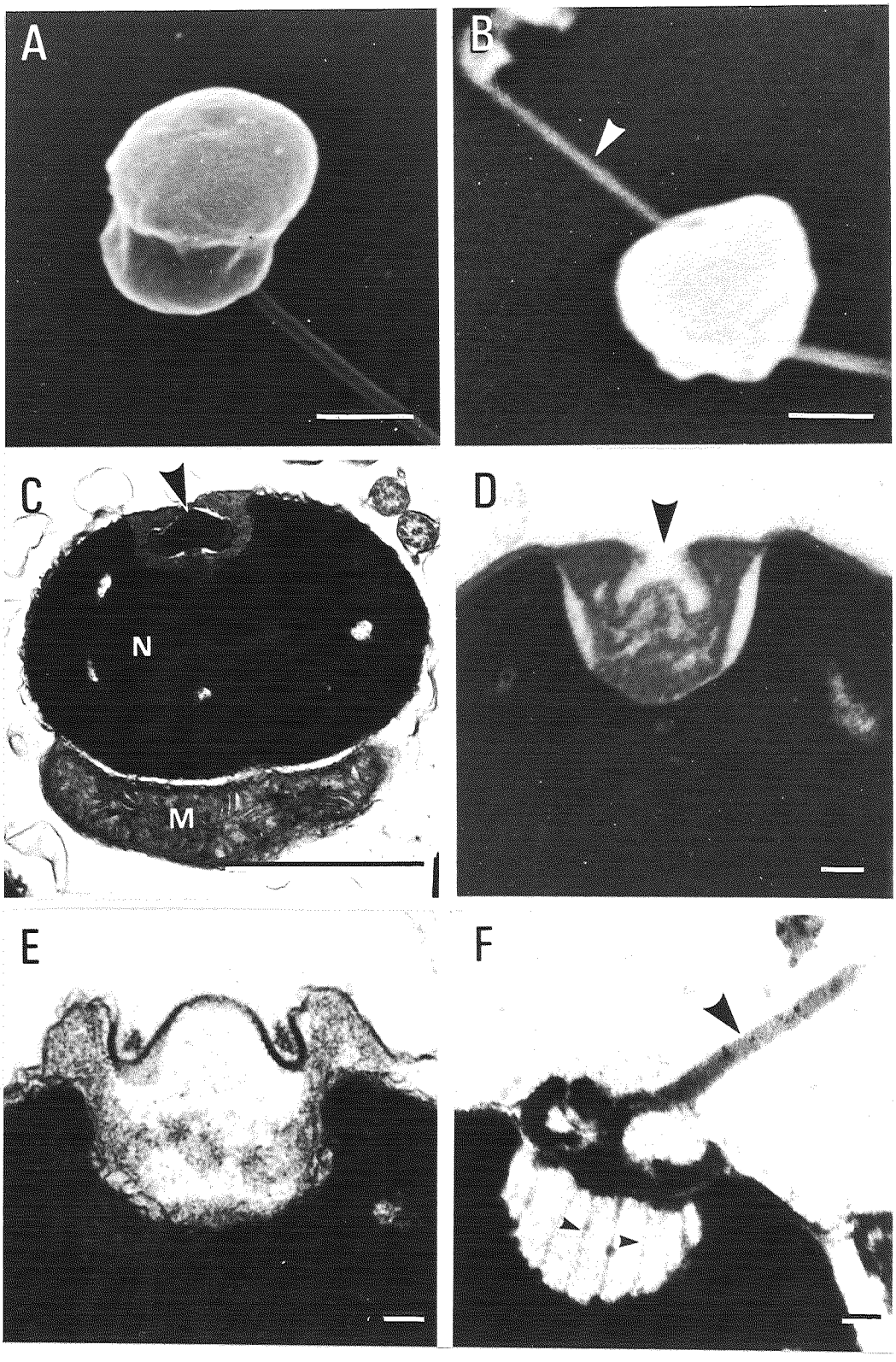
A
B
C
N
M
D
E
F

Explanation of Plate 30

Fig. 30. SEM (A) and TEM (B-D) of the early phase of fertilization in Amphipholis kochii. Scale, 1 μm. **A:** Contact of the spermatozoon with the egg surface by means of the acrosomal process (AP). The jelly coat has dissolved during SEM preparation. **B:** Fusion of the acrosomal process membrane and egg plasma membrane (black arrowheads). Note that the acrosomal fossa at the anterior portion of the sperm nucleus (N) is intact (white arrowhead). CG, cortical granule; FC, fertilization cone; M, mitochondrion. **C:** The spermatozoon incorporated into the egg cytoplasm through the fertilization cone (FC) 15 sec postinsemination. The fertilization cone comprises microfilaments (MF). CG, cortical granule material; FM, fertilization membrane; M, mitochondrion; N, nucleus. **D:** The fertilizing spermatozoon incorporated into the fertilization cone (FC) 20 sec postinsemination. Arrowheads indicate the bundle of microfilaments located in the acrosomal process. M, mitochondrion; N, nucleus.

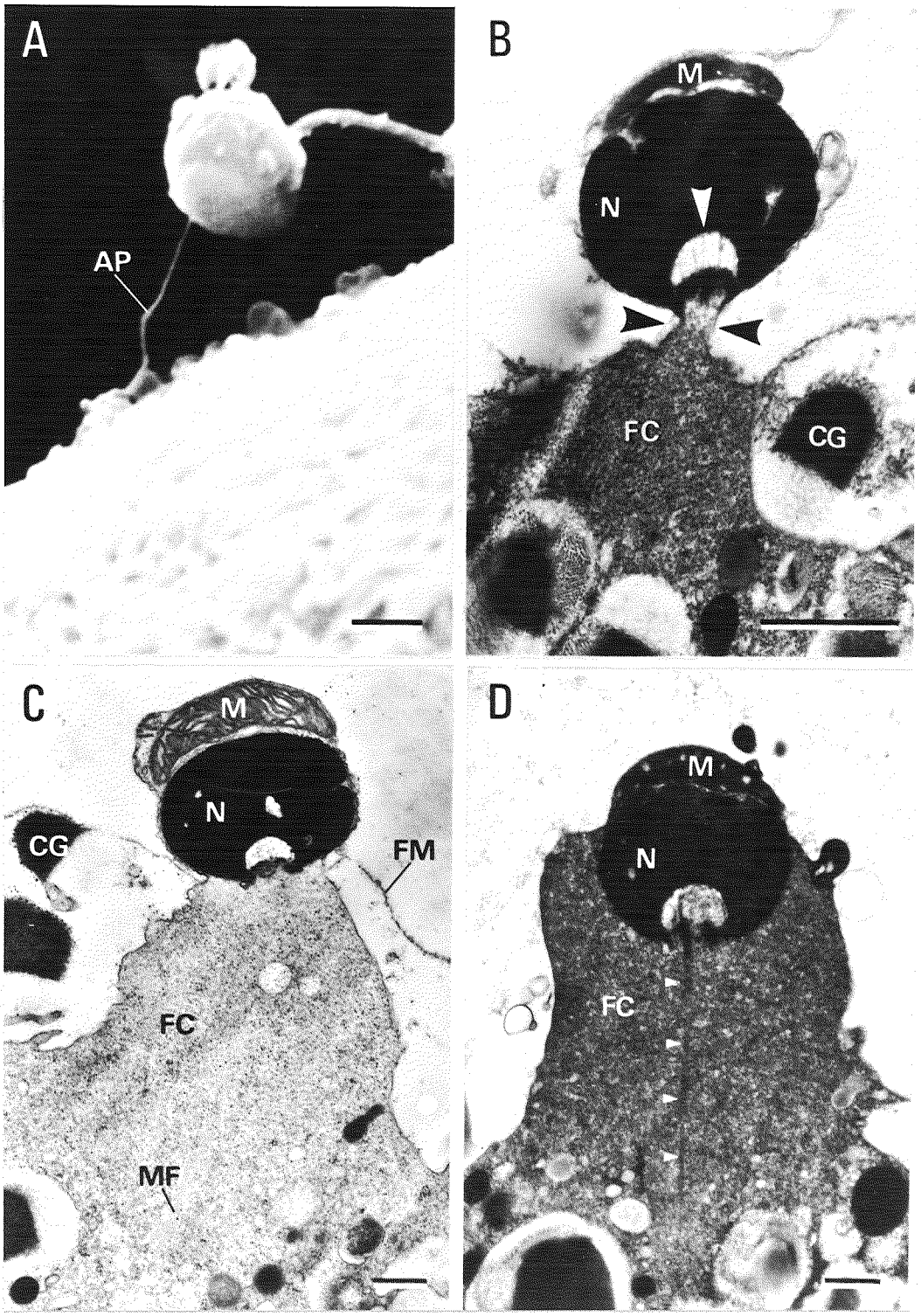
A
AP
B
M
N
FC
CG
C
M
N
CG
FM
FC
MF
D
M
N
FC

Explanation of Plate 31

Fig. 31. TEM of Amphipholis kochii eggs undergoing the cortical reaction. Scale, 1 μm. A: Part of the leading edge of the cortical reaction spreading from right to left. The vitelline coat (VC) has become elevated from the egg plasma membrane surface. The contents of the cortical granule are discharged by fusion of the membrane of the granule with the overlying egg plasma membrane (arrowheads). B: The discharged cortical granule. The peripheral fibrous (PF) material has become dispersed in the perivitelline space, and some of it (arrowheads) has become attached to the elevated vitelline coat. The central fibrous (CF) material remains near the egg surface. C: 20 sec postinsemination. The contents of the cortical granules (CF, PF) have been discharged into the perivitelline space. Some PF material is attached to the elevated vitelline coat (small arrowheads). The cortical granule located deeply from the egg surface is discharged by a fusion of its own membrane and the adjacent cortical granule membrane (large arrowheads).

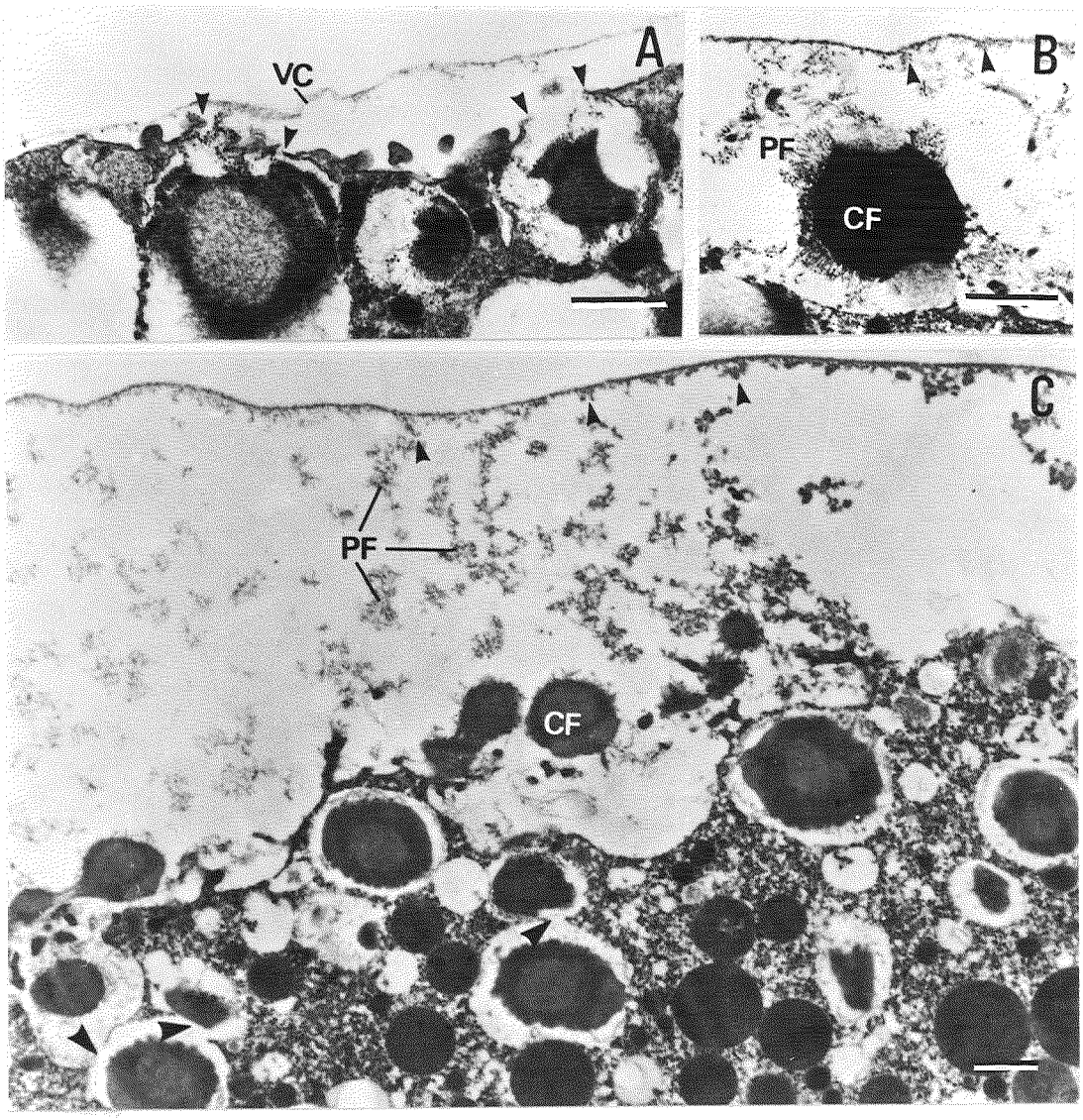
A
VC
B
PF
CF
C
PF
CF

Explanation of Plate 32

Fig. 32. Surface replicas of Amphipholis kochii eggs during fertilization membrane formation. Scale, 1 μm. **A:** The leading edge of the cortical reaction at 15 sec postinsemination. Arrow shows the direction of spread of the cortical reaction. The elevated vitelline coat fibers are woven into a sheet which has a smooth appearance (asterisk). **B:** The inner surface of the sheet made of the vitelline coat fibers at 15 sec postinsemination, showing that much fibrous material attached to it. Asterisks indicate cortical granule material that has become attached to the inner surface of the elevated vitelline coat during the procedure for surface replication. **C:** The fully-formed fertilization membrane at 5 min postinsemination. It has been folded to show its outer (O) and inner (I) surfaces.

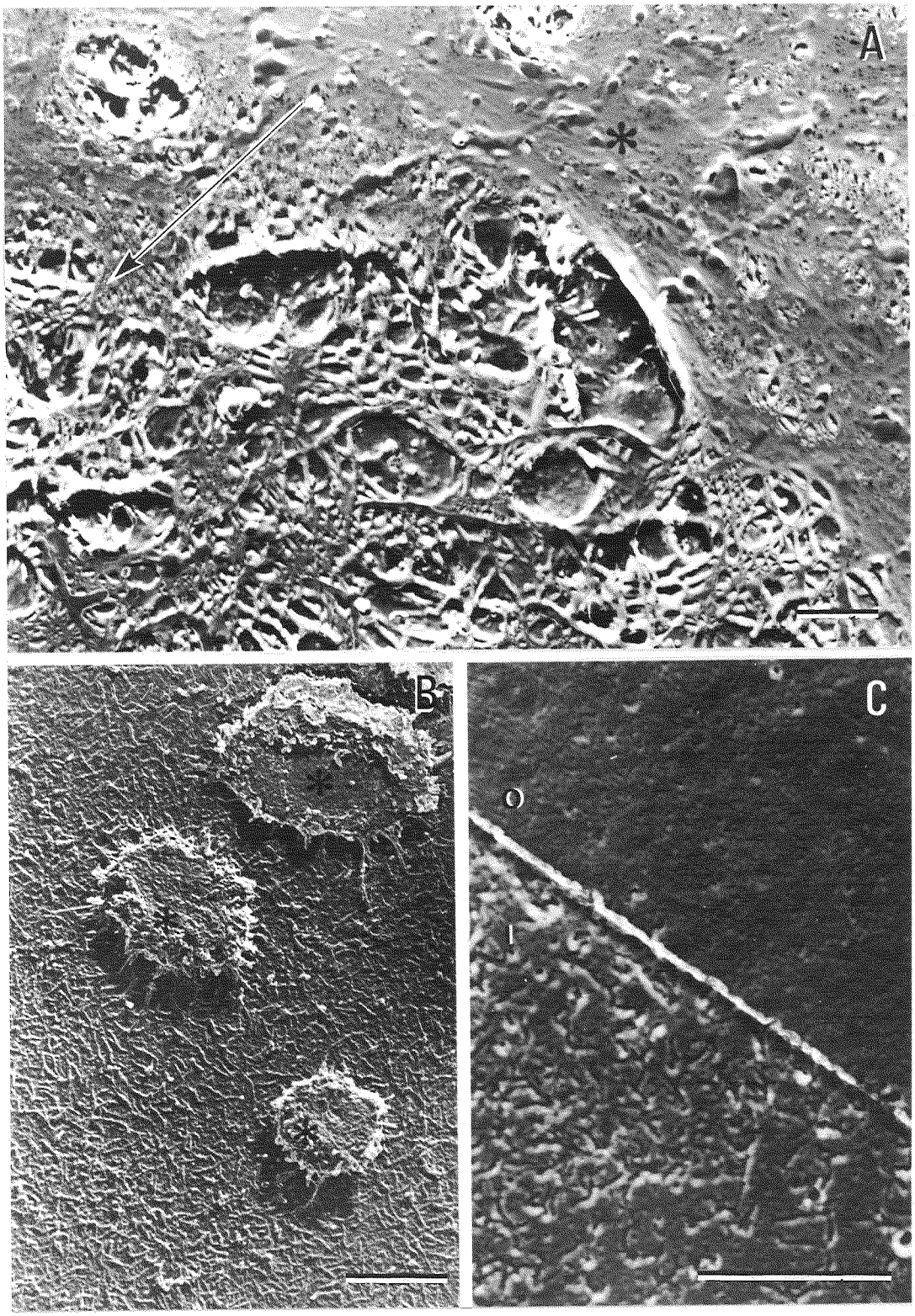
A
B
C
o
i

Explanation of Plate 33

Fig. 33. TEM of the developing (A, B) and the fully-formed (C) fertilization membranes of Amphipholis kochii. Scale, 0.1 μm. **A:** 1 min postinsemination. The membrane consists of dense outer and inner laminae and a translucent middle lamina. **B:** 2 min postinsemination. The inner surface of the membrane is lined with peripheral fibrous material of the cortical granules (arrowheads). **C:** 3 min postinsemination. The fertilization membrane is composed of an outer layer (OL), middle layer (ML) and inner layer (IL).

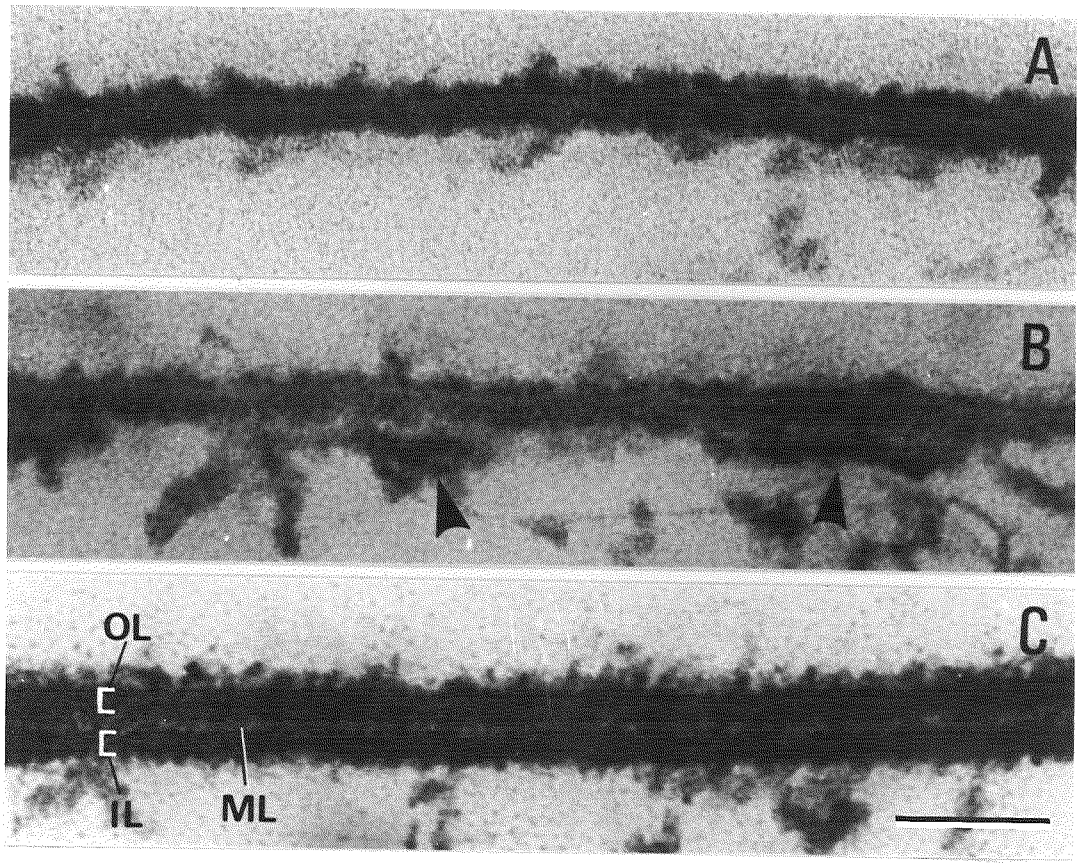
A
B
C
OL
C
C
IL
ML

Explanation of Plate 34

Fig. 34. TEM (A, C) and SEM (B) of Amphipholi kochii eggs during hyaline layer formation. Scale, 1 μm (A, C), 5 μm (B). **A:** 3 min postinsemination. The central fibrous materials of the cortical granules (CF) seem to fuse together to form the hyaline layer. Arrowheads show microvilli. **B:** A denuded egg surface at 3 min postinsemination. The fertilization membrane was removed to show fusion of the cortical granule material. **C:** 5 min postinsemination. The fertilization membrane (FM) and the hyaline layer (HL) can be seen.

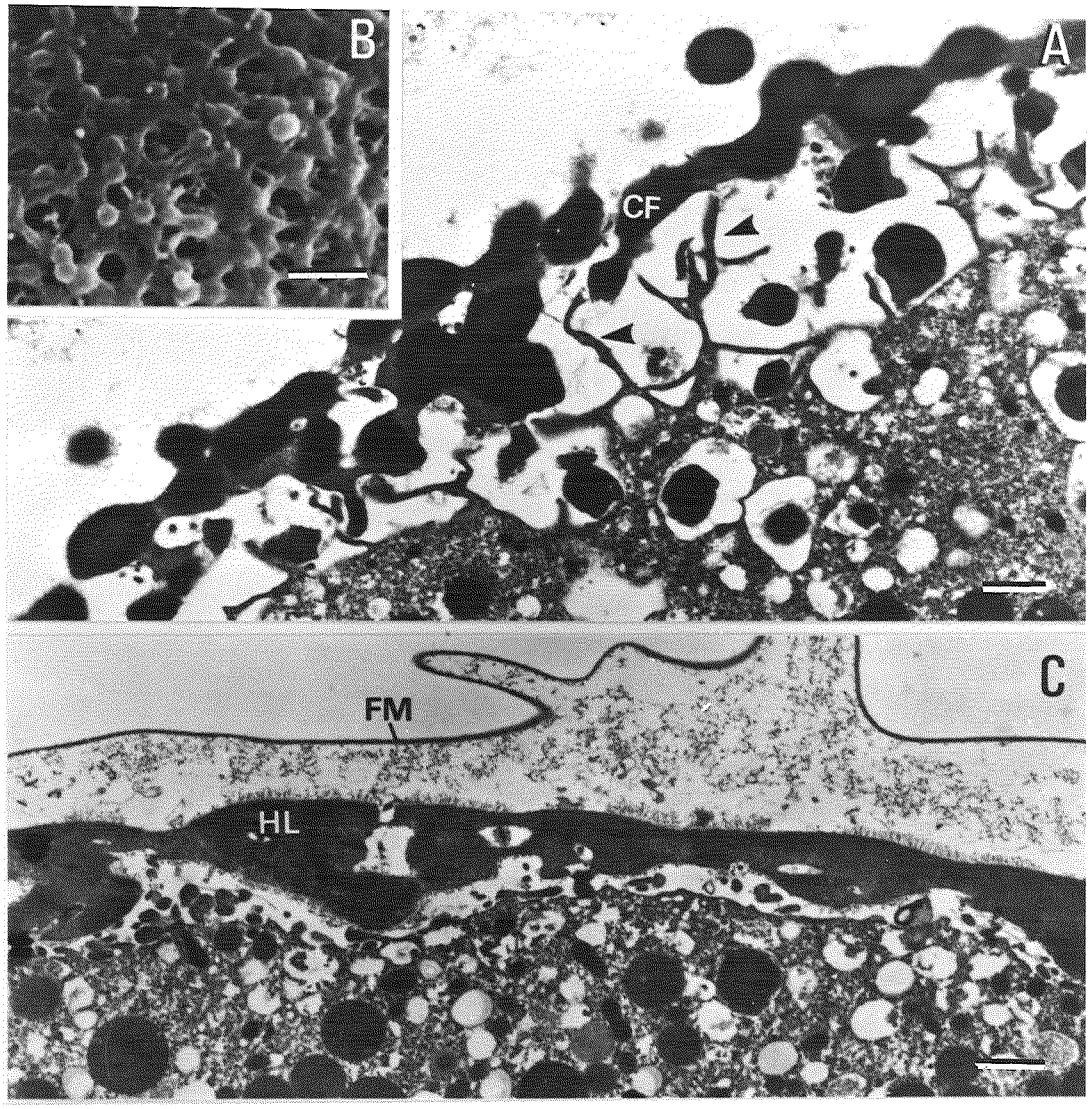
B
A
CF
C
FM
HL

Explanation of Plate 35

Fig. 35. TEM of the spermatozoa of Amphipholis kochii during its metamorphosis into a male pronucleus. Scale, 1 μm. **A:** The incorporated spermatozoon in the egg cortex. The sperm nucleus disperses at its lateral surface (arrowheads). Note that the sperm head has rotated about 30°. M, mitochondrion. **B:** The spermatozoon has dispersed to a greater extent than the sperm nucleus in Fig. 35A. The sperm head has rotated about 90°. M, mitochondrion. **C:** Longitudinal section of a dispersing spermatozoon, showing that the dispersion is latest at the acrosomal fossa (large arrowhead). Small arrowheads indicate vacuoles that elongate and surround the nucleus. M, mitochondrion. **D:** Dispersion of the sperm nucleus. The nucleus is still condensed at the acrosomal fossa (large arrowhead). Note that several elongated vacuoles (small arrowheads) surround the nucleus and form the male pronuclear envelope. **D:** The male proncleus 15 min postinsemination. The pronucleus is surrounded by a nuclear envelope, which possesses nuclear pores (arrowheads). Sperm mitochondrion (M) is still associated with the nucleus.

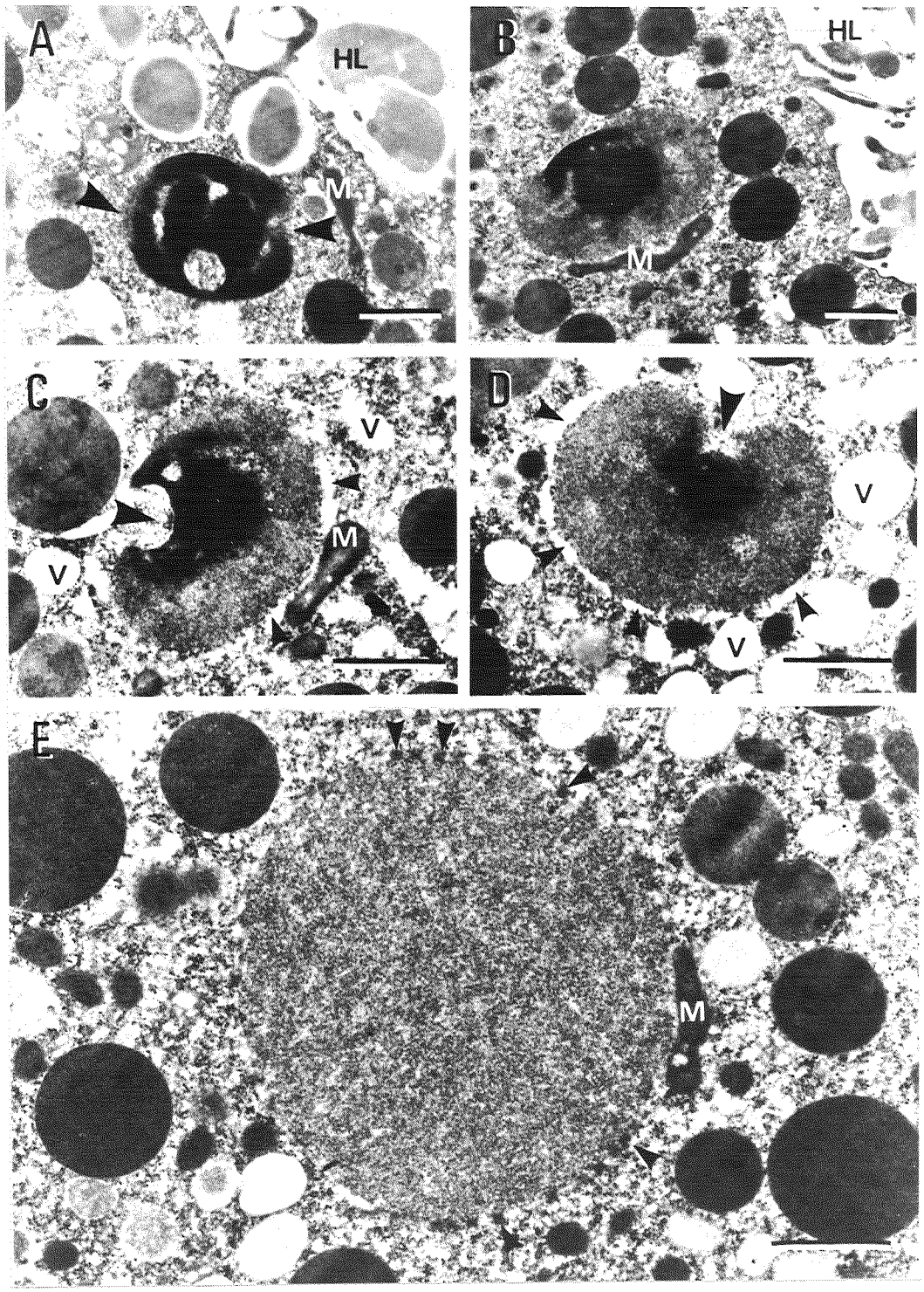
A
HL
M
B
HL
M
C
V
M
V
D
V
V
E
M

Explanation of Plate 36

Fig. 36. Epon thick sections of the normal monospermically fertilized eggs of Amphipholis kochii. Scale, 0.5 μm. **A:** 10 min postinsemination. The egg is in anaphase of the first meiotic division. The spindle and chromosomes are shown by single-arrowheads. Double-arrowhead indicates the male pronucleus. **B:** 45 min postinsemination. The male pronucleus (MP) becomes larger and moves inward to the central portion of the egg. Arrowhead shows the maternal chromosomes which disperse and fuse together to form the female pronucleus. **C:** Autoradiogram of the egg at 45 min postinsemination. Silver grains are found over the dispersing maternal chromosomes (arrowheads). **D:** Autoradiogram of the egg at 45 min postinsemination. The developing female (FP) and male (MP) pronuclei are seen. Grains are developed on both pronuclei. **E:** Autoradiogram of the egg at 60 min postinsemination, showing the initial stage of fusion of both pronuclei (FP, MP). Grains are seen on both pronuclei. **F:** Autoradiogram of the egg at zygote nucleus stage.

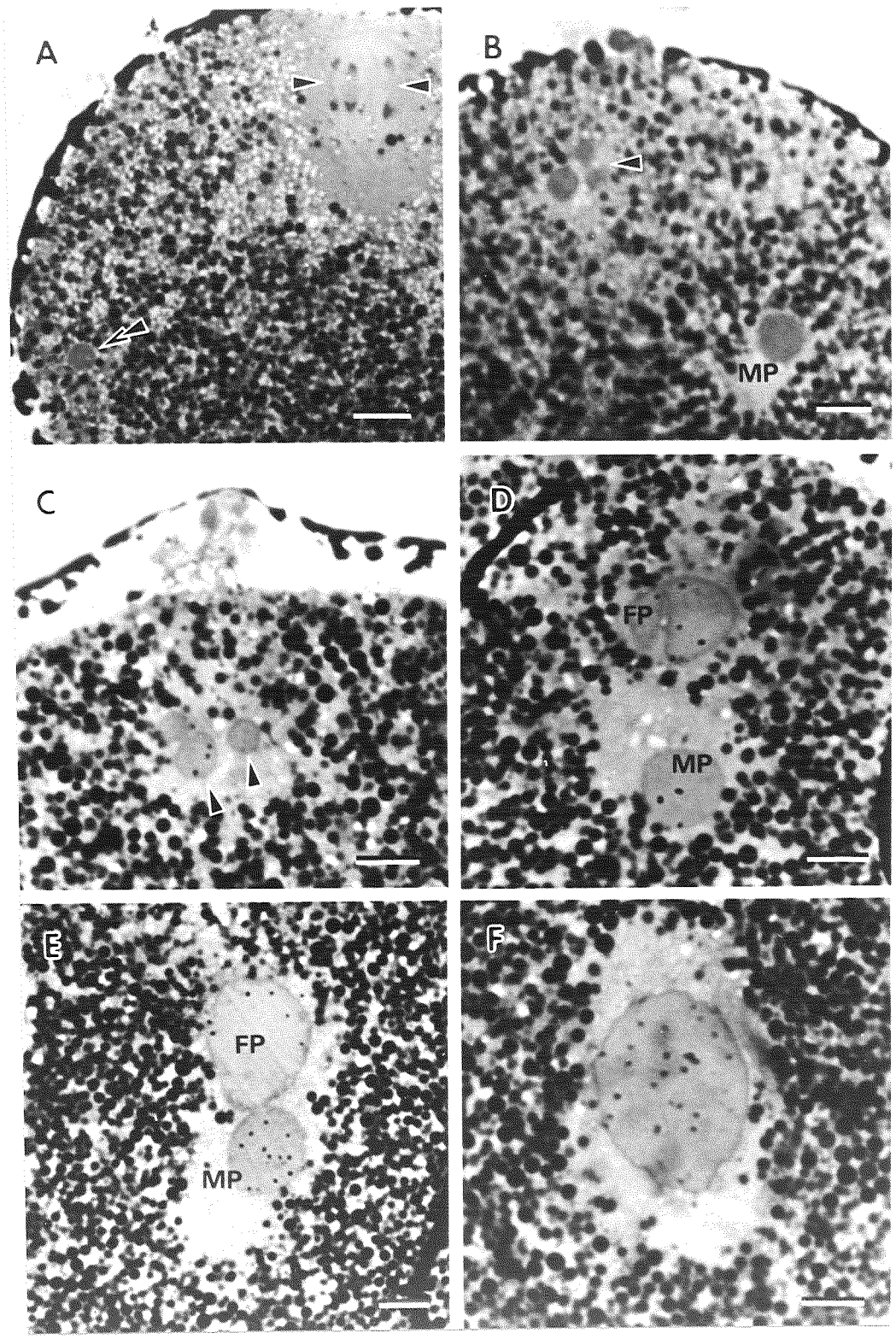
A
B
MP
C
D
FP
MP
E
FP
MP
F

Explanation of Plate 37

Fig. 37. TEM of the maternal chromosomes in Amphipholis kochii. Scale, 1 μm. **A:** The chromosomes (CH) at the first meiotic anaphase. The first polar body (PB) is forming. Note that the chromosomes are not associated with cisternae. **B:** The chromosomes (CH) after the second meiotic division. They were partially surrounded by vacuoles (arrowheads). The second polar body (PB) is still connected to the egg with narrow cytoplasmic bridge. **C:** The chromosomes (CH) during karyomere formation. The chromosomes are dispersed and partially surrounded by vacuoles (V) forming the nuclear envelope with nuclear pores (arrowhead). **D:** The irregularly shaped female pronucleus formed by fusion of the karyomeres.

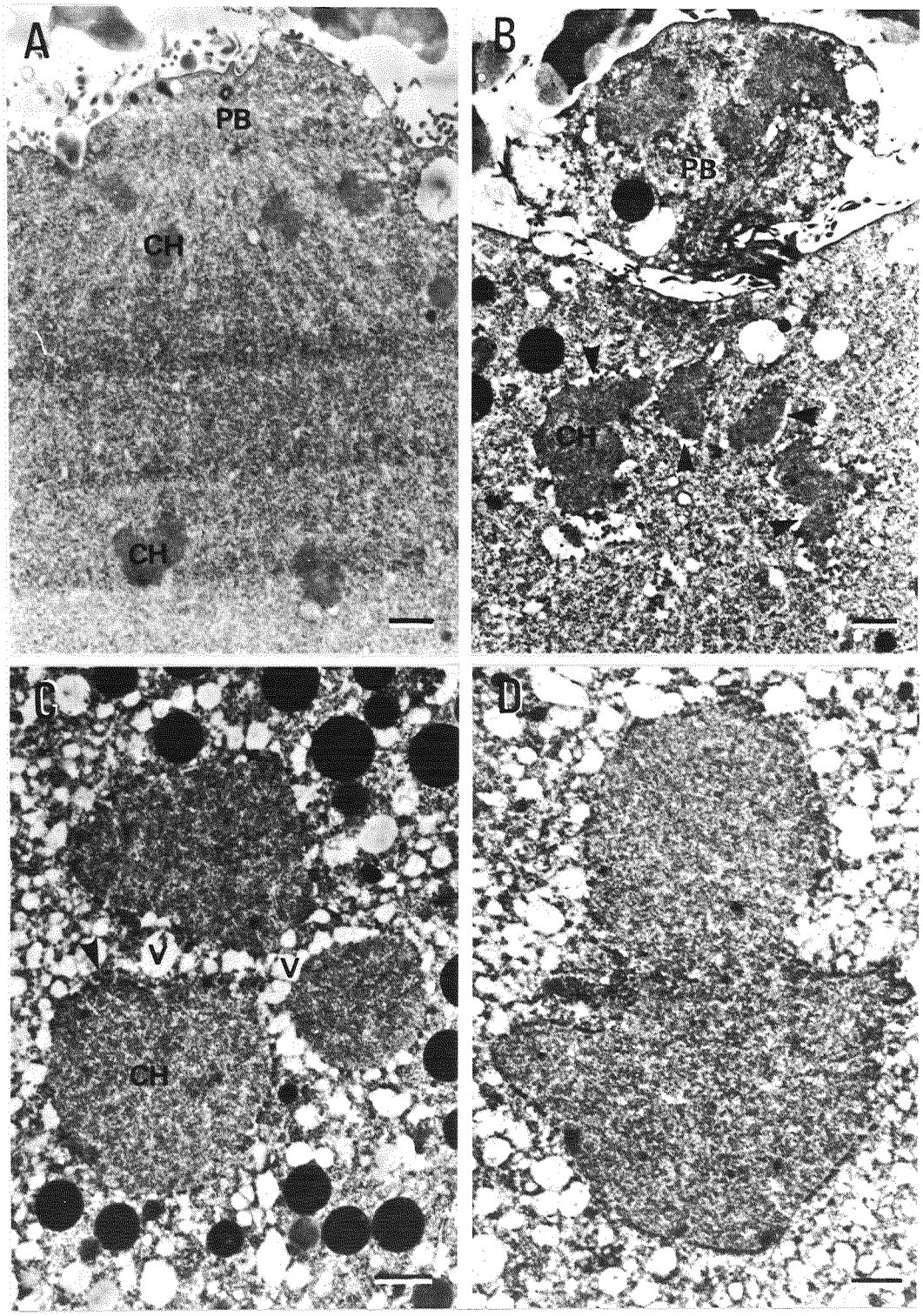
A
PB
CH
CH
B
PB
CH
C
V
V
CH
D

Explanation of Plate 38

Fig. 38. TEM of the male and female pronuclei encoutered in the central portion of the egg of Amphipholis kochii. Scale, 2 μm. **A:** The male pronucleus (MP) is smaller and denser than the female pronucleus (FP). **B:** The male (MP) and female (FP) pronuclei at the initial stage of fusion. Both pronuclei are jointed by the internuclear bridge (arrowheads) which may be formed by the disintegration of both pronuclear envelopes into vesicles. NO, nucleolus.

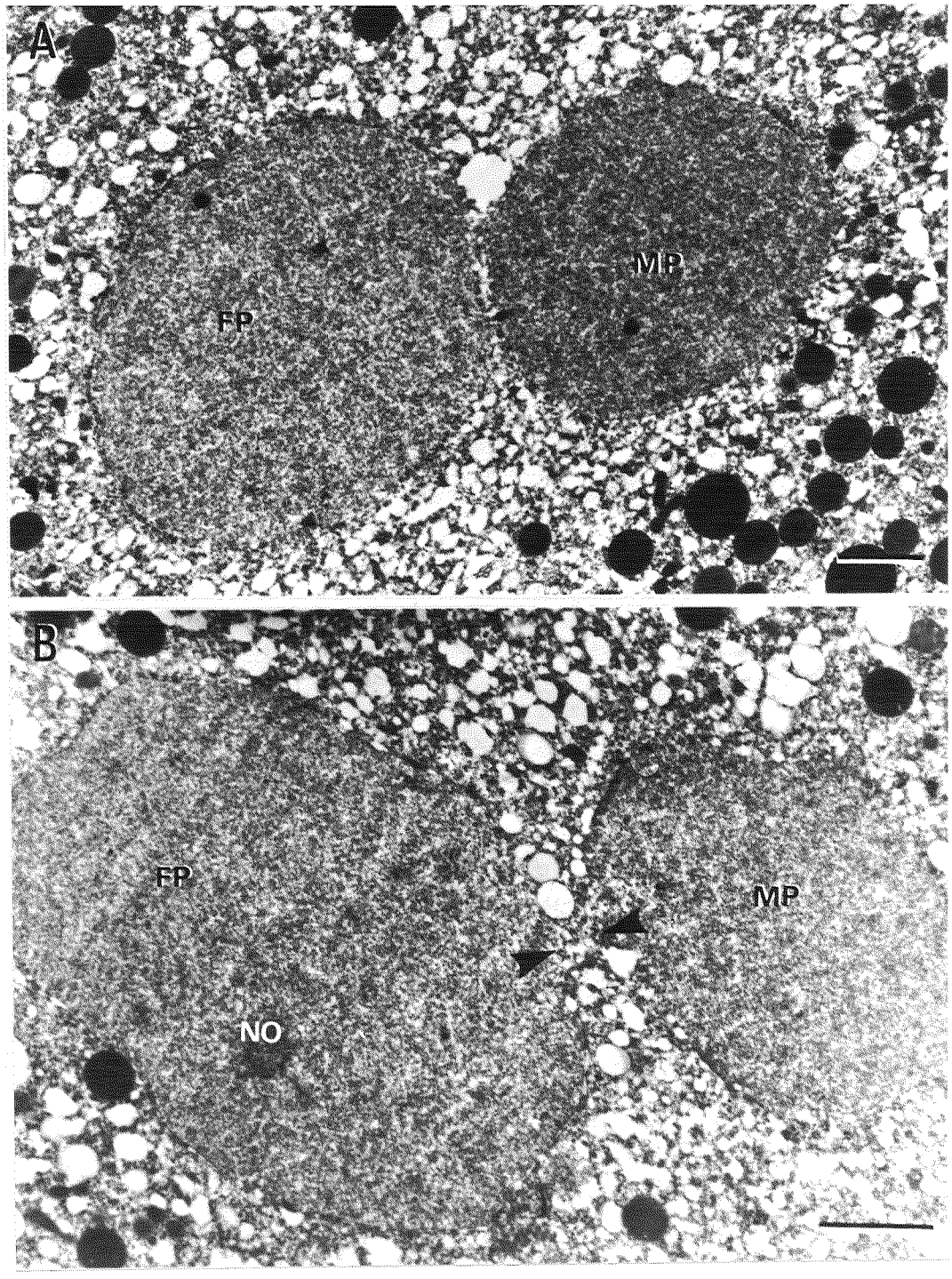
A
MP
FP
B
FP
MP
NO

Explanation of Plate 39

Fig. 39. TEM of the zygote nuclei of *Amphiopholis kochii*. Scale, 2 μm. **A**: Fusion of the male (MP) and female (FP) pronuclei. The internuclear bridge (arrowheads) are prominent. Note that the density of the both pronuclei is still different. **B**: Developing zygote nucleus. The internuclear bridge (arrowheads) has enlarged. Note that the density of the zygote nucleus is uniform. **C**: The fully-formed zygote nucleus.

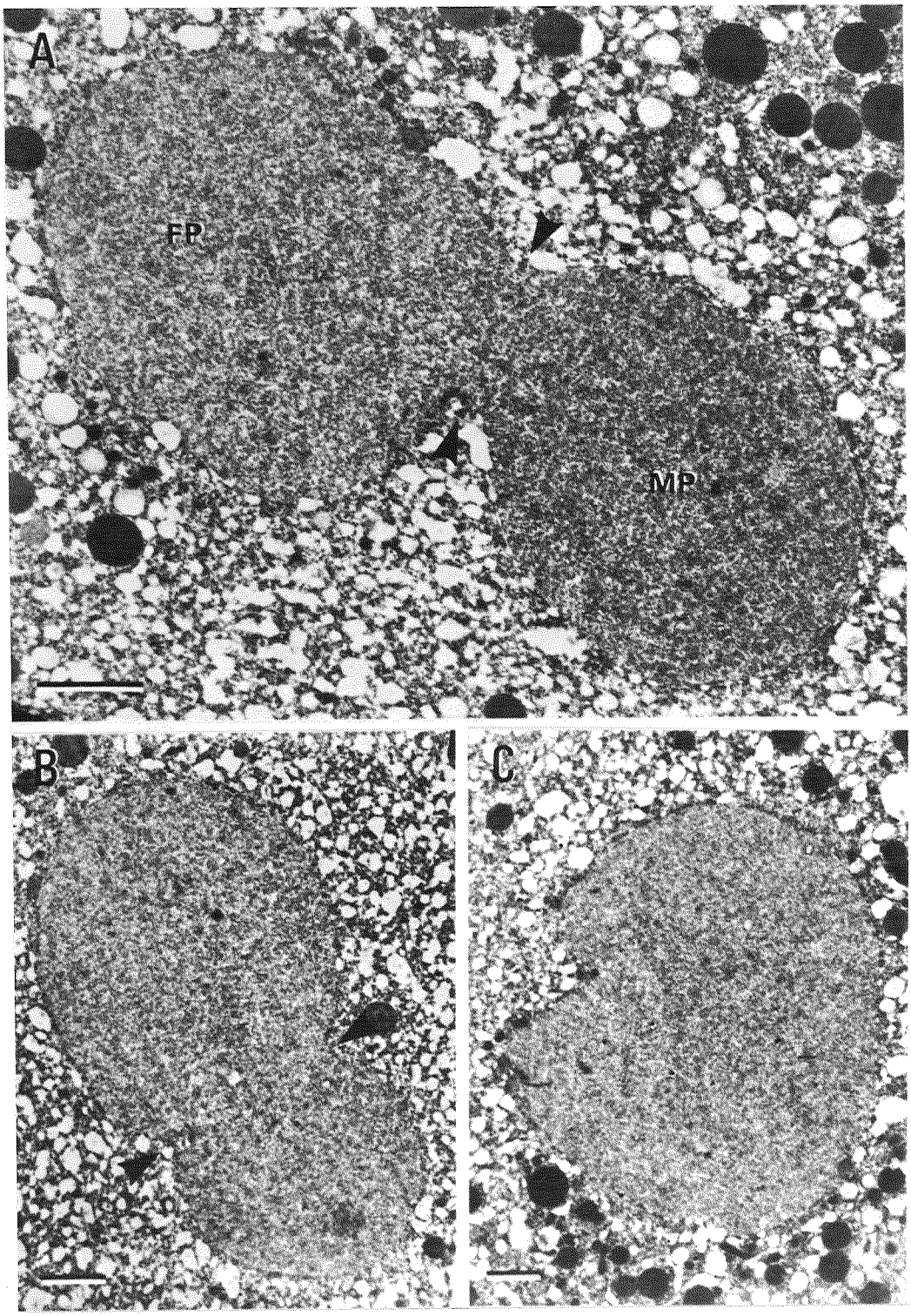
A
FP
MP
B
C

Explanation of Plate 40

Fig. 40. Autoradiograms of Amphipholis kochii eggs treated with colchicine from 30 min preinsemination (A, C) or 30 min postinsemination (B, D), and fixed at 60 min postinsemination. Scale, 10 μm. **A:** The maternal chromosomes (arrowhead) remain condensed state and show no DNA synthetic activity. **B:** The female pronucleus (FP) has formed and synthesized DNA. PB, polar body. **C:** Neither the maternal chromosomes (single-arrowheads) nor the sperm nucleus (double-arrowhead) have decondensed and synthesized DNA. **D:** Female (FP) and male (MP) pronuclear formation and DNA synthesis have occurred.

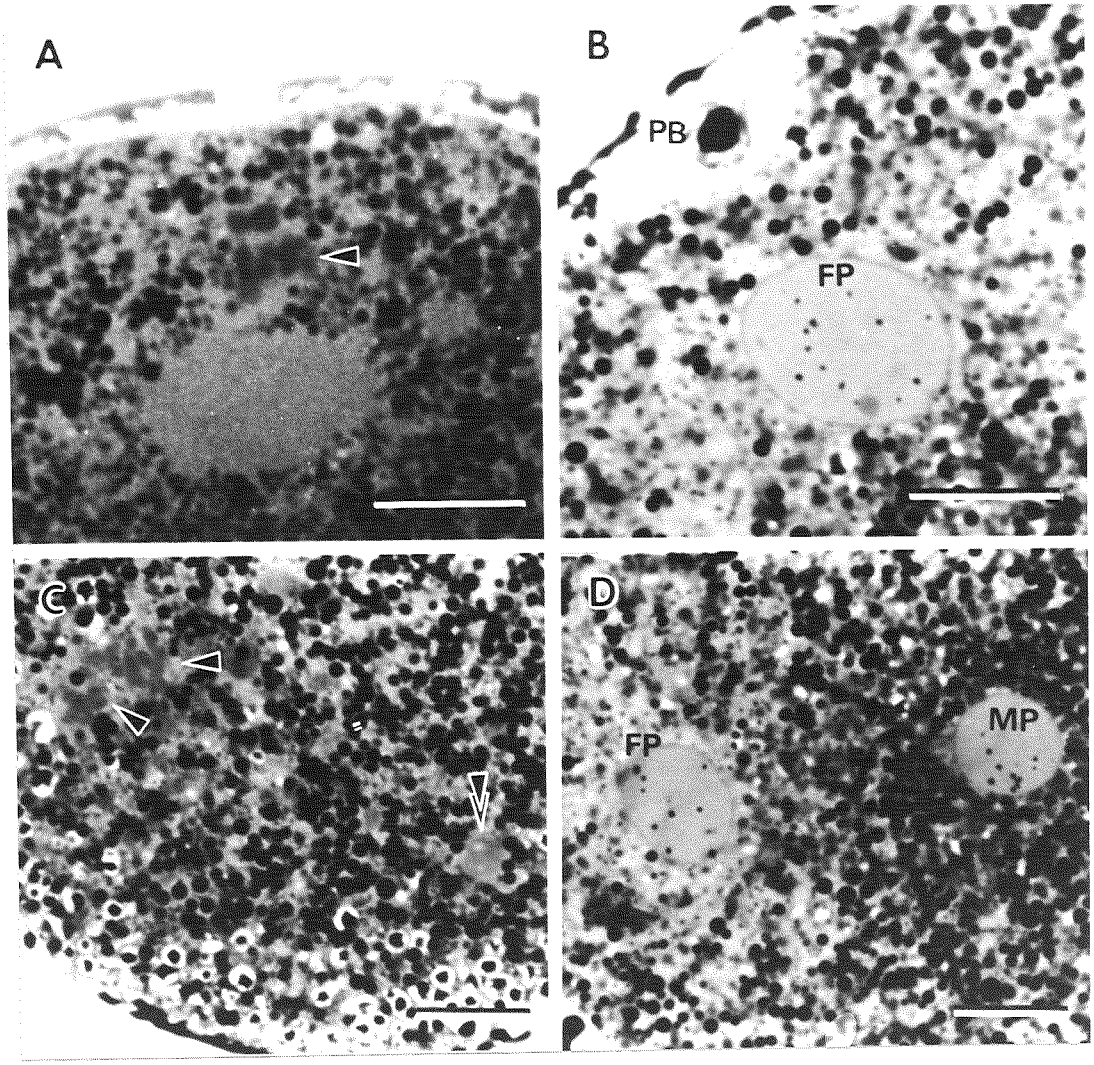
A
B
PB
FP
C
D
FP
MP

Explanation of Plate 41

Fig. 41. TEM of the maternal chromosomes in Amphipholis kochii eggs treated with colchicine. Scale, 1 μm. **A:** Treated from 30 min preinsemination and fixed at 60 min postinsemination. The chromosomes are not decondensed and surrounded by membranes. **B:** Treated from 30 min postinsemination and fixed at 45 min postinsemination. The chromosomes disperse and fuse together to form the female pronucleus. Note the nuclear envelope around the karyomeres.

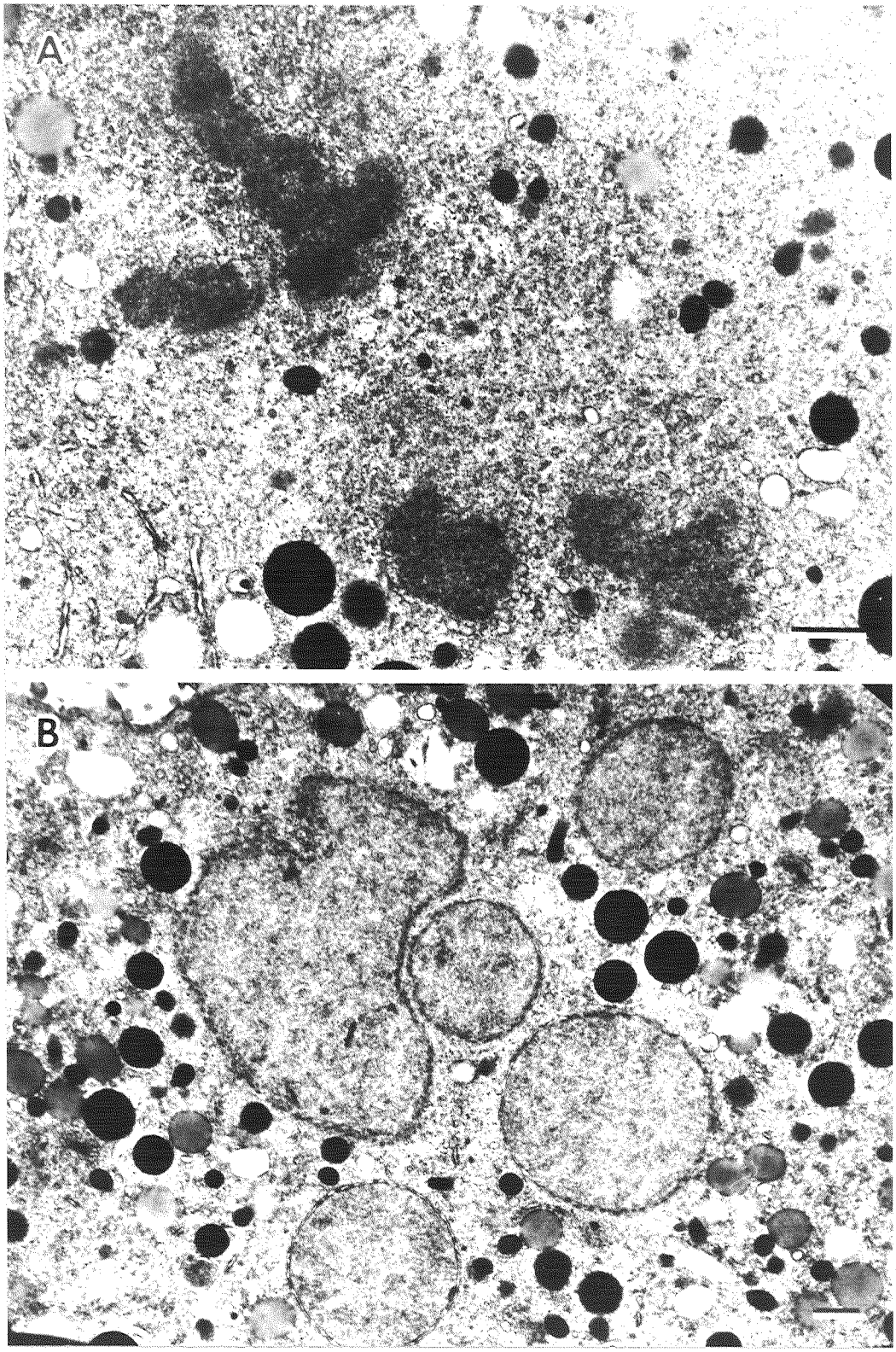
A
B

Explanation of Plate 42

Fig. 42. Autoradiograms of Amphipholis kochii eggs treated with cytochalasin B from 2 min postinsemination. Scale, 10 μm. **A:** 30 min postinsemination. Nuclear division, i.e., separation of chromosomes (arrowheads), has occurred but cytokinesis, i.e., polar body formation, has been inhibited. **B:** 45 min postinsemination. The maternal chromosomes are dispersing (arrowheads). **C:** 60 min postinsemination. The female pronucleus has been formed. Silver grains are observed over the female pronucleus, showing DNA synthesis in the female pronucleus. **D:** 60 min postinseminatiion. The female (FP) and male (MP) pronuclei before fusion. The female pronucleus (FP) is large as compared with that in the normal egg. Both pronuclei have synthesized DNA.

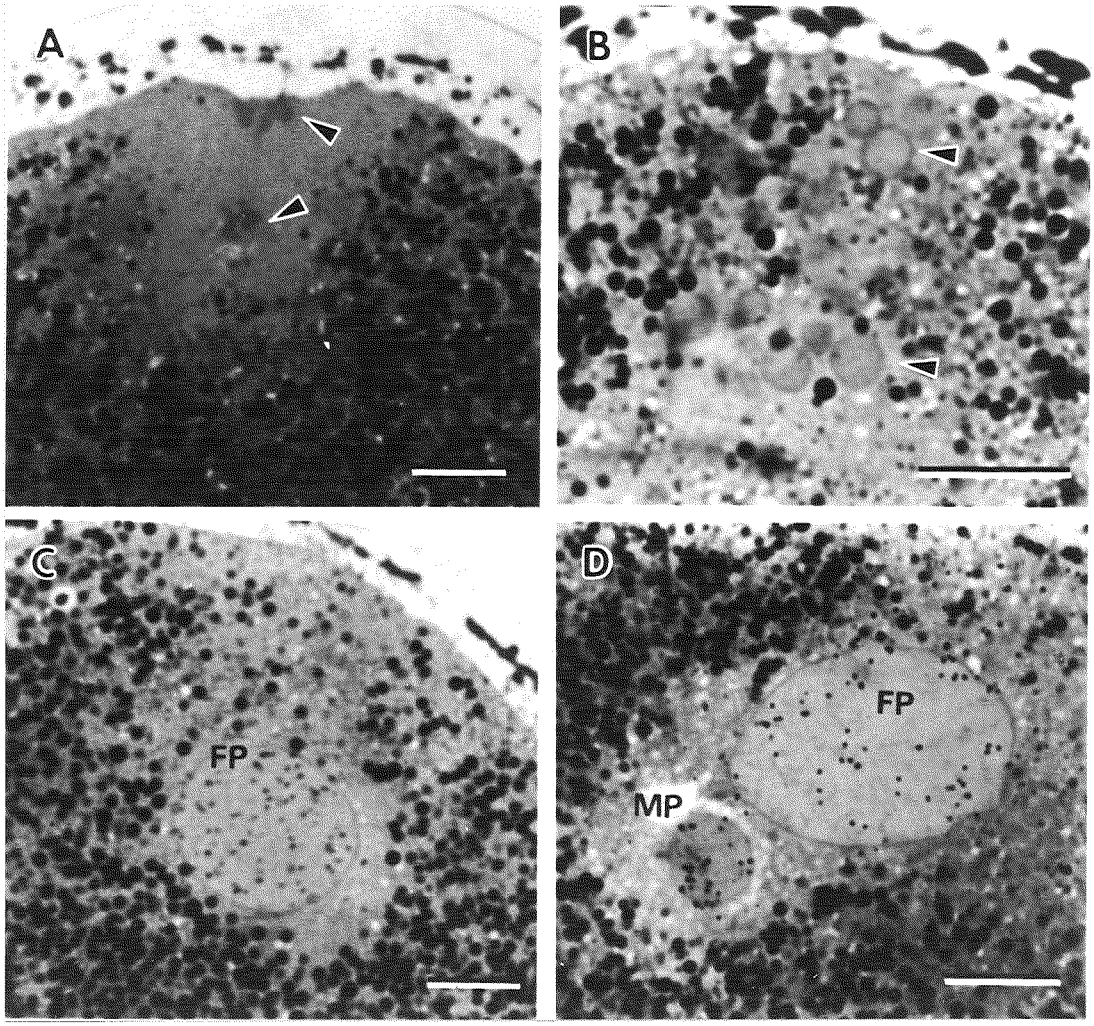
A
B
C
FP
D
FP
MP

Explanation of Plate 43

Fig. 43. TEM of the male pronucleus in Amphipholis kochii eggs treated with colchicine. Scale, 1 μm. **A:** Treated from 30 min preinsemination and fixed at 5 min postinsemination. The incorporated sperm nucleus disperses at its lateral portion (arrowheads). M, mitochondrion. **B:** Treated from 30 min preinsemination and fixed at 15 min postinsemination. The ellipsoidal sperm nucleus becomes circular showing the first dispersion, but it is not surrounded by membranes. M, mitochondrion. **C:** Treated from 30 min preinsemination and fixed at 45 min postinsemination. The second dispersion of the nucleus has not occurred. The nucleus is still naked. **D:** Treated from 15 min postinsemination and fixed at 30 min postinsemination. The nuclear envelope is disintegrated into vacuoles (arrowheads). M, mitochondrion. **E:** Treated from 15 min postinsemination and fixed at 45 min postinsemination. The nuclear envelope is completely removed from the nucleus. **F:** Treated from 30 min postinsemination and fixed at 45 min postinsemination. The developing male pronucleus shows further dispersion with nuclear envelope (the second dispersion).

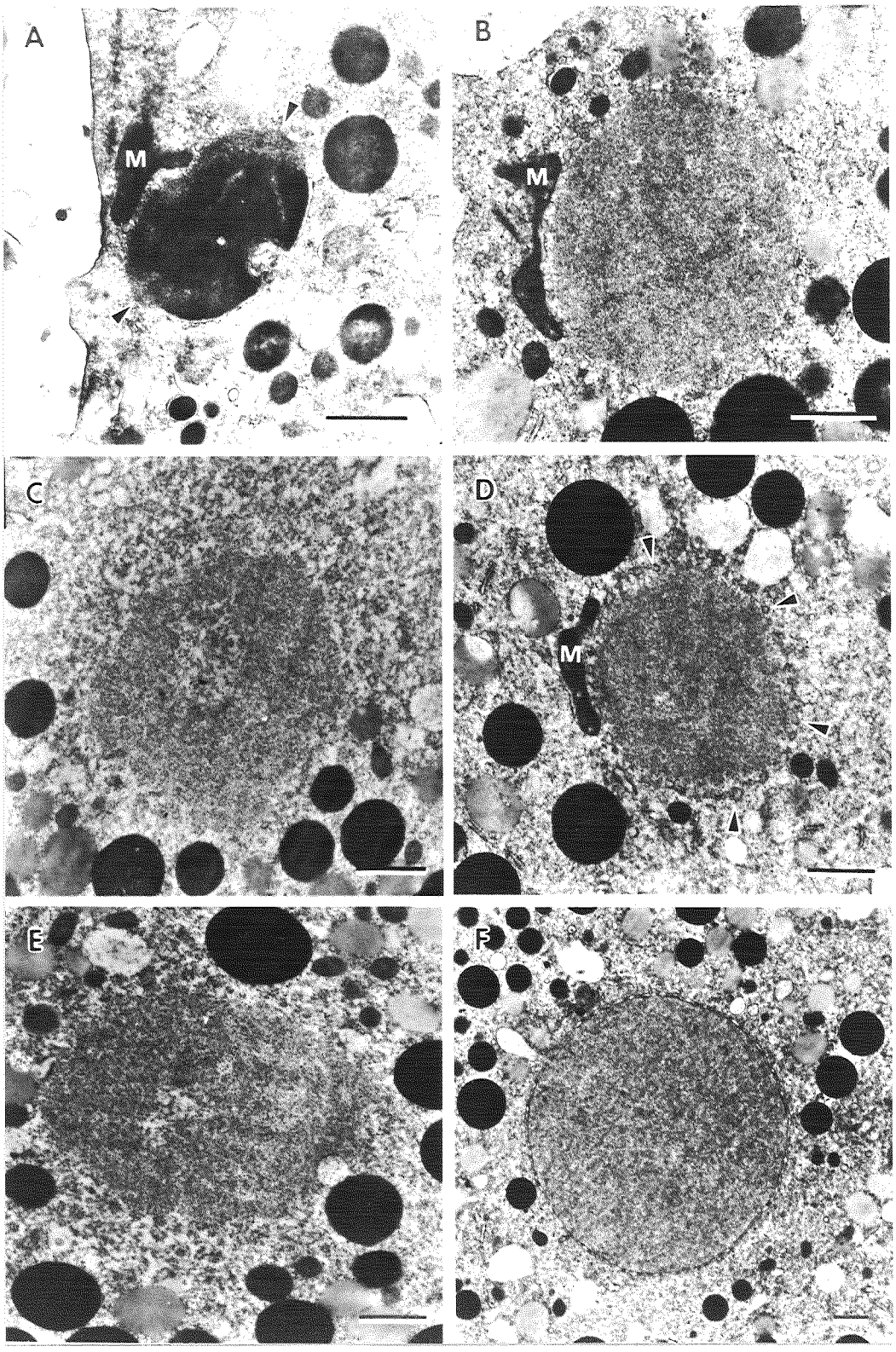
A
M
B
M
C
D
M
E
F